

**Chemogenomics Knowledgebase and TargetHunter For
Polypharmacology Analysis Of A Traditional Chinese Herbal Formula, "Sini
Decoction"**

by

Shifan Ma

Bachelor of Science, China Pharmaceutical University, 2012

Submitted to the Graduate Faculty of
School of Pharmacy in partial fulfillment
of the requirements for the degree of
Master of Science

University of Pittsburgh

2015

UNIVERSITY OF PITTSBURGH

SCHOOL OF PHARMACY

This thesis was presented

by

Shifan Ma

It was defended on

March 23th, 2015

and approved by

Paul Schiff, PhD, Professor

Xiang-Qun (Sean) Xie, PhD, Professor

Lirong Wang, PhD, Research Assistant Professor

Dissertation Advisor: Xiang-Qun (Sean) Xie, PhD., Professor

Copyright © by Shifan Ma

2015

**Chemogenomics Knowledgebase And Targethunter For
Polypharmacology Analysis Of A Traditional Chinese Herbal Formula, "Sini Decoction"**

Shifan Ma, M.S.

University of Pittsburgh, 2015

To enhance therapeutic efficacy and reduce adverse effects, practitioners of traditional Chinese medicine (TCM) often prescribe a combination of multiple herbs, called Traditional Chinese Herbal formulae (TCHF), according to the compatibility principle of TCM. To clarify the possible compatibility mechanism of formulae with systems polypharmacology analyses, we use Sini Decoction (SNT), which has been proven to be effective in treating cardiovascular diseases (CVD), as a model. The main components of SND are *Aconitum carmichaeli* Debeaux [Ranunculaceae], *Zingiber officinale* Roscoe [Zingiberaceae] and *Glycyrrhiza uralensis* Fisch. ex DC [Fabaceae]. In this research, we initially construct a chemical library with 347 reported constituents in SND, and narrowed the library to 40 compounds by selecting representative chemical structures. Then, we constructed several databases for the specific indications of SND, including heart failure, myocardial infarction, and shock, and an integrated database for CVD to perform high throughput docking with the 40 compounds in SND. Systems pharmacology is applied to investigate the polypharmacological mechanisms of SND formulae in treatment of

CVD. The predicted results showed that 31 ingredients in SND were associated with 33 targets related to the autonomic nervous system, the renin-angiotensin aldosterone system, blood coagulation, ionic channels and the glucocorticoid receptor. Through analysis of the compound-target interaction, we found multiple active chemical ingredients might interact with the same target, thus explaining the synergistic mechanisms of SND as “Jun (emperor) - Chen (minister) - Zuo (adjuvant) - Shi (courier)”. To validate the polypharmacological effects predicted by molecular docking, the experimental validation was further performed on three selected representative constituents (aconitine, liquiritin, and 6-gingerol) according to our predicted results. The results showed that the three constituents combination could produce the same cardiac effects in the rat heart failure model with the combination of three herbs in SND, and confirmed the three constituents we predicted are most likely the active constituents. This computational systems pharmacology data revealed that aconitine was the principal component of the formula, whereas liquiritin and 6-gingerol served as adjuvant ingredients, as 6-gingerol can enhance the cardiac effects of aconitine, and liquiritin can alleviate the arrhythmia caused by aconitine. The predictions are all congruent with the other reports and experiments results.

Key words: Synergistic Effect; Chinese Medicinal Formula; Sini Decoction; Polypharmacological Analysis

TABLE OF CONTENT

PREFACE.....	xii
1.0 INTRODUCTION	1
1.1 SINI DECOCTION	1
1.2 SYNERGISTIC EFFECT OF INGREDIENTS IN TCM	4
1.3 POLYPHARMACOLOGY AND MECHANISM STUDY FOR TCM	5
1.4 CARDIOVASCULAR DISEASES.....	7
2.0 METHODS AND MATERIAL.....	11
2.1 CARDIOVASCULAR DISEASES DATABASE CONSTRUCTION.....	11
2.1.1 Database Infrastructure	11
2.1.2 Cardiovascular Disease Knowledgebase Construction.....	11
2.1.3 Chemoinformatics Tools.....	12
2.2 COMPOUND LIBRARY CONSTRUCTION	14
2.3 TARGET PREDICTION.....	17
2.4 NETWORK CONSTRUCTION	17
2.5 EXPERIMENTS.....	19
2.5.1 Effect of SND on Normal Heart Function Measured by Hemodynamic Index.....	19
2.5.2 Effect of SND and Compounds on Heart Function of HF Rats.....	20
2.5.3 The Effect of Liquiritin on The Arrhythmia Induced by Aconitine (AC)	22

2.5.4 The Effect of Aconitine (AC) Combined with 6-Gingerol on Heart Function	22
2.5.5 The Validation of Predicted Targets for The Effective Compounds in SND	24
3.0 RESULTS	26
3.1 CARDIOVASCULAR DISEASES RELATED TARGETS AND DRUGS	26
3.2 DATABASE VALIDATION BY POLYPHARMACOLOGY OF ANTI-CVD DRUGS	34
3.3 POLYPHARMACOLOGY OF TARGETS OF SND COMPOUNDS	38
3.3.1 Target Prediction	38
3.3.2 Network Construction	38
3.3.3 Select Representative Active Constituents for Each Herb	41
3.3.4 Detailed Docking Information for Selected Constituents and Targets	43
3.3.5 Homology Model and Docking of Beta-1 Adrenergic Receptor	51
3.4 EXPERIMENTAL VALIDATION	53
3.4.1 The Effects of Drugs on Heart Failure	53
3.4.2 The Effect of Liquiritin on Arrhythmia Induced by Aconitine	57
3.4.3 The Effect of 6-Gingerol And Aconitine on Heart Function	60
3.4.4 The Validation of Predicted Targets with Constituents in SND	62
4.0 DISCUSSION	64
4.1 SYNERGISTIC EFFECT OF THREE INGREDIENTS IN SND	64
4.1.1 Major Constituents from Three Herbs Acting Synergistically on RAAS	66
4.1.2 Multiple Components Interact with Multiple Targets in the Coagulation System	69

4.1.3 Herbs in SND Acting Synergistically to Improve the Lipid Profile	70
4.1.4 <i>Glycyrrhiza Uralensis</i> can Alleviate Arrhythmia Caused by Aconitum	72
4.1.5 The Synergistic Effect of Ginger and Aconitum Pair	74
4.1.6 Compounds act on targets in autonomic nerves system (ANS).....	75
5.0 CONCLUSION.....	78
6.0 FUTURE PROSPECTIVE	80
APPENDIX. ABBREVIATION.....	81
BIBLIOGRAPHY	85

LIST OF TABLES

Table 1. Constituents and Their Chemical Structures in SND.....	14
Table 2. Comparison of the Experimental Data and the predicted Results.....	36
Table 3. Effect of SND on Normal Rats Measured by Hemodynamic Index	53
Table 4. Effect of Aconitine on Normal Rats Measured by Hemodynamic Index	53
Table 5. Effect of SND on HF Model Measured by Echocardiographic Data.....	56
Table 6. The Time of Premature Beats, Ventricular Tachycardia, and Cardiac Arrest.....	58
Table 7. The Dosage of Premature Beats, Ventricular Tachycardia, and Cardiac Arrest.....	59
Table 8. Summary of Hemodynamic Data with Combined Use of Aconitine and 6-gingerol....	61
Table 9. The Validated Interaction between SND Components and Predicted Targets.....	77

LIST OF FIGURES

Figure 1. Synergistic Effect of Sini Decoction for Cardiovascular Diseases	2
Figure 2. Distribution of Death	8
Figure 3. Targets for SND Related Indications and Other Cardiovascular Diseases	10
Figure 4. Overview of CVDPlatform HTDocking Procedure	13
Figure 5. Effect of SND on Normal Heart Function Measured by Hemodynamic Index	19
Figure 6. HF Model of Rats Induced by LAD Ligation and Drug Effect Evaluation	20
Figure 7. The Validation of Aconitine Acting on Beta-1 Adrenergic Receptor.....	24
Figure 8. Summary of CVD Related Targets	26
Figure 9. Drugs and Their Targets in Different Development Phases	28
Figure 10. Therapeutic Targets for MI and HF Ranked by The Number of Drugs.....	30
Figure 11. CVD Related Pathways in CVDPlatform.	31
Figure 12. Validation of CVDPlatform	34
Figure 13. Network for Compound-Target Interaction	40
Figure 14. Interaction Network of Representative Compounds and Their Targets.....	42
Figure 15. Detailed Interaction Mode of ACE with Lisinopril and 6-Gingerol.	43
Figure 16. Detailed Interaction Mode of MAOB with Coumarin Analog and Liquiritin	44

Figure 17. Detailed Interaction Mode of HMGCR with Mevastatin and Constituents in SND..	47
Figure 18. Detailed Interaction Mode of PPARG with Retinoic Acid and Glycyrrhetic Acid	48
Figure 19. Interaction Mode of AChE with Dihydrotanshinone I and Constituents in SND.....	49
Figure 20. Homology Modeling and Docking Analysis of Beta-1 Adrenergic Receptor.	51
Figure 21. Echocardiography in HF Rats with Sham Operation, HF, and Drug.....	55
Figure 22. Effects of Drugs on MASSON and HE Stained Results in HF Rats.	57
Figure 23. ECG of Normal, Premature Beats, Ventricular Tachycardias, and Cardiac Arrest...	58
Figure 24. The Dosage of Premature Beats, Ventricular Tachycardia and Cardiac Arrest.....	59
Figure 25. The Time of Premature Beats, Ventricular Tachycardia and Cardiac Arrest	59
Figure 26. The Change Rate of HR and dp/dt after treatment of Propranolol and Aconitine.....	63
Figure 27. The Prediction of Synergistic Effect Mechanism for SND.....	64
Figure 28. Multiple Targets from the RAS System and Coagulation Pathway.....	68
Figure 29. Interconversion of Cortisone and Cortisol Catalyzed by 11 β -HSD 1 and 2	73

PREFACE

I am heartily thankful to my advisor, Dr. Xiang-Qun Xie, whose encouragement, guidance and support from the initial to the final level enabled me to get in touch, and have a deeper understanding of the project. Dr. Xiang-Qun Xie has been my inspiration as I hurdle all the obstacles in the completion this research work.

I am sincerely grateful for the help and instruction I got from my co-advisor Dr. Lirong Wang. He gave me detailed and feasible guidelines and suggestions all through the project and during the two-year of MS program. He constructed the database, and developed HT-Docking and TargetHunter online program and made the high throughput virtual screen in this thesis came true. This part is the bases of this thesis.

I would like to thank Dr. Hai Zhang and his groups. This thesis would not have been possible without their previous work and always support. They did the constituents isolation and identification from aconitum, licorice and ginger in SND, laying the foundation for this thesis. They also did work to explore the synergistic effect of SND in ADME aspect, which made the work more complete. Furthermore, they validated the active constituents we selected via virtual screening, and continued to work on validation of predicted targets and molecular mechanisms for synergistic effect of Sini Decoction.

I would like to thank Dr. Zhiwei Feng, who taught me to do manual docking and homology modeling construction. He made this work more complete.

I would like to thank Dr. Peng Yang, who taught me how to select constituents with diverse chemical structures.

I would like to express my gratitude to Dr. Haibin Liu, who gave me kind suggestions at the initial of this project. His work on other project inspired me a lot for this thesis.

I would like to show my gratitude to all the members in Dr. Xiang-Qun Xie's group, who helped a lot in the two years.

I would like to thank you my parents, who support me all the time.

Lastly, I offer my regards and blessings to all of those who supported me in any respect during the completion of the project.

1.0 INTRODUCTION

1.1 SINI DECOCTION

Sini decoction (SND) is a traditional Chinese herbal formula consisting of three different herbs: *Aconitum Carmichaelii* Debeaux [Ranunculaceae] (AC), *Zingiber Officinale* Roscoe [Zingiberaceae](ZO), and *Glycyrrhiza Uralensis* Fisch. ex DC. [Fabaceae] (GU). SND is officially recorded in the Chinese pharmacopoeia 2010 edition and has been used to treat cardiovascular diseases for many years. AC is the principal herb in SND, and it plays the main pharmacological actions of this formula. ZO is the assistant and complement herb, and GU is the herb that reduces the toxicity induced by AC, and guides AC and ZO to their target tissues [1].

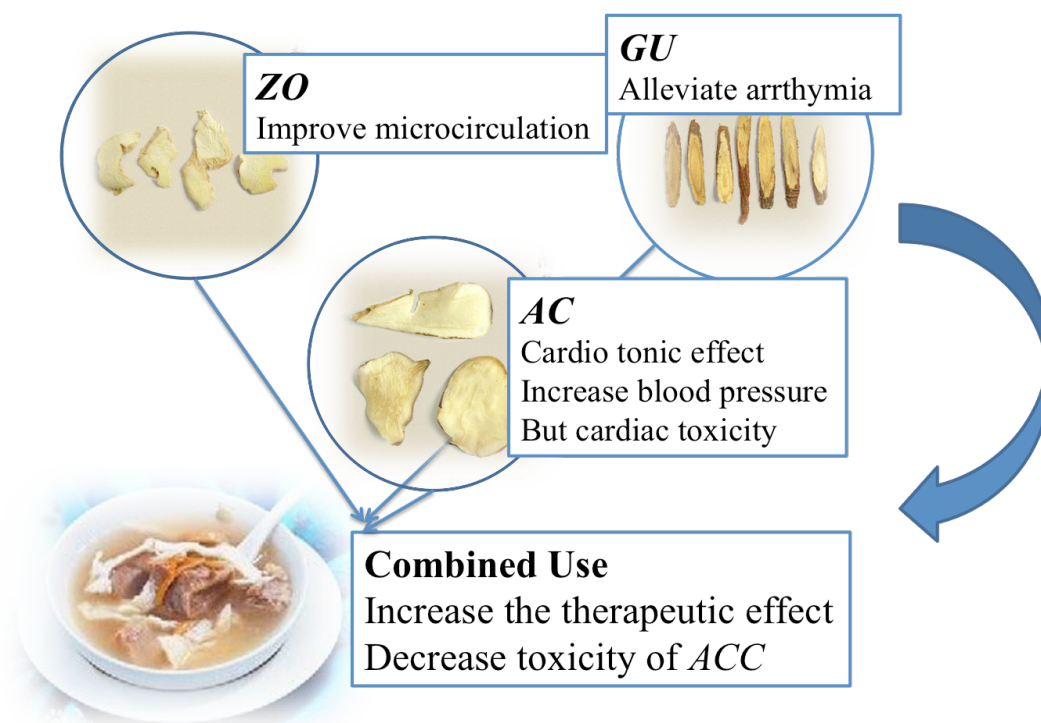


Figure 1. Synergistic Effect of Sini Decoction for Cardiovascular Diseases

The three herbs in Sini Decoction have limited therapeutic effect or have some toxic effect when used alone. However, if used in combination, they will have improved therapeutic effect with reduced toxicity.

Traditional Chinese medicine (TCM) often holistically restores the balance of Yin-Yang in the body energy, thus reviving the body's normal function and homeostasis. Herein, SND, a well-known life rescue medication, is recorded in the *Treatise on Febrile Diseases* and other ancient Chinese medical textbooks to improve Yang deficiency, thus restoring the balance of Yin-Yang to treat different types of cardiovascular and other diseases, such as myocardial infarction (MI) [2], congestive shock, liver failure [3], hyperlipidemia [4], diabetes [5], and heart failure (HF) [1]. Although the single herbal medicine AC can treat cardiovascular diseases, it will cause cardiac toxicity but it can be made safer and the therapeutic effect enhanced by combination with the two herbal medicines of ZO and GU [6]. On the hand, ZO and GU have

less efficacy comparing with AC when used alone to treat CVD. Accumulated evidence has proved that SND can treat cardiovascular diseases with decreased toxicity and increased efficacy in combination with ZO and GU especially heart failure and myocardial infarction. Some previous studies focused on the pharmacokinetic profile of Sini Decoction, to study the synergistic effects among the three herbs on rat models [2, 7-9].

It is common knowledge that a multi-herbal formula exerts therapeutic efficacy through synergistic effect of its multiple ingredients that attack multiple targets in multiple channels. Though many compounds have been isolated and identified in Sini Decoction [10], revealing the holistic mechanism of the pharmacological action of SND remains a difficult task due to the unknown active compounds and the unknown synergistic actions that take place in SND. Additionally, it is time-consuming, costly, and tedious to use the traditional methods for active components screening, potential targets identification, and TCM formulae mechanism understanding [11].

Recently, the combined use of computational screening and polypharmacology analysis is emerging as a promising way to identify the potential drug targets in TCM and to clarify the pharmacological mechanisms of the formula [7, 12]. As a system biology-based methodology, system pharmacology offers an effective approach to evaluate TCMs' polypharmacological effects at the molecular level for exploring the complex interactions of small molecules and proteins in a biological system. Therefore, in our research, systems polypharmacology is employed to screen the active components from the medical herbs. We then verified the targets predicted and pharmacological actions in the rat models we built.

Previous studies by our collaborators have identified 51 chemical ingredients in SND [10, 13-16]. The results provided a material basis for further polypharmacology analysis. In the

present study, we applied our established *in silico* docking approach to predict potential targets of the SND active ingredients. Firstly, we constructed a biological network of the interactions between the chemical compounds and target proteins at the molecular or systematic level based on our prediction. Then we investigated the effects of selective components in SND. Finally, we validated the predicted targets on the rat models of myocardial infarction and heart failure caused by coronary artery ligation. The combined approaches offer a deeper understanding of the pharmacological mechanisms of SND, and may provide a novel and efficient way to dissect the compatibility mechanism of TCMs.

1.2 SYNERGISTIC EFFECT OF INGREDIENTS IN TCM

To get efficacy-enhancing and toxicity-reducing effects of TCM, formulas containing several medicinal herbs are usually required based on clinical treatment experience in China. For complicated or multi-factorial diseases, accumulating evidence indicates that TCM can usually achieve a better therapeutic efficacy using multiple drugs with common and different pharmacological targets instead of one drug-one target [17]. TCM is an empirical healthcare system under the guidance of the TCM theory based on several millennia of treatment. Typically, the medicinal herbs in a formula can be classified into principal (Jun), assistant (Chen), complement (Zuo), and guide (Shi) components according to their roles in the prescription, in which the principal herb performs the main pharmacological actions, and the others perform synergistic actions to yield maximal therapeutic efficacy with minimal adverse effects [17, 18]. According to the polypharmacological theory, these essential multi-components play multiple

pharmacological roles by reacting with different but related targets: this is also known as the compatibility mechanism [19-21]. Network polypharmacology is used to unravel synergistic mechanism of drug combinations in TCM [20].

It is possible that the multiple compounds in the SND formula could interact with multiple targets and act synergistically to heal illnesses. However, it is a time-consuming, costly and challenging task to identify the essential potential target and understand the systematic mechanism for the TCM formulae experimentally. Thus in this study, we applied computational network pharmacological approaches and high throughput virtual screening to investigate the potential target for the synergistic effect of SND ingredients at the molecular level.

1.3 POLYPHARMACOLOGY AND MECHANISM STUDY FOR TCM

Systems biology is an emerging area of biology, which utilizes experimental and computational approaches to evaluate and integrate large datasets in a systematical way. Systems biology also examines and analyzes regulatory networks with large datasets, in order to identify how the elements are joined to form a functional system [22]. Polypharmacology, a concept that one or multiple drugs can modulate multiple targets to treat disease, is an important application of systems biology in drug discovery [22]. Polypharmacology might involve multiple drugs acting on multiple targets in the context of network regulating physiological responses in disease process [12]. So polypharmacology is very useful in the discovery of novel drugs and suitable combination medications for complex diseases, such as cancer, in which drugs act on multiple therapeutic targets in a complex pathological network. Systems pharmacology often use network

analysis of drug-target interaction as an approach [20]. On the other hand, polypharmacology is believed to reduce on-target and anti-target adverse effect, and drug resistance, thus improving drug safety, preventing side effects and drug tolerance [22]. Taken together, systems polypharmacology analysis can lead to new therapeutic directions with improvement on both the safety and efficacy of existing medications [23].

Given the complex pathological mechanism and therapeutic pathways involved in cardiovascular diseases, polypharmacology analysis is often performed to understand the synergistic effect of drugs reacting with multiple therapeutic targets in the overlapping signaling pathways [24]. Polypharmacology analysis can not only help to unravel the mechanism of actions of primary targets for existing drugs in the context of a whole organism, but also predict possible off-target therapeutic and adverse effects [25] and guide combination therapy [26]. On the other hand, TCM is about herbal formulations with multiple herbs, involving multiple constituents, acting on multiple targets in overlapping therapeutic pathways to attain a synergistic effect with higher efficacy and reduced side effects to treat disease. Therefore, systems pharmacology offers an effective approach to evaluate polypharmacological effects of traditional Chinese herbal formula at the molecular level to explore the interactions between small chemical molecules and targets in a pathological system. Moreover, polypharmacology are often used with computational methods, such as fragment-based methods [27], Gaussian Ensemble Screening (GES) polypharmacology fingerprints [28], *in silico* polypharmacology [29], and data mining [11] to avoid the spending of large amount of cost and time. Herein, we perform a polypharmacology study combined with computational approaches to screen active components from the three herbs in SND, to predict and to validate their corresponding targets and pharmacological actions.

1.4 CARDIOVASCULAR DISEASES

Cardiovascular diseases are the leading cause of death in the world (accounting for 31% in the distribution of all causes of death, as shown in **Figure 2A**) [30], accounting for 28% in non-communicable diseases (NCD) [31] caused death worldwide.

Cardiovascular diseases (CVDs) are a group of disorders of heart and blood vessels, including: coronary heart disease or ischaemic heart disease (e.g. heart attacks), cerebrovascular disease (e.g. stroke), peripheral arterial disease, rheumatic heart disease (damage to the heart muscle and heart valves caused by rheumatic fever), congenital heart disease (inherent malformations of heart structure), deep vein thrombosis, and cardiac arrhythmias. An estimated 17.5 million people died from CVDs in 2012, representing 31% of all global deaths (**Figure 2A**) [32]. Among these deaths caused by CVDs, an estimated 7.4 million deaths were due to coronary heart disease (heart attack, accounting for 46% and 38% in cardiovascular diseases caused deaths for male and female respectively) and 6.7 million deaths were due to cerebrovascular disease (stroke, accounting for 34% and 37% in cardiovascular diseases caused deaths for male and female respectively), as shown in **Figure 2C and 2D** [30, 33].

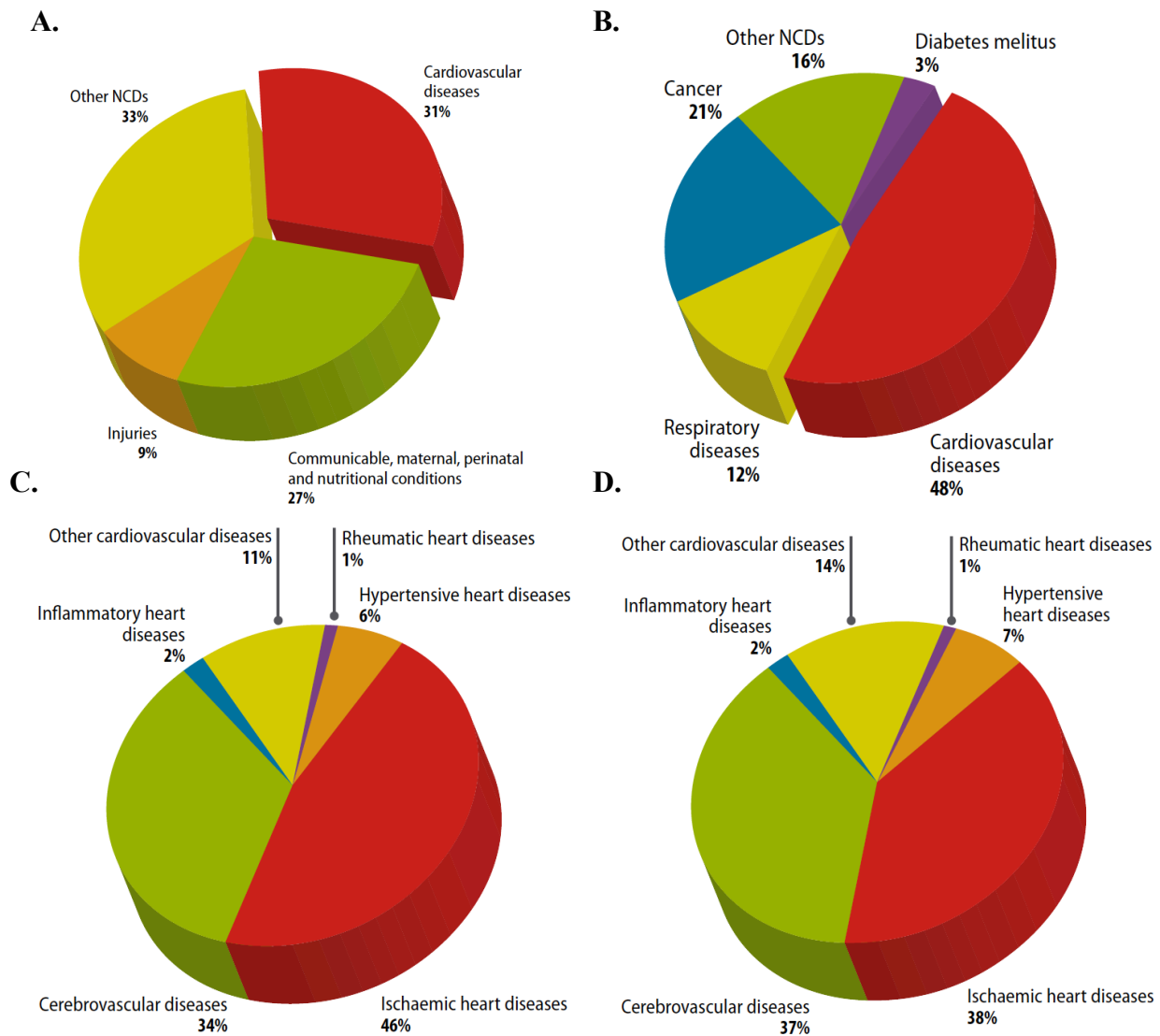


Figure 2. Distribution of Death

(A) The distribution of all causes of death in the world per year in 2013; (B) The distribution of death caused by different non-communicable diseases (NCD); (C, D) The distribution of death caused by different cardiovascular diseases in female (C) and male (D). Data was collected from WHO website.

Heart attack, stroke, heart failure, myocardial infarction (MI), shock and other complications are mainly due to the failure of the blood supply to the heart, brain, and other tissues by the circulation, caused by the formation of blockage in blood vessels or the impairment of heart function. The causes of heart failure and other indications are usually the presence of a combination of some common risk factors, such as tobacco use, unhealthy diet and obesity, physical inactivity and harmful use of alcohol, hypertension, diabetes and hyperlipidemia [32, 34]. Although there are many different complications and disorders in cardiovascular diseases that can be treated with different drugs and corresponding targets, these disorders share similar risk factors and pathological pathways [35]. We can see from **Figure 3**, the protein targets involved in the SND indications, such as coronary disease, MI, shock, and heart failure, overlap each other and also overlap with these targets involved in other cardiovascular diseases. Thus, when we study some specific cardiovascular diseases, we would better evaluate CVD as a whole.

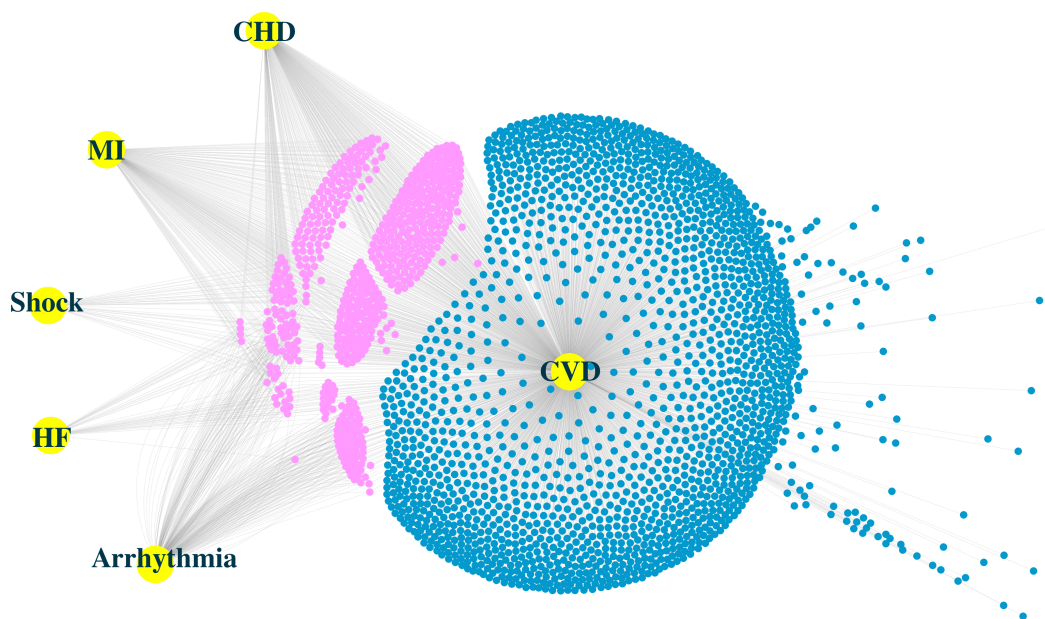


Figure 3. Targets for SND Related Indications and Other Cardiovascular Diseases

Targets in pathological pathways of SND indications, including coronary heart disease, myocardial infarction, heart failure, shock, and arrhythmia, represent by pink nodes; the other targets related with the etiology for other cardiovascular diseases are in blue; the yellow large nodes stand different types of diseases.

Abbreviations: CHD, coronary heart disease; MI, myocardial infarction; HF, heart failure.

Sini Decoction has been widely used in China for centuries as a rescue in emergencies to treat some cardiovascular diseases, such as heart failure, MI, and congestive shock. Since it is hard to consider those diseases individually, we then just put all the therapeutic targets together as a database to study Sini Decoction. Instead, we considered the cardiovascular diseases as whole to study the molecular mechanism of SND.

2.0 METHODS AND MATERIAL

2.1 CARDIOVASCULAR DISEASES DATABASE CONSTRUCTION

2.1.1 Database Infrastructure

CVDPlatform was rooted from our established web-interface molecular database prototype CBID (www.CBLIgand.org/CBID) [36], which is constructed with a MySQL (<http://www.mysql.com>) [37] database and an apache (<http://www.apache.org/>) web server, and implemented with our house chemoinformatics tools.

2.1.2 Cardiovascular Disease Knowledgebase Construction

CVD related proteins and genes. The candidate proteins related to cardiovascular diseases were data mined from literature and public database, including PubMed (www.ncbi.nlm.nih.gov/pubmed), PubChem (pubchem.ncbi.nlm.nih.gov/), DrugBank (<http://www.drugbank.ca>), Potential Drug Target Database (<http://www.dddc.ac.cn/pdtd>), Therapeutic Targets Database (<http://bidd.nus.edu.sg/group/ttd/>), ClinicalTrials.gov

(clinicaltrials.gov/) and PharmGkb (www.pharmgkb.org), up to 984 candidate proteins were collected, and their corresponding X-ray crystallographic structures were obtained directly from RSCB Protein Data Bank (www.rcsb.org/pdb) to build the CVD specific chemogenomics database (www.cbligand.org/CVD).

CVD pathways (currently 269 records). The CVD related pathways was achieved via the public database KEGG [38] (<http://www.genome.jp/kegg/>) and DrugBank [39] using our in house data-mining tools.

CVD bioassays. The corresponding bioassays for the target genes and proteins, which are used to validate our prediction, have been collected from a batch of literature and public resource, like PubChem [40], ChEMBL [41], and DrugBank [39].

2.1.3 Chemoinformatics Tools

The *CVDPlatform* provides both chemogenomics and chemoinformatics data to explore the potential CVD targets and off-targets, ADME and toxicity profile, to evaluate molecular properties, as well as to calculate drug-likeness. We have implemented several chemoinformatics tools and powerful algorithms in the platform to assist CVD drug design and target identification, as showed below.

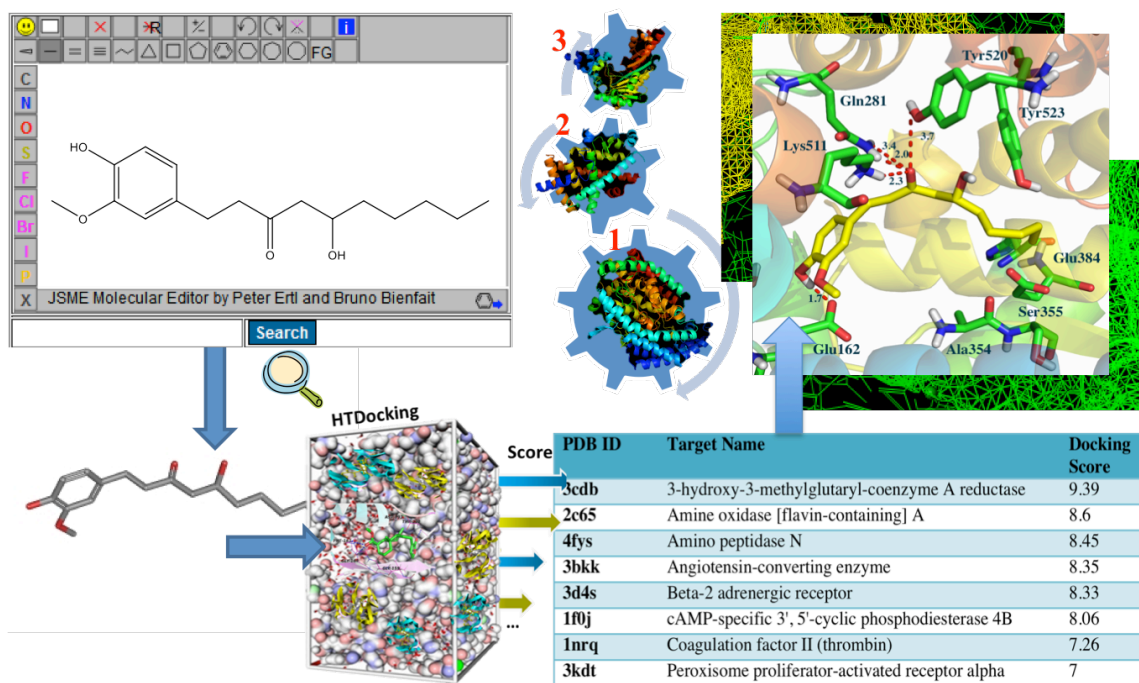


Figure 4. Overview of CVDPlatform HTDocking Procedure

HTDocking. We constructed online high-throughput docking program in our *CVDPlatform*. HTDocking online program aims to explore multiple druggable therapeutic targets, their interacted small chemical compounds, and their potential pharmacology. We use AutoDock in this HT-Docking program to offer a multi-facet capability, high performance rate and enhanced accuracy [42]. It can provide predicted binding affinity values (ΔG values) for different poses of each compound in the binding pockets [43]. The docking score in the HT-docking program is served as a measurement for the binding affinity. The calculation of docking score is $pKi = -\log(\text{predicted } Ki)$ and the predicted $Ki = \exp^{(\Delta G * 1000 / (1.987191 * 298.15))}$. We can rank the potential therapeutic targets for cardiovascular diseases according to the docking score from each protein structure. Top listed targets with higher docking scores may have higher binding affinity

or more chance to interact with our input compounds. The workflow of HTDocking is shown in **Figure 4**.

2.2 COMPOUND LIBRARY CONSTRUCTION

Based on previous studies on chemical analyses of Sini decoction (SND) [44], 347 compounds were reported in SND, with 196 constituents in GU, 49 constituents in AC and 102 constituents in ZO. We selected 40 representative compounds with diverse chemical structure, which have been identified and isolated, including 25 constituents in AC, 13 constituents in GU, and 2 constituents in ZO (as shown in **Table 1**). The structures were obtained from the Chemical Book (www.chemicalbook.com), NCBI PubChem database (www.ncbi.nlm.nih.gov/pccompound), Scifinder [45] (<http://scifinder.cas.org/scifinder>), and saved to files in SDF format and SMILES format for further analysis.

Table 1. Constituents and their chemical structures in SND

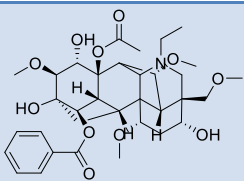
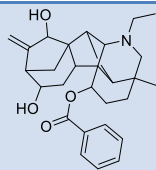
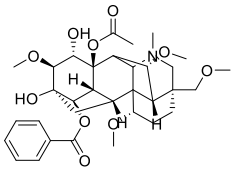
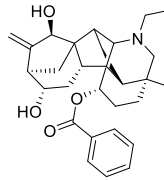
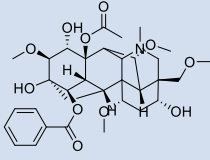
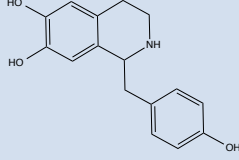
Name	Structure	Name	Structure
1 Aconitine AC		20 Benzoylnapelline	
2 Hypaconitine		21 Isobenzoylnapelline	
3 Mesaconitine		22 Higenamine	

Table 1 continued

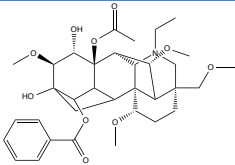
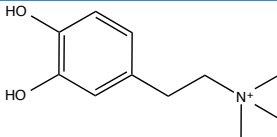
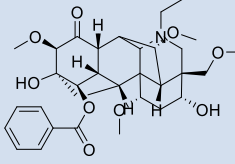
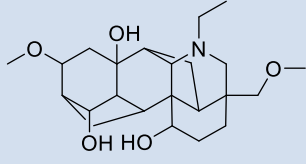
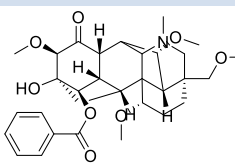
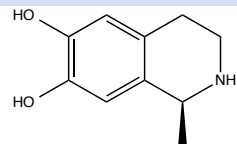
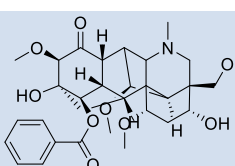
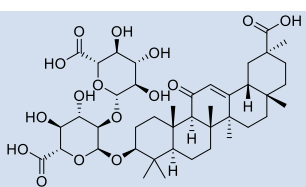
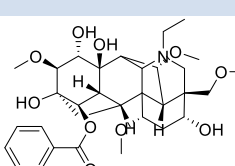
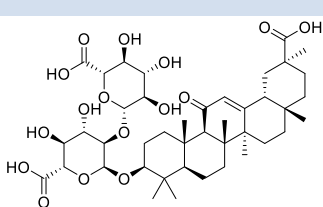
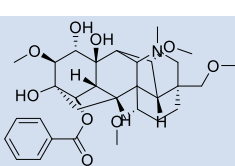
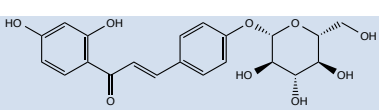
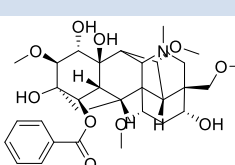
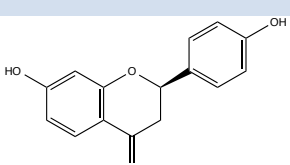
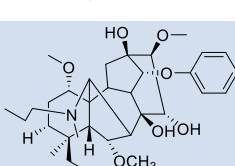
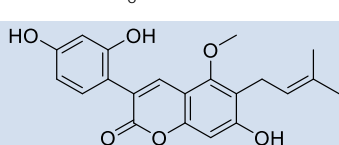
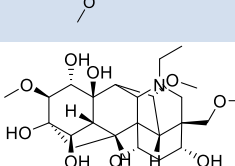
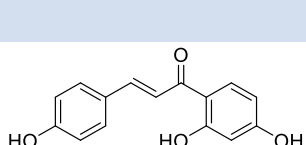
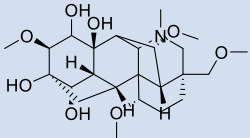
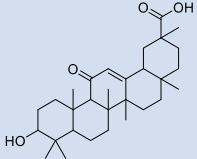
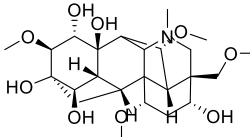
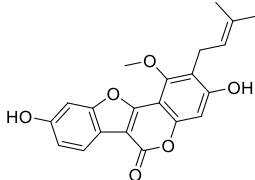
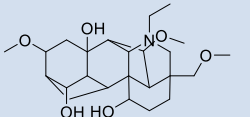
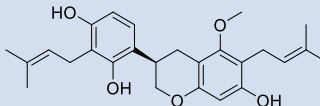
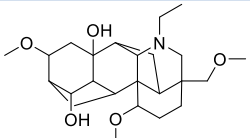
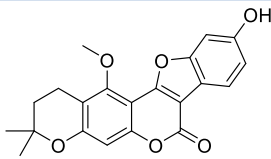
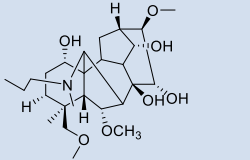
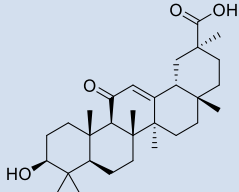
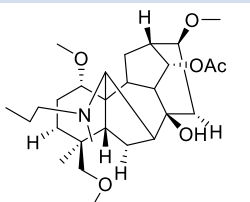
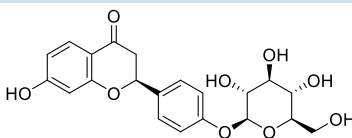
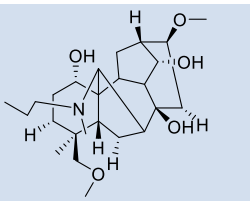
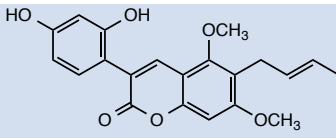
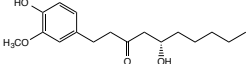
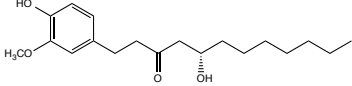
4	Deoxyaconitine		23	Coryneine	
5	Pyroaconitine		24	Isotalatizidine	
6	Pyrohypaconitine		25	Salsolinol	
7	Pyromesaconitine		26	Glycyrrhizic Acid	
8	Benzoylaconine		27	Glycyrrhizin	
9	Benzoylhypaconine		28	Isoliquiritin	
10	Benzoylmesaconine		29	Liquiritigenin	
11	Benzoyldeoxyaconine		30	Glycyamarin	
12	Aconine		31	Isoliquiritigenin	

Table 1 continued

13	Hypaconine		32	Glycyrrhetic Acid	
14	Mesaconine		33	Glycyrol	
15	Neoline		34	Licoricidin	
16	Talatisamine		35	Iso-Glycyrol	
17	Fuziline		36	Glycyrrhetic Acid	
18	14-Acetyl-Talatisamine		37	Liquiritin	
19	Talatizidine		38	Glycyrin	
39	6-Gingerol		40	8-gingerol	

1-25 are from AC, 26-38 are from GU, 39 and 40 are from ZO

2.3 TARGET PREDICTION

Molecular docking, which is commonly applied to rational drug discovery, is frequently used to predict the interaction between small molecules and its corresponding target proteins,. In this study, the molecular docking approach was applied to predict the possible interaction between the 40 components from SND and the 984 target proteins we collected in our database.

All the docking studies were done by Sybyl-X (version 1.3, TRIPOS, Inc.), using co-crystal structures of target proteins. The protein structures need a preparation process before docking, involving the addition of hydrogens, removal of co-crystallized ligands and water molecules, addition of charges, fixation of side chain amide and side chain bumps to optimize interaction with surrounding residues and group atoms, and stage minimization. The binding site of the target protein in molecular docking was defined according to the key residues and known ligand position reported in literature using Surflex-Dock. For each of the compounds, the proteins with docking score larger than 6 were selected as its potential targets.

2.4 NETWORK CONSTRUCTION

Construction of a target-compound network for a specific herb formula is helpful and reasonable to identify and further evaluate potential targets and synergistic effect of compounds in SND in the context of disease pathways. Cytoscape 3.0.2 was used to generate the network plot between targets and compounds in order to predict possible targets for synergistic effect and

to understand the underlying principle of herbal formulation. Cytoscape is a standard computational tool that is frequently used in the biological field to generate, analyze and visualize the graphical network, where nodes represent targets or compounds, and edges stand for interaction between targets and compounds.

2.5 EXPERIMENTS

2.5.1 Effect of SND on Normal Heart Function Measured by Hemodynamic Index

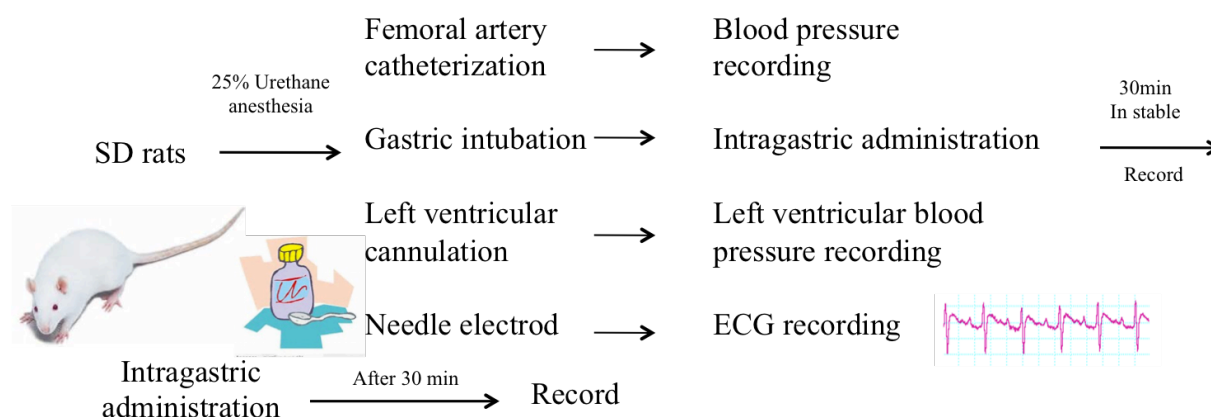


Figure 5. Overview of Experimental Procedure for Effect of SND on Normal Heart Function Measured by Hemodynamic Index

All of the animal studies followed the relevant national legislation and local guidelines, and were performed at the Centre of Laboratory Animals of the Second Military Medical University (Shanghai, China). The surgical procedures were performed using the well-established techniques. All surgeries were performed under 25% urethane anesthesia and all efforts were made to minimize suffering. Five Sprague-Dawley (SD) rats were anesthetized with an intraperitoneal injection of Urethane (1.4 g/kg, i.p.) and placed in a supine position on a table for the operations. The first polyethylene catheter connected to a pressure transducer, which was equipped with a polygraph, was inserted into the right carotid artery and then advanced into the left ventricle cavity to record left ventricular systolic (LVSP) and end-diastolic pressures (LVEDP) and heart rate (HR). The second polyethylene catheter was inserted into the lower

abdominal aorta through the left femoral artery to record systolic blood pressure (SBP), diastolic blood pressure (DBP). The third polyethylene catheter was placed in stomach fundus for drug administration. The HR, LVSP, LVEDP, SBP, DBP, MBP, maximal rate of pressure development (+dp/dt) and decline (−dp/dt) were analyzed by LabChart software. Thirty minutes after surgery, when the hemodynamic parameters are in stable, the rats were administrated Intragastrically with Sini Decoction. After 30 minutes, the hemodynamic parameters (HR, LVSP, LVEDP, SBP, DBP, MBP, maximal rate of pressure development (+dp/dt) and decline (−dp/dt)) were recorded and analyzed to see whether SND can have effect on heart function of normal rats.

2.5.2 Effect of SND and Compounds on Heart Function of HF rats

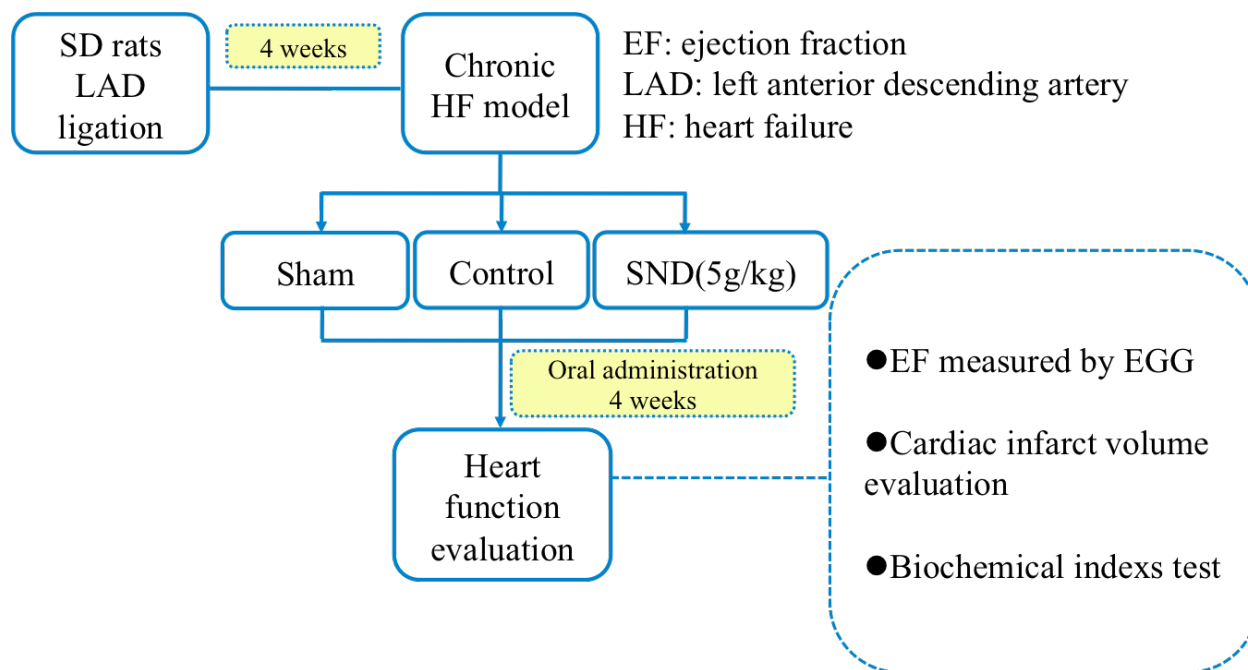


Figure 6. Overview of Experimental Procedure for HF Model of Rats Induced by LAD Ligation and Drug Effect Evaluation

2.5.2.1 HF model of rats induced by LAD ligation and drug administration The surgical procedures were performed using the well-established technique. All surgeries were performed under diethyl ether anesthesia and all efforts were made to minimize suffering. Rats were anesthetized with diethyl ether and placed in a supine position on a table for the operations. The left anterior descending artery (LAD) was occluded. To prevent infection, rats were given penicillin (40,000 units) after the operation for 3 days. Fifty animals survived throughout the experiment, including 40 LAD rat and 10 sham rats (without ligation). Forty LAD rats were randomly divided into four groups, 10 in HF model (water), 10 in herbs group (SND, 5g/kg), 10 in components group (three herbs extract, 15mg/kg) and 10 in compounds group (three active compounds, 1 mg/kg). All drugs were given through oral administration began at 4 weeks after surgery. The drugs were diluted with distilled drinking water and administered orally with a volume of 5mL/kg body weight once every morning for 4 weeks (**Figure 5**) [46] [2].

2.5.2.2 Echocardiography assessment Echocardiography was performed 21 days after surgery according to reported methods. Ten rats from each group were anesthetized by intraperitoneal injection of 100 mg /kg ketamine. After cleaning the rat chest, the cardiac short axis (papillary level), left ventricle end-diastolic dimension (LVIDd), and left ventricle end-systolic dimension (LVIDs) were measured using a Visual Sonics Vevo770 machine equipped with 23 (or 30) MHz transducers to assess systolic function. The ejection fraction (EF) was calculated from the left ventricle end-diastolic volume (LVEDV) and the left ventricle end-systolic volume (LVESV) as $EF\% = [(LVEDV - LVESV)/LVEDV] \times 100$. The data calculations were performed using a single blind method (**Figure 6**) [47, 48].

2.5.2.3 Morphometric analysis Myocardial tissues in the left ventricle (LV) of sacrificed rats (approximately 2 mm in thickness) were removed after echocardiography assessment. Samples were fixed in 4% pre-cooled paraform aldehyde for 72 h and embedded in paraffin for histological studies. Paraffin-embedded tissues were sectioned into slices about 5 mm thicknesses. Masson's trichromatic stain was performed to assess myocardial fibrosis. Images were visualized under an optical microscope at $\times 400$ magnification [49].

2.5.3 The effect of Liquiritin on the arrhythmia induced by Aconitine (AC)

Male SD rats weighing 280-300 g were equally divided into two groups randomly: A (AC) and B (AC and Liquiritin). SD rats were anesthetized with an intraperitoneal injection of urethane (1.4 g/kg, i.p). The rats were intravenously injected with the normal saline in group A, and with 4 mg/kg Liquiritin in group B. After 5 min, 10 μ g/ml aconitine was injected to the rats in a constant speed of 0.1ml/min. The cardiac function test was performed on the PowerLab 8/35 (AD instrument, Australia), and the rats were connected to PowerLab through three electrocardiograph electrodes. The electrocardiogram was recorded to show the time of the appearance of premature beats, ventricular tachycardias and cardiac arrest, and to calculate the dosage of aconitine, at which could lead to premature beats, ventricular tachycardias and cardiac arrest [50].

2.5.4 The effect of aconitine (AC) combined with 6-gingerol on heart function

Male SD rats weighing 280-300 g were equally divided into four groups randomly: A (aconitine (AC), 10ug/kg), B (AC, 10ug/kg, and 6-gingerol, 70ug/kg), C (AC, 5ug/kg), and D (AC, 5ug/kg, and 6-gingerol, 35ug/kg). SD rats were anesthetized with an intraperitoneal injection of Urethane (1.4 g/kg, i.p.). The first polyethylene catheter connected to a pressure transducer, which was equipped with a polygraph, was inserted into the right carotid artery and then advanced into the left ventricle cavity to record left ventricular systolic (LVSP), end-diastolic pressures (LVEDP) and heart rate (HR). The second polyethylene catheter was inserted into the lower abdominal aorta through the left femoral artery to record systolic blood pressure (SBP), diastolic blood pressure (DBP), and medium blood pressure (MBP). The third polyethylene catheter was connected with a needle that inserted into the femoral vein for intravenous drug administration. The HR, LVSP, LVEDP, SBP, DBP, MBP, maximal rate of pressure development (+dp/dt) and decline (−dp/dt) were analyzed by LabChart software. Thirty minutes after surgery, when the hemodynamic parameters are in stable, normal saline was injected to the rats in group A and C, and 70ug/kg and 35ug/kg 6-gingerol were injected to rats in group B and D respectively. After 5 minutes, the rats were intravenously injected with the 10μg/ml aconitine in group A and B, and with 5μg/ml aconitine in group C and D. Then after 30 minutes, the hemodynamic parameters (HR, LVSP, LVEDP, SBP, DBP, MBP, maximal rate of pressure development (+dp/dt) and decline (−dp/dt)) were recorded and analyzed, if they were in stable, to evaluate whether 6-gingerol can improve the effect of aconitine on heart function.

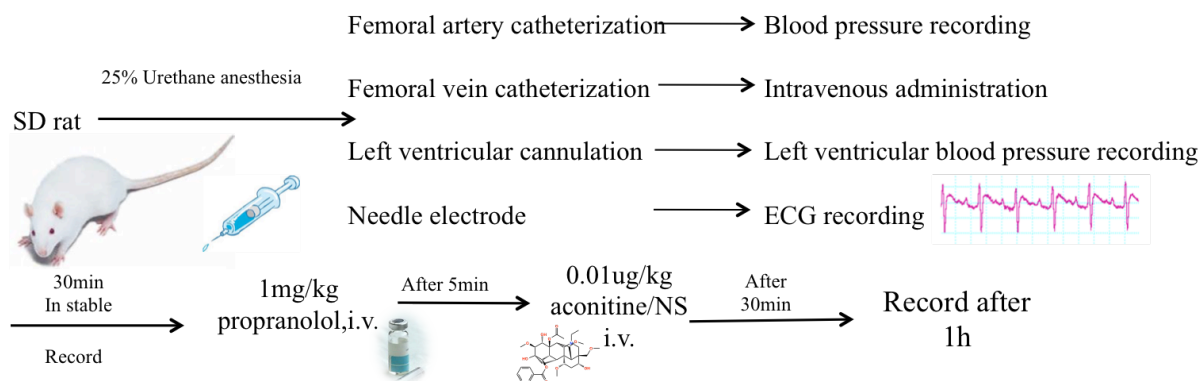


Figure 7. The Overview for Experimental Procedure of Validation of Aconitine Acting on Beta-1 Adrenergic Receptor

2.5.5 The validation of predicted targets for the effective compounds in SND

2.5.5.1 The validation of aconitine acting on beta-1 adrenergic receptor

SD rats were equally divided into four groups randomly: A (normal saline (NS) and AC), B (Propranolol (PRO) and AC), C (PRO and SND), and D (propranolol and NS). As described in 2.5.5, SD rats were anesthetized with an intraperitoneal injection of urethane (1.4 g/kg, i.p), the cardiac function was performed on the PowerLab 8/35 (AD instrument, Australia), and the rats were connected to PowerLab through three electrocardiograph electrodes to record the hemodynamic index HR, LVSP, LVEDP, SBP, DBP, MBP, maximal rate of pressure development (+dp/dt) and decline (−dp/dt) was recorded by PowerLab, and analyzed through Labchart software to validate whether the effective compounds in SND agitated Beta adrenergic receptor. (**Figure 7**) Thirty minutes after surgery, the rats were intravenous injected with the propranolol in group B, C, and D after the hemodynamic condition is stable. After 5 min, 10 µg/ml aconitine, SND, and saline were injected to the rats in a constant speed. After 30 min, the hemodynamic parameters were then recorded and analyzed when the blood pressure was stable

to see whether propranolol can block the effect of SND and aconitine on heart function in rats, in order to validate whether the effective compounds in SND agitated beta-1 adrenergic receptor (**Figure 7**).

3.0 RESULTS

3.1 CARDIOVASCULAR DISEASES RELATED TARGETS AND DRUGS

CVDPlatform (www.cbligand.org/CVD) archived 984 cardiovascular diseases related target proteins, corresponding with 924 FDA-approved and clinical trial CVD drugs, 276 cardiovascular related pathways and 2080 active chemical compounds associated with therapeutic targets of CVDs, and 350765 references.

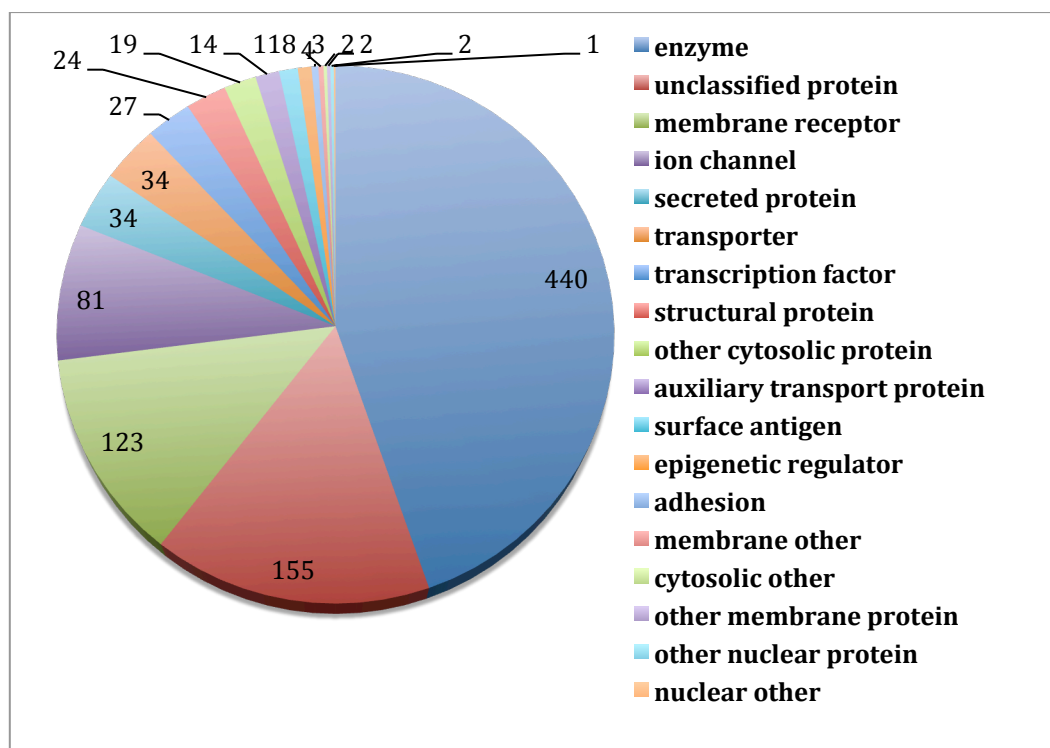


Figure 8. Summary of CVD related targets

Figure 8 illustrated detailed target information about the cardiovascular diseases database (*CVDPlatform*). The majority of CVD target proteins are 440 enzymes, including angiotensin converting enzyme (ACE), 3-hydroxy-3-methylglutaryl-coenzyme A reductase (HMGCR), renin (REN), and prothrombin (Coagulation factor II, FII). In addition, 123 membrane receptors, such as beta-1 adrenergic receptor (ADBR1), beta-2 adrenergic receptor (ADBR2), muscarinic acetylcholine receptor M1, M2, M3 (ACM1, 2, 3), alpha-1 adrenergic receptor (ADAR1), type-1 angiotensin II receptor (AGTR1), and 81 ionic channels, such as voltage-dependent N-type calcium channel subunit alpha-1 (CAC1) are also included in these 984 target proteins.

Statistical analysis was performed on the number of drugs in the different development phases according to their therapeutic targets. The corresponding targets were ranked according to the total number of drugs, and the top 20 targets were listed in **Figure 9**. Not surprisingly, we can easily find the well-known therapeutic targets with anti-cardiovascular disease drugs in the market. For example, 12 approved drugs act on beta-1 adrenergic receptor to decrease heart rate, myocardia contraction and conduction to treat hypertension, heart failure, shock, and other complications; several approved drugs act on potassium, sodium, and calcium channels to treat stroke, cerebral hemorrhage, coronary artery disease, heart failure, hypertension, arrhythmias, and other disorders; some well-known anti-hypertension agents act on targets in renin-angiotensin-aldosterone system, such as angiotensin converting enzyme, angiotensin receptor type I, and renin, to treat heart failure and coronary artery disease. Moreover, some relative new targets have attracted more attention recently, with larger percentage of drugs in phase 1 and phase 2 compared with traditional targets, such as Endothelin-1 receptor (EDNRA) and renin (Renin)

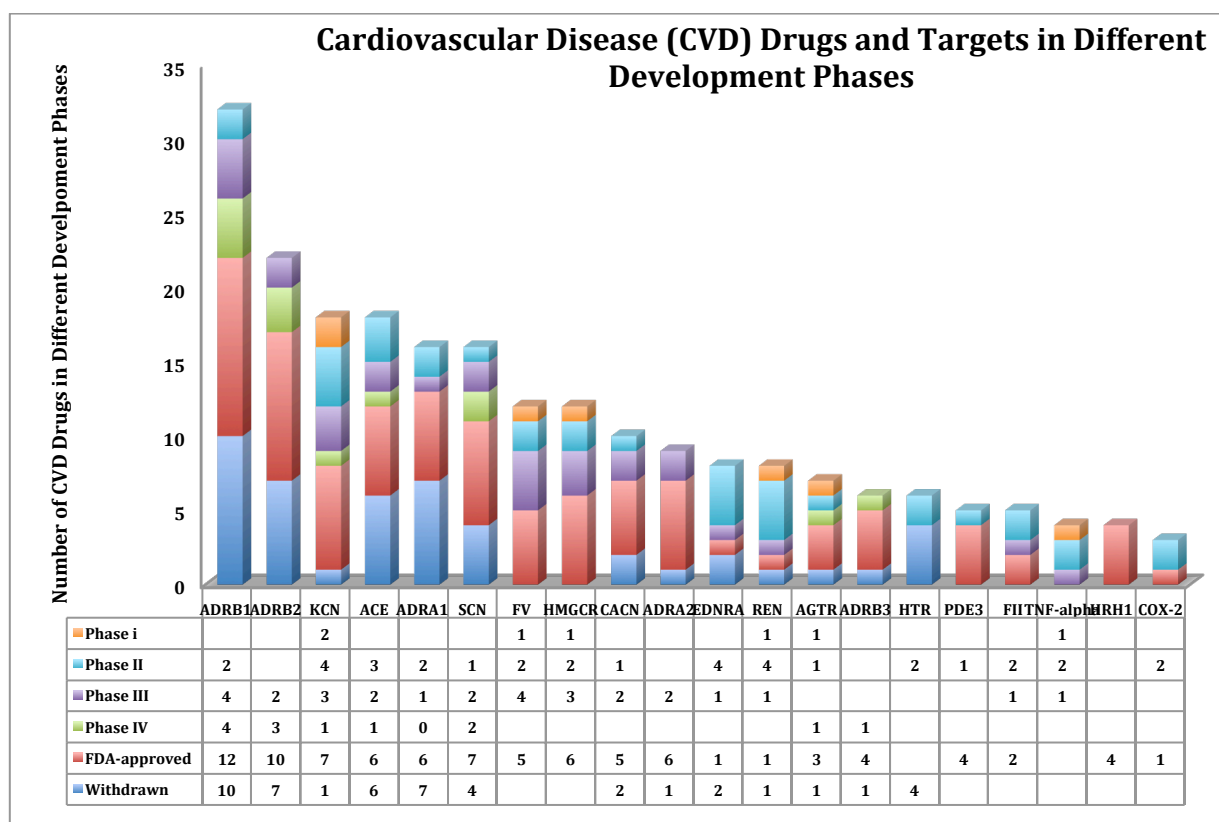


Figure 9. Drugs and Their Targets in Different Development Phases

These approved and clinical trial CVD drugs were classified by different phases, distinguished by distinct colors. The red and blue columns indicate the approved and discontinued CVD drugs, respectively. The orange, light blue, purple and green lines denote clinical trial drugs in phases I, II, II and IV respectively.

Abbreviations: ADRB1, Beta-1 adrenergic receptor; ADRB2, Beta-2 adrenergic receptor; KCN, Potassium channel; ADRA1, Alpha-1 adrenergic receptor; SCN, Sodium Channel; ACE, Angiotensin Converting Enzyme; CACN, Voltage-dependent L-type calcium channel; FV, Coagulation Factor V; HMGCR, 3-hydroxy-3-methylglutaryl-coenzyme A reductase; ADRA2, Alpha-2 adrenergic receptor; EDNRA, Endothelin-1 receptor; REN, Renin; AGTR, Angiotensin II receptor; ADRB3, Beta-3 adrenergic receptor; HTR, serotonin receptor; PDE3, cGMP-inhibited 3',5'-cyclic phosphodiesterase; FII, Coagulation Factor II; TNF-alpha, Tumor necrosis factor alpha; HRH1, Histamine H1 receptor, COX-2, Prostaglandin G/H synthase 2

Interestingly, some targets have a number of drugs that have already been withdrawn from the market or discontinued in the early phase of clinical trials. The ADBR1, ion channels, and ACE are targets with both the strong therapeutic effect and a toxic potential, having almost equal number of approved and withdrawn drugs. For instance, ADBR1 have strong cardiac inotropic effect, which is not only important for its therapeutic effect but also poisonous sometimes for a long time use. However, the cardiovascular disease agents are often used in a long term to control the blood pressure, lipid profile, and plasma glucose level within a normal range in order to reduce the risk of many cardiovascular complications, such as heart failure, heart attack, and stroke. Some long-term side effects that cannot be recognized in the early clinical trial might be found in patients after entering into market. Also, the criteria for the acceptable drug toxicity are different for cardiovascular diseases and some more fetal chronic diseases like cancers. Some toxicity effects that are tolerated for anticancer drugs may not be allowed for anti-CVD agents (**Figure 9**).

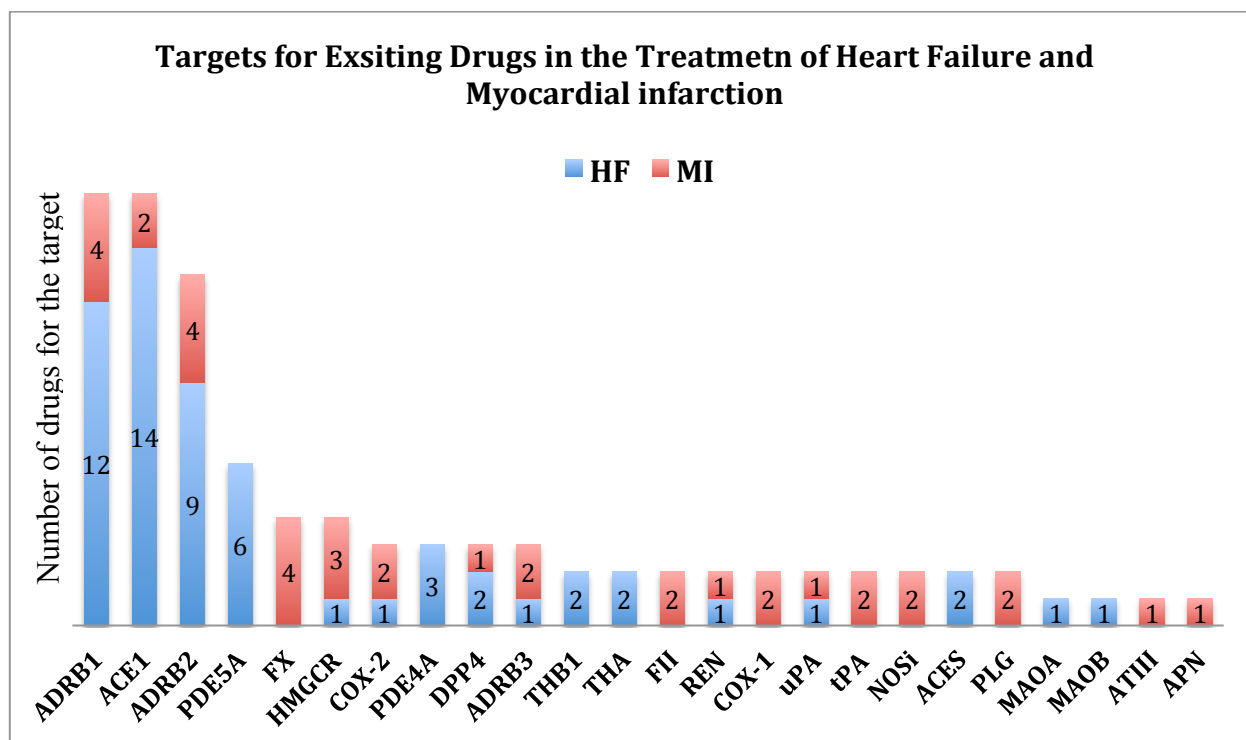


Figure 10. Therapeutic Targets for MI and HF ranked by the number of drugs

These approved and clinical trial drugs were classified by treatment for MI and HF, distinguished by distinct colors. The red columns indicate MI drugs; the blue columns denote HF drugs. The targets are ranked by the total number of drugs for the treatment of two diseases.

Abbreviations: MI, myocardial infarction; HF heart failure; ADBR1, beta-1 adrenergic receptor; ACE1, angiotensin converting enzyme1; ADBR2, beta-2 adrenergic receptor; PDE5A, cGMP-specific 3', 5'-cyclic phosphodiesterase; FX, coagulation factor X; HMGCR, 3-hydroxy-3-methylglutaryl-coenzyme A reductase; COX-2, Prostaglandin G/H synthase 2; PDE4A, cAMP-specific 3',5'-cyclic phosphodiesterase 4A; DPP4, Dipeptidyl peptidase-4; ADBR3, beta-3 adrenergic receptor; THB1, truncated haemoglobin; THA, Thermosipho africanus; FII, coagulation factor II; REN, renin; COX-1, Prostaglandin G/H synthase 1; uPA, Urokinase-type plasminogen activator; tPA, Tissue-type plasminogen activator; NOSi, Nitric oxide synthase, inducible; ACES, Acetylcholinesterase; PLG, Plasminogen receptor; MAOB, Amine oxidase [flavin-containing] B; MAOA, Amine oxidase [flavin-containing] A; ATIII, Antithrombin III; APN, Aminopeptidase N

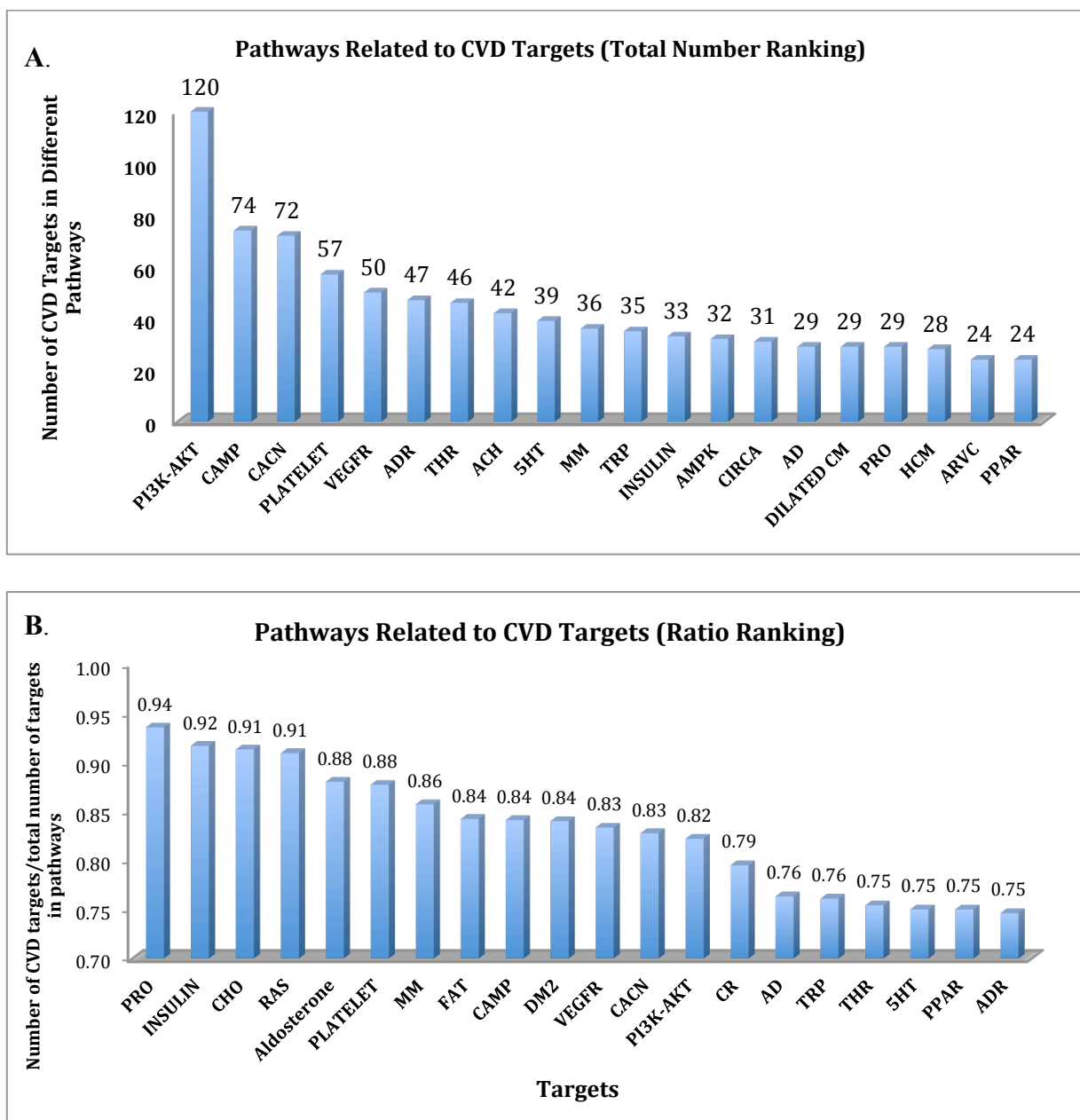


Figure 11. CVD Related Pathways in *CVDPlatform*

The CVD related pathways were plotted according to the number of CVD targets involved. (A) The top 20 pathways with more than 20 CVD targets involved were listed. (B) The number of CVD drugs in a pathway was divided by the total number of the targets in the pathway.

Abbreviation: PI3K-AKT, PI3K-Akt signaling pathway; CAMP, cAMP signaling pathway; CACN, Calcium signaling pathway; PLATELET, Platelet activation; VEGFR, Vascular smooth muscle contraction; ADR, Adrenergic signaling in cardiomyocytes; THR, Thyroid hormone signaling pathway; CHO, Cholinergic synapse; 5HT, Serotonergic synapse; MM, Multiple

myeloma; TRP, Inflammatory mediator regulation of TRP channels; INSULIN, Insulin signaling pathway; AMPK, AMPK signaling pathway; CR, Circadian rhythm; AD, Alzheimer's disease; DILATED CM, Dilated cardiomyopathy; PRO, Protein digestion and absorption; HCM, Hypertrophic cardiomyopathy; ARVC, Arrhythmogenic right ventricular cardiomyopathy; PPAR, Peroxisome proliferator-activated receptor signaling pathway.

In addition, these targets emphasized in the cardiovascular diseases, are also in the top list for the targets involved in the specific indications for SND, such as heart failure and myocardial infarction, like ADBR1, ACE, ADBR2, HMGCR, indicating the reliability to use cardiovascular diseases as a whole to inspect the therapeutic effects and targets for SND (**Figure 10**).

The statistic of CVD targets was also plotted according to the pathways the CVD targets involved (as shown in **Figure 11**). Since some pathways might contain much more targets than other pathways, using the number of CVD therapeutic targets involved in different pathways, as a measurement of correlation with CVD seems not fair. Thus, we used the total number of proteins in a pathway to divide the number of CVD targets involved in that pathway, as a measurement of correlation between that pathway and CVD, as shown in **Figure 11B**. **Figure 11A** shows the top list pathways with more than 20 targets involved. **Figure 11B** shows the top list pathways with a higher ratio of targets involved in the CVD treatment. Two groups of pathways occupy a large percentage of the top list pathways: pathways regulating blood pressure and pathways involved in the ADME of protein, fat, and carbohydrates. Firstly, we found many pathways involved in the regulation of blood pressure were on the top list pathways, such as cholinergic and adrenergic pathway in automatic nervous system (ANS), renin-angiotensin-aldosterone system pathways (RAAS), calcium signaling pathway, and pathways directly acting on heart to control heart rhythm and cardiac muscles. Secondly, pathways that regulate plasma glucose and lipid level play an important role in treatment of CVD, such as protein digestion and

absorption, insulin signaling pathway, fat digestion and absorption, and Peroxisome proliferator-activated receptor (PPAR) signaling pathway. Furthermore, we can see 76% targets in the Alzheimer's disease pathological pathways are also discovered as therapeutic targets for cardiovascular diseases.

3.2 CVDPLATFORM VALIDATION USING POLYPHARMACOLOGY ANALYSIS OF ANTI-CVD DRUGS

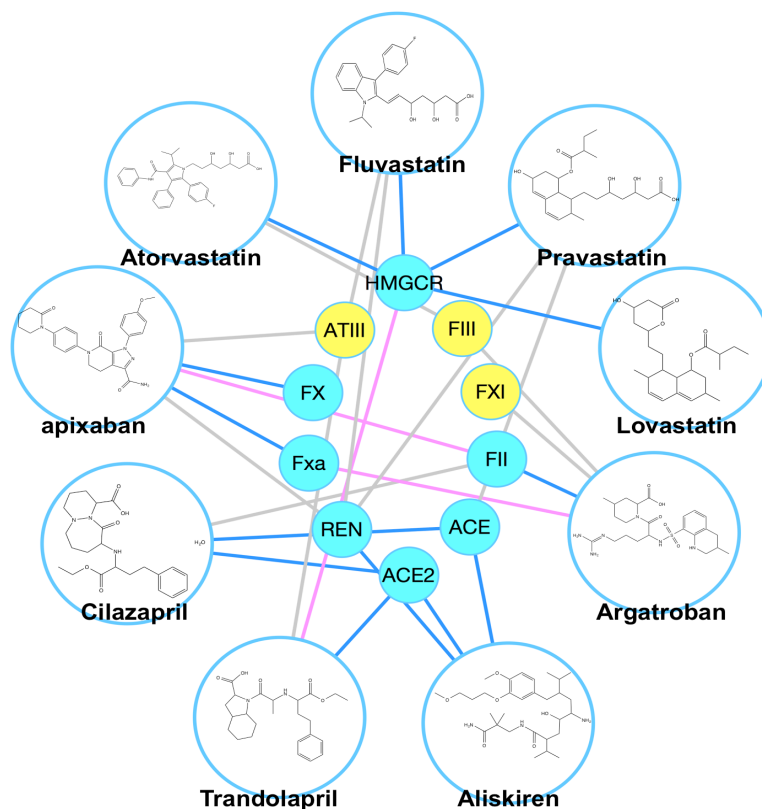


Figure 12. Validation of *CVDPlatform*

Validation of CVD database using polypharmacology analysis of FDA-approved anti-CVD drugs. The large circles (cyan) represent FDA-approved CVD drugs (Atorvastatin, Fluvastatin, Pravastatin, Lovastatin, Cilazapril, Trandolapril, Aliskiren, Argatroban, and Apixaban). Each drug is linked to its predicted targets by edges. Among them, the blue nodes and edges denote the known therapeutic targets for the drugs and their interactions. Yellow nodes represent predicted potential targets without experimental validation and they are linked by cyan and pink edges to their corresponding drugs.

Abbreviation: HMGCR, 3-hydroxy-3-methylglutaryl-coenzyme A reductase; ACE, Angiotensin-converting enzyme; ATIII, Antithrombin-III; FII, coagulation factor II; FIII, coagulation factor III; FX, Coagulation factor X; Fxa, Coagulation factor Xa; FXI, Coagulation factor XI; REN, Renin

As a validation procedure, we used our established computational chemogenomics methods in CVD database to predict the potential targets for 9 FDA-approved drugs, including four HMG CoA reductase (HMGCR) inhibitors (Atorvastatin, Fluvastatin, Pravastatin, and Lovastatin), two angiotensin converting enzyme (ACE) inhibitors (Cilazapril and Trandolapril), a renin (REN) inhibitor (Aliskiren), a prothrombin (FII) antagonist (Argatroban), and a coagulation factor X (FX) inhibitor (Apixaban). The potential target proteins for the nine anti-CVD drugs were predicted and ranked by docking scores. These associations were plotted as a polypharmacological interaction network (**Figure 12**).

Firstly, we compared our predicted drug-target connections against the reported ones. Not surprisingly, the known therapeutic targets for these agents such as HMGCR, ACE, REN, FX, and FII are ranked on the top of the corresponding predicted targets list in our results. For example, HMGCR is the protein ranked the first in the lists of target proteins for Pravastatin, Lovastatin, and Fluvastatin; prothrombin was distinguished from other targets with higher score ranked the first for Argatroban; Aliskiren (renin ranked the first) and Cilazapril (ACE ranked the third) also have their known therapeutic targets easily identified on the top lists. Moreover, our predicted binding affinities for these targets were consistent with the bioactivity data via comparing the docking scores with the experimental K_i or K_d values (**Table 2**). Furthermore, some additional predicted interactions were also validated by bioassays reported in literature or PubChem, indicating the reliability of the HTDocking program in *CVDPlatform* (**Table 2**). In addition, the other predicted associations, though no experimental validation so far, could be clues for the discovery of novel targets and indications of the existing drugs.

Table 2. Comparison of the Experimental Data and the Predicted Results

Target	Drug	Docking Score	Exp pKi	Exp Ki(nM)	Reference/ PubChem ID
Coagulation Factor Xa	Apixaban	8.75	9.09	0.8	J. Med. Chem., (2007) 50:22:5339
Coagulation Factor II	Argatroban	8.04	8.39	4	J. Med. Chem., (2003) 46:17:3612
Coagulation Factor III	Argatroban	7.27	7.40	39	J. Med. Chem., (2003) 46:17:3612
3-Hydroxy-3-Methylglutaryl-Coenzyme A Reductase	Lovastatin	7.52	8.22	6	AID83293
Coagulation Factor Xa	Argatroban	6.26	5.27	5300	AID766528
Angiotensin-Converting Enzyme	Captopril	9.12	8.76	1.7	AID37801
Renin	Captopril	8.98	8.76	1.7	AID198995
Coagulation Factor II	Apixaban	6.54	5.50	3100	AID302354
Cholinesterase	Lovastatin	7.22	5.95	1100	AID1093611
3-Hydroxy-3-Methylglutaryl-Coenzyme A Reductase	Fluvastatin	11.83	IC50=28nM		Bioorg. Med. Chem. Lett., (2005) 15:4:1027
Renin	Aliskiren	6.58	IC50=0.5nM		AID371780
3-Hydroxy-3-Methylglutaryl-Coenzyme A Reductase	Atorvastatin	10.57	IC50=0.227nM		AID625271
3-Hydroxy-3-Methylglutaryl-Coenzyme A Reductase	Pravastatin	8.37	IC50=5.59nM		AID625271
Angiotensin-Converting Enzyme	Trandolapril	8.53	IC50=0.93nM		AID39767
Urokinase-Type Plasminogen Activator Precursor	Fluvastatin	7.69	Potency=56.2nM		AID540303
Glucocorticoid Receptor	Fluvastatin	7.32	Potency=264.8nM		AID720692

The discovery of novel combination therapies, with improved pharmacological therapeutic effects and reduced side effects, is another application of poly-pharmacology analysis for approved drugs on the market [51]. According to clinical studies and literature reports, renin inhibitor (Aliskiren) is often used with angiotensin converting enzyme (ACE) inhibitors (Ramipril, NCT01432106; Lisinopril, NCT00994253; Enalapril, NCT00853658), and / or angiotensin II receptor (AGTR) inhibitor (Valsartan, NCT01432106) to attain enhanced effects on hypertension regulation, heart failure (HF) and coronary diseases control. There are four targets in RAAS: angiotensinogen (AGT), renin, ACE, and angiotensin II receptor type 1 (AGTR). Renin converts angiotensinogen to angiotensin I. Angiotensin I is then catalyzed by ACE to form angiotensin II. Angiotensin II is the most potent compound in the system acting on AGTR to regulate blood pressure. The effect of these four targets can be amplified when they work together to treat disease. So we can also predict the combination use of Aliskiren with Cilazapril or Trandolapril for hypertension treatment. HMGCR inhibitors, like Atorvastatin, are reported to be used in combination with ACE inhibitors (Ramipril, NCT01321255; Enalapril, NCT01271985) and AGTR antagonists in clinical trials to treat some complications in cardiovascular diseases. The combination medication of ACE inhibitors (Cilazapril and Trandolapril) and HMGCR inhibitors (Atorvastatin, Fluvastatin, Pravastatin, and Lovastatin) may reduce blood pressure, LDL and cholesterol level, thus lowering the risk for heart attack and stroke.

3.3 POLYPHARMACOLOGY OF TARGETS OF SND COMPOUNDS

3.3.1 Target Prediction

As shown in **Table 2**, 33 targets related to the therapeutic effect of SND were linked with 31 components by molecular docking. Components deoxyaconitine (4), neoline (15), talatisamine (16), 14-acetyl-talatisamine (18), talatizidine (19), coryneine (20), isoliquiritigenin (31), and glycyrrhetic acid (36) were ruled out due to low affinity to all the candidate proteins. Most candidate target proteins are shared by more than one component. ADRB1, ADRB2, M3AChR (M3 muscarinic acetylcholine receptor), FII, HMGCR (3-hydroxy-3-methylglutaryl-coenzyme A reductase), ACE, and renin can be good examples of potential targets with large number of connected components, 20, 11, 11, 12, 11, 10, and 14 respectively. These potential targets might play a critical role for SND to achieve its therapeutic effects. Actually, only 10 target proteins have just one corresponding component, suggesting a high rate of cross-targets shared by multiple components in SND formulation, which magnifies the possibility for synergistic effect. We built a network for target-compound interaction for SND to investigate the synergistic effect of the SND.

3.3.2. Network construction

A TCM prescription usually contains several herbs. The formula is based on the principle of “Jun-Chen-Zuo-Shi”, also known as “emperor-minister-adjuvant-courier”. “Jun” (emperor)

is mainly applied to treat the primary symptoms of the disease; “Chen” (minister) is used to reinforce the effects of “Jun” or deal with contingent indications; “Zuo” (adjuvant) plays an important role in lessening or eliminating toxic side effects of “Jun” or “Chen” and aids to cure collateral symptoms; “Shi” (courier) assists in transferring or leading other herbs to the target organs or tissues [52]. Unfortunately, the essential components and corresponding targets have not been identified in many formulae including SND, while precise mechanisms remain to be addressed by a molecular approach. We attempted to analyze and interpret the compatibility mechanism of SND formulation through the construction of a target-compound network.

As illustrated in **Figure 13**, the bilateral graphical network incorporated 64 nodes and 178 edges, where the edges encode interaction and the nodes represent potential targets (in squares) or compounds (in circles). The target proteins with smaller sizes, outside the main circle, are only targeted by one herb. Potential targets in the main circle are linked to multiple compounds, and might exert synergistic therapeutic efficacies [53]. To further evaluate the effects of three herbs in the SND formulation, we divided the components by their origin herbs and distinguish them by different colors: 1 to 25 are from AC (in light blue), 26 to 38 are from GU (in fuchsias), 39 and 40 are from ZO (in dark blue).

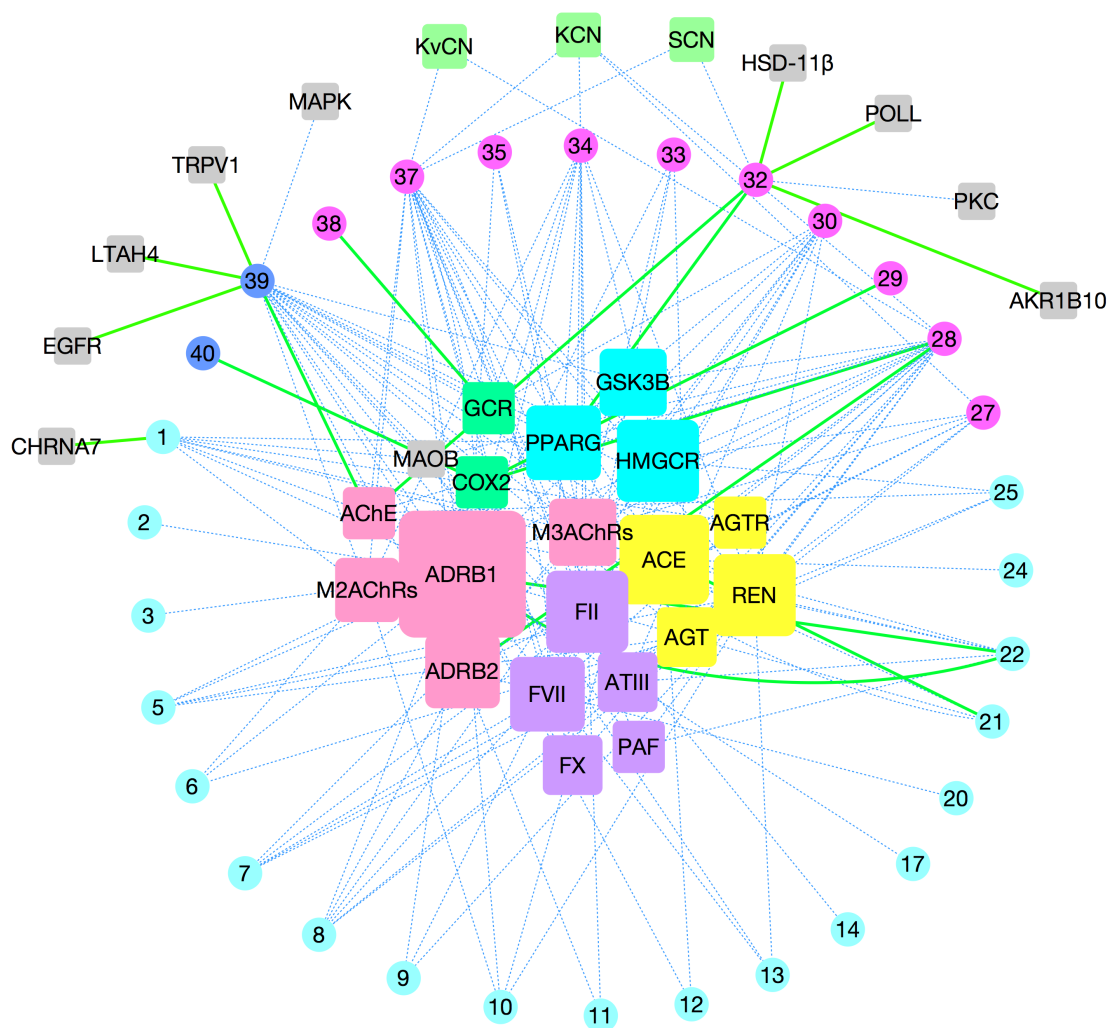


Figure 13. Network for Compound-Target Interaction

Thirty-one compounds were predicted to interact with 33 potential protein targets. The squares represent the targets, while the circles represent the compounds. Different color was applied to represent components from different herbs and potential targets from different physiological system: components from AC in light blue, GU in magenta, ZO in deep blue; targets from RAS system in yellow, autonomic nervous system in rubber red, coagulation system in purple, targets related to lipid metabolism in light blue, and targets relevant to immune and inflammatory process in light green. In addition, the sizes of the targets (squares) refer to the number of interactions with compounds. The edges stand for interactions: blue dashed edges stand for interactions without validation; green solid edges stand for validated interactions.

Abbreviation: HMGCR, 3-hydroxy-3-methylglutaryl-coenzyme A reductase; AChE, Acetyl cholinesterase; ACE, Angiotensin-converting enzyme; AGT, Angiotensinogen; ATIII,

Antithrombin-III; FII, coagulation factor II; FVII, coagulation factor VII; FX, Coagulation factor X; KCN, Potassium channel; KvCN, Potassium voltage-gated channel; PAF, Platelet activating factor; SCN, Sodium channel; M3AChR, M3 muscarinic acetylcholine receptor; M2AChR, M2 muscarinic acetylcholine receptor; ADRB1, Beta1 adrenergic receptor; ADRB2, Beta2 adrenergic receptor; PPARG, Peroxisome proliferator-activated receptor gamma; GSK3B, Glycogen synthase kinase 3 beta; GCR, Glucocorticoid receptor; COX-2, Prostaglandin G/H synthase 2.

3.3.3 Select representative active constituents for each herb

In order to study the specific molecular mechanism, we needed to narrow down the compounds into three representative ones for bioassay tests. We selected liquiritin, 6-gingerol, and aconitine as active constituents to represent licorice, ginger, and aconitum respectively, according to three criteria: first, the corresponding targets for the three constituents can represent most targets of all the ingredients, especially the important targets with therapeutic effect we used in validation, such as beta-1 adrenergic receptor; second, the three constituents need to be tested, identified, and isolated from herbs extract previously, so that they are available to be obtained and used in further experimental validation. We then constructed a network for the interaction between three selected compounds (liquiritin, 6-gingerol, and aconitine) and their corresponding predicted targets, as shown in **Figure 7**.

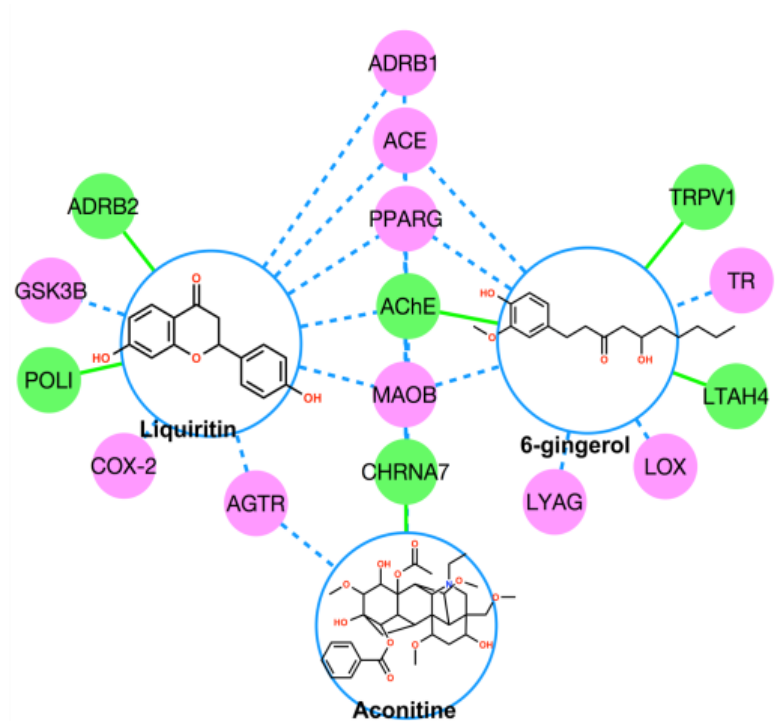


Figure 14. Interaction Network of Representative Compounds and Their Targets

The large circles (cyan) with chemical structures represent the three representative constituents (Liquiritin, 6-gingerol, and Aconitine) we selected for each of three herbs (Liquorice, Ginger, and Aconitium) in Sini Decoction. Each constituent is linked to its predicted targets, represented by nodes. Among them, the green nodes and edges denote the known targets of the compounds. Pink nodes represent new predicted targets without validation and they are linked to their corresponding constituents by blue dashed edges.

Abbreviation: HMGCR, 3-hydroxy-3-methylglutaryl-coenzyme A reductase; AChE, Acetyl cholinesterase; ACE, Angiotensin-converting enzyme; AGTR, Angiotensin II receptor; ATIII, Antithrombin-III; ADRB1, Beta1 adrenergic receptor; ADRB2, Beta2 adrenergic receptor; PPARG, Peroxisome proliferator-activated receptor gamma; GSK3B, Glycogen synthase kinase 3 beta; COX-2, Prostaglandin G/H synthase 2.

3.3.4 Detailed Docking Information for Selected Constituents and Targets

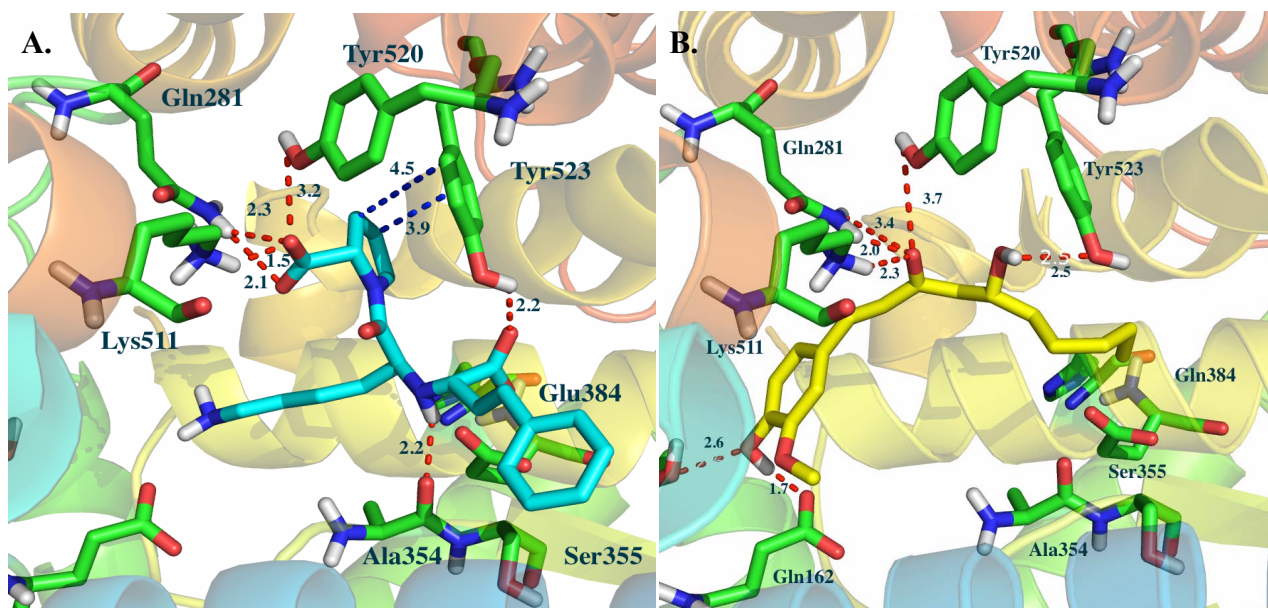


Figure 15. Detailed Interaction Mode of ACE with Lisinopril and 6-Gingerol

Interaction of ACE (angiotensin converting enzyme) (PDB Entry: 1O86) [41] with lisinopril (ACE inhibitor) (A) in co-crystal structure and with 6-gingerol (B) predicted by molecular docking. Hydrogen-bond bindings are indicated by red dashed line with measured distance, and some hydrophobic interactions (especially the π - π interactions) are displayed as dark blue dashed line with measured distance. Residues are shown in green, Lisinopril in blue, and 6-gingerol in yellow.

The interaction mode of 6-gingerol with ACE, comparing to ACE with ACE inhibitor Lisinopril is shown in **Figure 15**. We can see that Lisinopril has a carboxylic acid and 6-gingerol has a ketone, they are located in a position close to several hydrogen donors from three amine acids residues: Tyr520, Gln281, and Lys511. Both these two compounds form four hydrogen bonds with these residues at a range of distance from 1.5Å to 3.2Å, and from 2.0Å to 3.7Å, respectively. Additionally, Lisinopril forms two hydrogen bonds with the hydroxyl in Tyr523

and the ketone in Ala354, and have a π - π interaction with Tyr523, contributing to its high binding affinity ($K_i=0.27\text{nM}$). On the other hand, 6-gingerol has two complementary hydrogen bonds with Glu162 and Tyr523 in a distance of 1.7\AA and 2.5\AA respectively, indicating a similar binding affinity between ACE and Lisinopril [54].

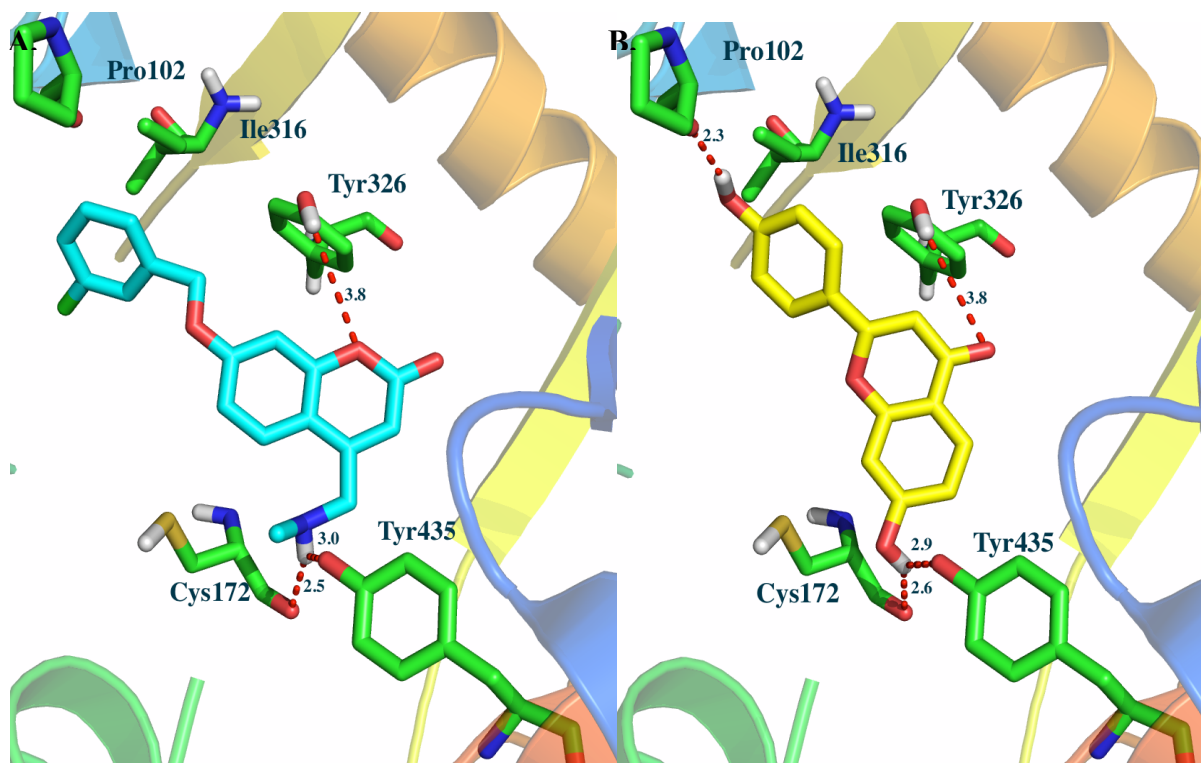


Figure 16. Detailed Interaction Mode of MAOB with Coumarin Analog and Liquiritin

Interaction information of MAOB (monoamine oxidase B) (PDB Entry: 2V61) [55] with coumarin analog (A) in co-crystal structure and with liquiritin (B) predicted by molecular docking. Hydrogen-bond bindings are indicated as red dashed line with measured distance, and some hydrophobic interactions are displayed as dark blue dashed line with measured distance. Residues are represented in green, liquiritin in yellow, and coumarin analog in blue.

As shown in **Figure 16**, liquiritin and coumarin analog was located into the same pocket with the similar poses and interact with similar residues. Both liquiritin and coumarin analog form three hydrogen bonds with the hydroxyl groups in residue Tyr326, the aldehyde groups in Tyr435 and Cys172. Additionally, Liquiritin forms another hydrogen bond with Pro102, which may enhance its binding affinity.

We can see from **Figure 17**, mevastatin, known as HMGCR inhibitor, interacts with residues in both chain A and chain B in the HMGCR tetramer crystal structure (PDB Entry: 1HW8). When being positioned into the same pocket as mevastatin, aconitine has a similar binding pose and interacts with similar residues with mevastatin, such as residues Glu559, Asn755, His752, Leu853, and Lys735 in chain A, and residues Ser661, Lys691, Ser684, Asp690, and Arg590 in chain B. However, 6-gingerol and liquiritin, which have a smaller molecular size, cannot occupy the large pocket between two chains, and they mainly interact with residues in chain B, such as Ser661, Lys691, Ser684, Asp690, and Arg590, while merely forming a few hydrophobic interactions with chain A. Thus in accordance with less interaction with chain A, 6-gingerol and liquiritin may have lower binding affinity or less chance to interact with HMGCR compared with mevastatin and aconitine.

To be specific, both 6-gingerol and liquiritin form three hydrogen bonds respectively with residues Asp690, Ser661, and Arg590 in chain B; the phenolic hydroxyl in liquiritin also forms a hydrogen bond with Ser684. The binding modes of Mevastatin and Aconitine are similar with each other. Both of them formed hydrogen bonds with Lys735, Arg590, Ser661, and Leu853, but they had slight difference: the distances for Aconitine to form hydrogen bonds with Ser661 (2.4Å) and Arg590 (2.7Å) are shorter than Mevastatin (3.8Å and 3.9Å), while the

distance between Aconitine (1.7Å) and Lys735 is farther than Mevastatin (3.3Å), indicating that Aconitine is closer to chain B than Mevastatin. Mevastatin and Aconitine had hydrophobic interaction with similar residues, such as Lys692 in chain A. However, the interaction mode for Mevastatin also shown its identical characteristic, which distinguished Mevastatin from other Aconitine. Mevastatin formed two hydrogen bonds with the carboxylic acid in residues Ser684 (in chain B) and Glu559 (in chain A) respectively, and formed other hydrogen bonds with amide in Asn755, and guanidine in Arg690. In contrast, Aconitine could not have hydrogen binding with Asn755, Arg690, Ser684, and had less chance to form one hydrogen bond with the carboxylic acid in Glu559 with a long distance (4.4Å). However, Aconitine might form three additional hydrogen bonds with Arg590 with a distance of 3.4Å, 2.3Å, and 2.0Å, while Mevastatin did not.

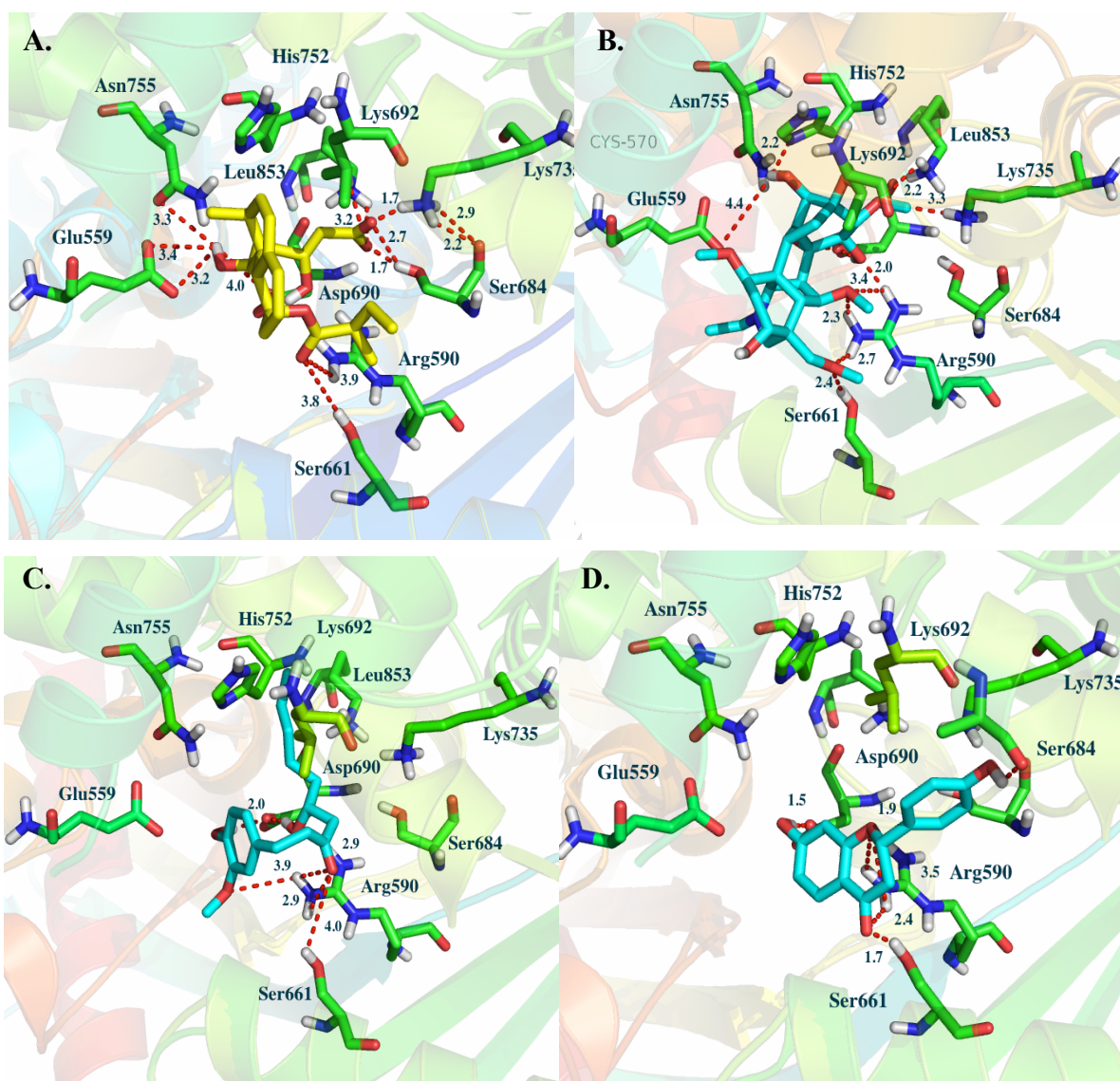


Figure 17. Interaction Mode of HMGCRC with Mevastatin and Constituents in SND

Interaction information of HMGCRC (3-hydroxy-3-methylglutaryl-coenzyme A reductase) (PDB Entry: 1HW8) [56] with Mevastatin (A) in co-crystal structure, and with aconitine (B), 6-gingerol (C), and liquiritin (D) predicted by molecular docking. Hydrogen-bond bindings are indicated by red dashed line with measured distance, and some hydrophobic interactions are displayed as dark blue dashed line with measured distance. Residues are represented in green, mevastatin in yellow, liquiritin, 6-gingerol, and aconitine in blue.

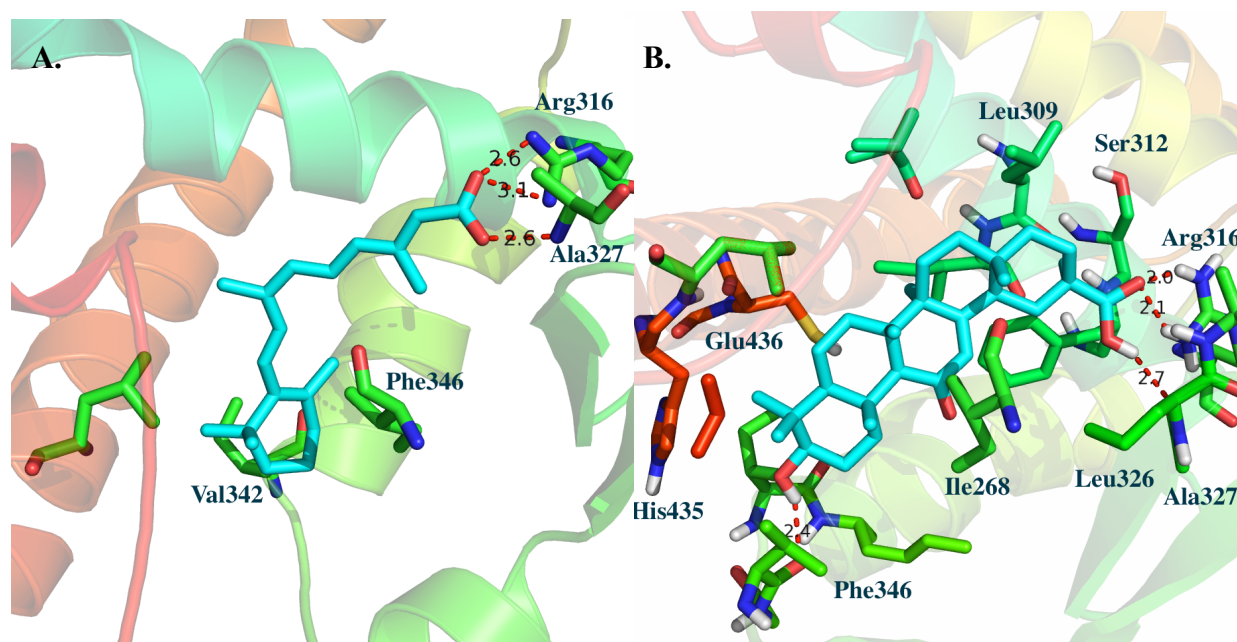


Figure 18. Interaction Mode of PPARG with Retinoic Acid and Glycyrrhetic Acid

Interaction information of PPARG (PDB Entry: 1FM6) [57] with (9cis)-retinoic acid (A) in co-crystal structure and with glycyrrhetic acid (B) predicted by molecular docking. Hydrogen-bond bindings are indicated as red dashed line with measured distance, and some hydrophobic interactions are displayed as dark blue dashed line with measured distance.

We can see from Figure 18, glycyrrhinic acid (B) (2.0Å, 2.1Å, and 2.7Å) formed three same hydrogen bindings with residues Arg316 and Ala327 within a distance of 2.7 Å, which are similar as the co-crystal ligand (9cis)-retinoic acid (A) (2.6Å, 2.6Å, and 3.1Å). In contrast to (9cis)-retinoic acid, glycyrrhinic acid also forms an additional hydrogen bond with Phe346 with a distance of 2.4 Å, indicating a higher binding affinity. Moreover, glycyrrhinic acid fits into the same pocket with similar poses as (9cis)-retinoic acid, and forms hydrophobic interactions with almost the identical residues around them, such as Val342, Phe346, Ile 268, Leu326, Leu309, and Gly436.

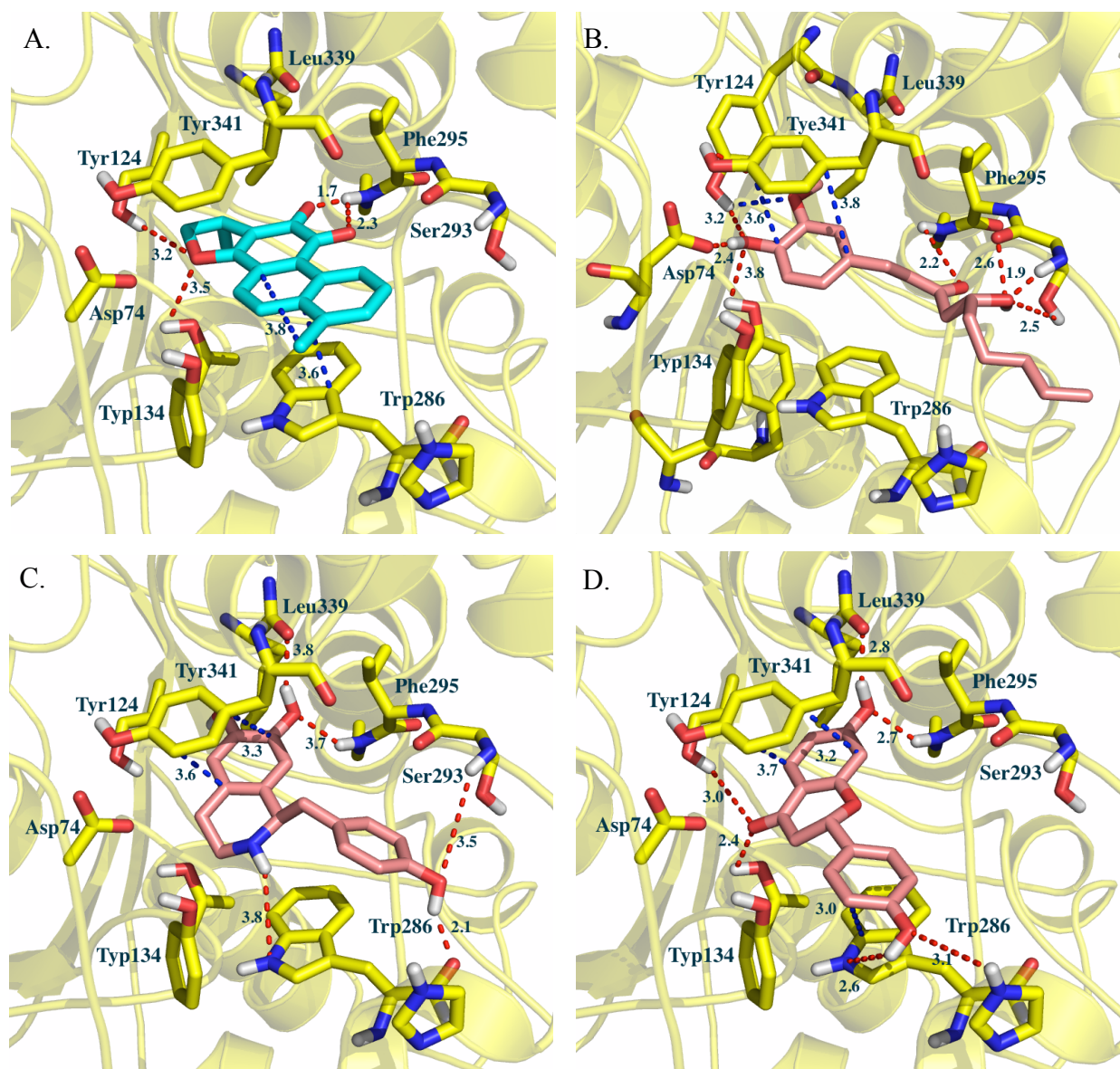


Figure 19. Interaction Mode of AChE with Dihydrotanshinone I and Constituents in SND

Interaction information of AChE (Acetylcholinesterase) (PDB Entry: 4M0E) with Dihydrotanshinone I (A, in blue) in co-crystal structure, and with 6-gingerol (B, in red), higenamine (C, in red), and liquiritin (D, in red) predicted molecular docking. Hydrogen bonds are indicated as red dashed line with measured distance, and some hydrophobic interactions are displayed as dark blue dashed line with measured distance.

As shown in **Figure 19**, 6-gingerol, liquiritin and higenamine fitted into the same pocket with similar poses compared with Dihydrotanshinone I in the co-crystal structure. The benzoyl ring in 6-gingerol, the aromatic rings in liquiritin and higenamine formed π - π interactions with benzoyl ring in residue Tyr341 in AChE within a distance of 4 Å. This observation was in agreement with interaction mode between Dihydrotanshinone I and AChE in the co-crystal structure (PDB Entry: 4M0E). Additionally, Liquiritin also formed another π - π interaction with residue Trp286 in AChE, in accordance with π - π interaction of Dihydrotanshinone I and Trp286 in co-crystal structure. Moreover, liquiritin, as well as 6-gingerol formed hydrogen bonds with residues Phe295, Tyr124, and Tyr134, similar to Dihydrotanshinone I in the co-crystal structure. Liquiritin formed three additional hydrogen interactions with Trp286, Trp285 and Leu339 in AChE in a distance of 2.3 Å and 3.0 Å individually. Although higenamine did not form the π - π interaction with Trp286 and some hydrogen bonds with Tyr 341 and Tyr124 as the ligand in co-crystal structure did, it formed two additional hydrogen interactions with carboxyl groups in Leu339, Trp285, and Trp286 respectively to recoup the potential binding affinity. As for 6-gingerol, its hydroxyl group and ketone group interacted with Phe295 and Ser293 respectively, forming two hydrogen bonds, to compensate the loss of π - π interaction with Trp286.

3.3.5 Homology Model and Docking of Beta-1 Adrenergic Receptor

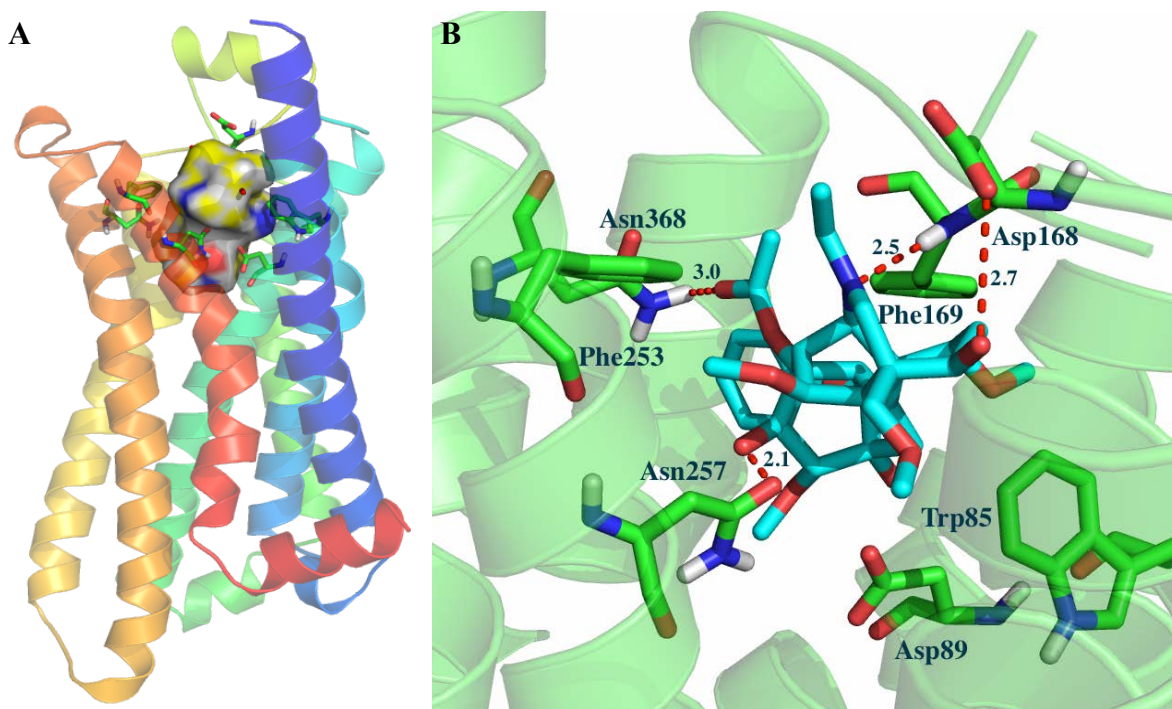


Figure 20. Homology Modeling and Docking Analysis of Beta-1 Adrenergic Receptor.

(A) Homology model for beta-1 adrenergic receptor and the binding site we defined by the key residues in reports. (B) Detailed interaction information for docking analysis for aconitine and beta-1 adrenergic receptor.

Since ADBR1 has no available crystal structure, we built homology model for human beta-1 adrenergic receptor based on the crystal structure of human beta-2 adrenergic receptor (PDB Entry: 2R4R) co-crystal structure with 65% sequence similarity (Shown in **Figure.20A**). The pocket is defined according to the key residues in literature reports as shown in **Figure 20A**. The detailed docking mode is shown in **Figure 20B** that the ketone and amide in aconitine can form hydrogen bonds with the amide in Asn368 and Phe169 respectively. The hydroxy groups in

aconitine can also form hydrogen binding with residues Asn257, Asp168, and Asp89 respectively. Hydrophobic interactions are also formed between aconitine and residues Phe253 and Trp85 in beta-1 adrenergic receptor.

3.4 EXPERIMENTAL VALIDATION

3.4.1 The Effects of Drugs on Heart Failure

3.4.1.1 Effect of SND on Normal Heart Function Measured by Hemodynamic Index

Table 3. Effect of SND on Normal Rats Measured by Hemodynamic Index

		Before Drug Administration	After SND administration
SBP	mmHg	101.9±23.0	119.8±20.2**
DBP	mmHg	84.7±18.0	102.1±16.7**
MBP	mmHg	93.8±20.4	111.6±18.4**
HR	bpm	387±21	399±9*
LVSP	mmHg	137.2±9.2	154.4±12.2
LVEDP	mmHg	9.1±5.6	9.5±5.7
+dp/dt_{max}	mmHg/s	4952.1±596.0	5902.8±511.6*

Table 4. Effect of Aconitine on Normal Rats Measured by Hemodynamic Index

		Before Drug Administration	After AC (10µg/kg) Administration
SBP	mmHg	96.7±11.4	112.7±10.5**
DBP	mmHg	67.5±10.4	82.7±10.4**
MBP	mmHg	80.1±11.1	94.9±10.0**
HR	bpm	388±47	412±57*
LVSP	mmHg	108.6±6.6	121.5±6.2*
LVEDP	mmHg	8.9±3.0	7.6±3.0*
+dp/dt_{max}	mmHg/s	3473.1±367.4	4078.1±402.0*

SBP, systolic blood pressure; DBP, diastolic blood pressure; medium blood pressure; HR, heart rate; LVEDP, left ventricular end-diastolic pressure; LVSP, left ventricular systolic pressure; $+dp/dt_{\max}$, the maximum rate of change of ventricular systolic Values; AC, aconitine. Data shows as mean \pm SD, n=5, * p<0.05, ** p<0.01

We assessed the effect of SND and aconitine on normal heart function on rats using the hemodynamic parameters as measurements. As shown in Table 3, treatment with SND resulted in a significant improvement in normal heart function, as reflected by an increase of left ventricular systolic (LVSP, from 137.2 ± 9.2 to 154.4 ± 12.2) and end-diastolic pressures (LVEDP, from 9.1 ± 5.6 to 9.5 ± 5.7) and heart rate (HR, from 387 ± 21 to 399 ± 9), systolic blood pressure (SBP, from 101.9 ± 23.0 to 119.8 ± 20.2), diastolic blood pressure (DBP, from 84.7 ± 18.0 to 102.1 ± 16.7), maximal rate of pressure development ($+dp/dt$, from 4952.1 ± 596.0 to 5902.8 ± 511.6). We further evaluated the effect of aconitine (as an constituents we predicted to be representative and active in aconitum) on normal heart function on rats. As Table 3 shown, we observed almost the same cardio inotropic effect on rats treated with aconitine as on rats treated with SND, with an dramatic increase in the hemodynamic indexes (LVSP, from 108.6 ± 6.6 to 121.5 ± 6.2 ; SBP, from 96.7 ± 11.4 to 112.7 ± 10.5 ; DBP, from 67.5 ± 10.4 to 82.7 ± 10.4 ; MBP, 80.1 ± 11.1 to 94.9 ± 10.0 ; HR, from 388 ± 47 to 412 ± 57 ; $+dp/dt$, from 3473.1 ± 367.4 to 4078.1 ± 402.0), merely with trifling discrepancy in HR (from 388 ± 47 to 412 ± 57). Our results match results the previous studies focus on SND, and validated that aconitine have similar effect on heart function with SND, showing the rationality of choosing aconitine as the constituents to represent AC.

3.4.1.2 Echocardiographic Assessment

We examined the systolic function in sham operated and HF rats compared to HF rats treated with SND, using echocardiography. As shown in **Figure 21**, two-dimensional M-mode echocardiography in rat models with sham operation, HF and drugs-treated groups showing evidence of cardiac failure with chamber dilation in HF rat. Drug administration prevented the development of chamber dilatation in HF rats. This result shown that the HF model was successfully established, and treatment with SND in HF rats resulted in a significant improvement in left ventricle (LV) systolic function.

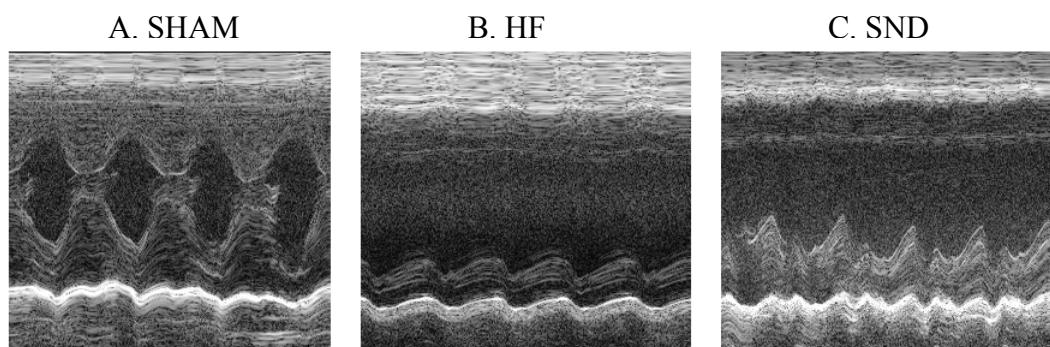


Figure 21. Echocardiography in HF Rats with Sham Operation, HF, and Drug

The summary data for echocardiographic measurements for HF models was shown in **Table 5** and **Table 6**, depicting a dramatic decline in ejection fraction, fractional shortening, and stroke volume in HF models compared with sham operation group. However, these reductions were significant improved in HF rats treated with SND at 21 days of follow-up. Moreover, the notably raised left ventricular volume and diameters in systole and diastole detected in HF models were also compromised by the treatment with SND. The results indicated that the HF model was successfully established and SND treatment had therapeutic effects on the established HF models.

Table 5. Effect of SND on HF Model Measured by Echocardiographic Data

	SHAM	HF	SND+HF
LVIDs (mm)	2.68±0.90	8.52±0.51 [*]	7.82±0.59
LVIDd (mm)	6.45±0.67	9.86±0.55 [*]	9.54±0.70
LVESV (mL)	30.38±20.61	397.60±52.93 [*]	329.50±57.91
LVEDV (mL)	214.36±50.25	549.72±66.78 [*]	511.90±87.93
EF (%)	86.98±6.89	27.73±1.64 [*]	35.58±4.27 [▲]
FS (%)	59.23±10.29	13.68±0.86 [*]	18.03±2.47 [▲]

^{*}*p*<0.05 comparing HF and sham animals,

[▲]*p*<0.05 comparing drug treatment and HF animals.

LVEDV, left ventricular end-diastolic volume; LVESV, left ventricular end-systolic volume; LVIDd, left ventricular internal diameter in diastole; LVIDs, left ventricular internal diameter in systole; EF, ejection fraction; FS, fractional shortening; SV, stroke volume; HR, heart rate; HF, heart failure; MI, myocardial infarction.

Sham, sham operations, Sham surgery is a faked surgical intervention that omits the step thought to be therapeutically necessary. It is an important scientific control that isolates the specific effects of the treatment as opposed to the incidental effects caused by anesthesia, the incisional trauma, pre- and post-operative care.

Data are shown as mean ± S.D.

3.4.1.3 Effects of Drugs on MASSON

The HE-stained images of left ventricular tissue were shown in **Figure 22**, where cardiomyocytes in the sham group were orderly arranged, and the nuclei were lightly stained. Thickening and lengthening of myocardial fibers could be observed in model group.

Cardiomyocyte hypertrophy and cellular degeneration significantly improved in the different drug groups in contrast with those in the model group.

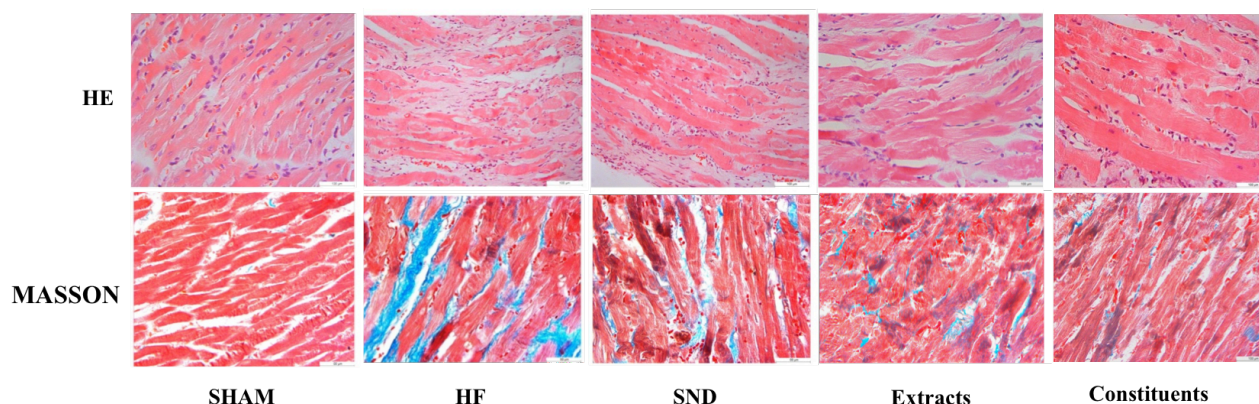


Figure 22. Effects of Drugs on MASSON and HE Stained Results in HF Rats

For HE stain, Hematoxylin and eosin stain is one of the principal stains in histology. Hematoxylin is a dark blue or violet stain that is basic and positive, binding to basophilic substances, coloring DNA/RNA (nuclei of cells), keratohyalin granules, and calcified material. Eosin is a red or pink stain that is acidic and negative, which binds to acidophilic substances, such as proteins, and colors them in various shades of red, pink and orange. For Masson's trichrome staining, a three-color staining protocol used in histology: red color represents keratin and muscle fibers, blue or green color represents collagen and bone, light red or pink stands for cytoplasm, and dark brown to black stands for cell nuclei.

3.4.2 The Effect of Liquiritin on Arrhythmia Induced by Aconitine

The typical electrocardiograms of normal ECG (A), premature beats (B), ventricular tachycardia (C) and cardiac arrest (D) are shown in **Figure 23**. **Table 7 (Figure 25)** shows the time of the occurrence of premature beats, ventricular tachycardia and cardiac arrest, they are 6.60 ± 1.88 min, 7.82 ± 2.42 min, and 14.33 ± 2.60 min respectively in group A, and 8.20 ± 2.06 min, 11.36 ± 2.46 min, and 25.28 ± 3.51 min in group B, indicating that the use of 4 mg/kg Liquiritin

could significantly delay the time for occurrence of premature beats, ventricular tachycardia and cardiac arrest induced by aconitine (10 μ g/ml in a speed of 0.1ml/min, i.v.). Calculated with the time and the concentration of the aconitine, the dosages of aconitine, under which could lead to premature beats, ventricular tachycardia and cardiac arrest are shown in **Table 7 (Figure 25)**, 21.30 \pm 4.72 μ g/kg, 25.19 \pm 6.26 μ g/kg, and 46.72 \pm 6.60 μ g/kg in group A, and 31.41 \pm 7.85 μ g/kg, 43.42 \pm 8.90 μ g/kg, and 97.72 \pm 18.96 μ g/kg in group B. The dosages of aconitine which causes premature beats, ventricular tachycardias and cardiac arrest interventions with Liquiritin are nearly two times than that in group A. It is supposed that the Liquiritin could probably ease the arrhythmia caused by aconitine, and thus reduce the toxicity of aconitine. (**Table 8 and Figure 24**)

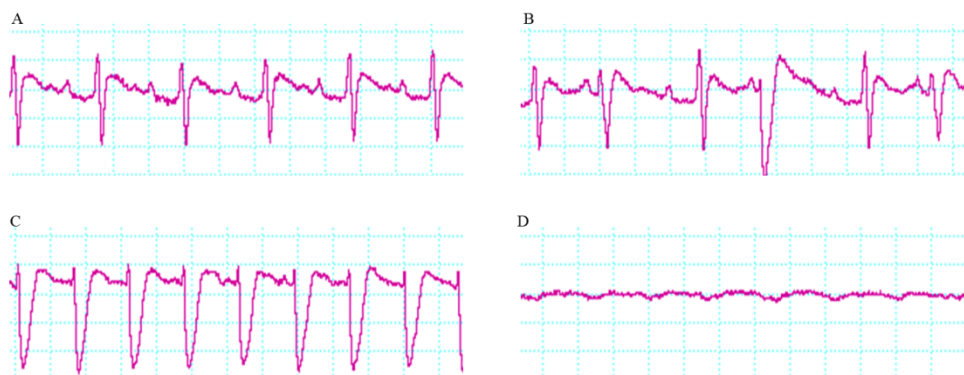


Figure 23. Typical ECG of Normal condition, Premature Beats, Ventricular Tachycardias, and Cardiac Arrest

Table 6. The Time of Premature Beats, Ventricular Tachycardia, and Cardiac Arrest

	Aconitine	Aconitine+ 4 mg/kg Liquiritin
Premature Beats	6.60 \pm 1.88 Min	8.20 \pm 2.06 Min
Ventricular Tachycardia	7.82 \pm 2.42 Min	11.36 \pm 2.46* Min
Cardiac Arrest	14.33 \pm 2.60 Min	25.28 \pm 3.51* Min

* p < 0.05 vs group aconitine

Table 7. The Dosage of Aconitine under occurrence of Premature Beats, Ventricular Tachycardia, and Cardiac Arrest

	Aconitine	Aconitine+ 4 mg/kg Liquiritin
Premature Beats	21.30±4.72 µg/kg	31.41±7.85* µg/kg
Ventricular Tachycardia	25.19±6.26 µg/kg	43.42±8.90* µg/kg
Cardiac Arrest	46.72±6.60 µg/kg	97.72±18.96** µg/kg

* p <0.05, ** p <0.01 vs group aconitine

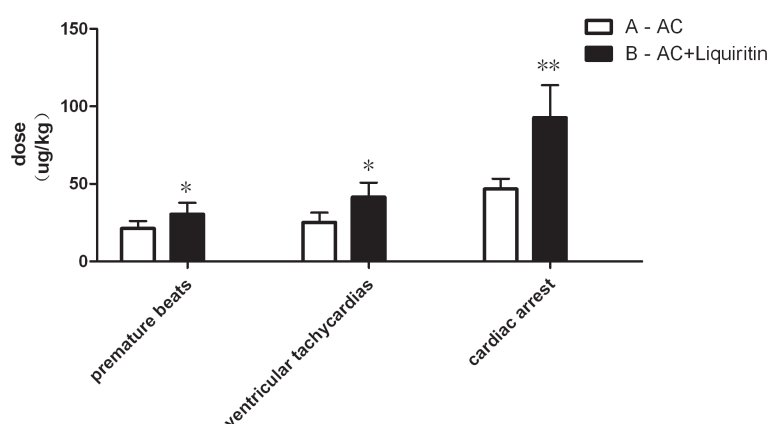


Figure 24. The dosage of aconitine under the occurrence of premature beats, ventricular tachycardia and cardiac arrest

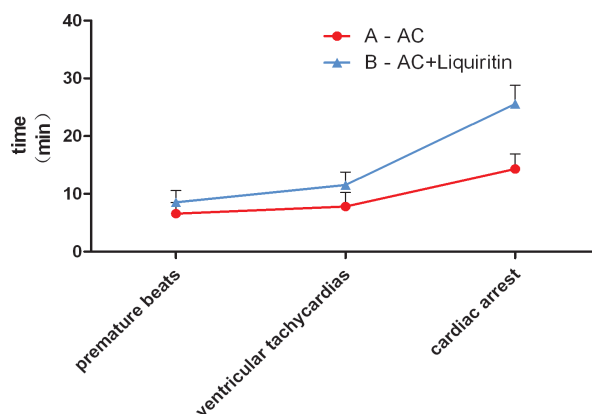


Figure 25. The occurrence time of premature beats, ventricular tachycardia and cardiac arrest

3.4.3 The Effect of 6-Gingerol And Aconitine on Heart Function

We assessed the effect of aconitine combined with 6-gingerol on heart function compared with aconitine alone by hemodynamic measurements. As shown in **Table 9** treatment with aconitine resulted in a significant improvement in heart function, as reflected in an increase of left ventricular systolic (LVSP) and end-diastolic pressures (LVEDP) and heart rate (HR), systolic blood pressure (SBP), diastolic blood pressure (DBP), maximal rate of pressure development (+dp/dt). Combined with 6-gingerol (aconitine: 6-gingerol= 1:7), the inotropic cardiac effect of aconitine was further enhanced with significant raise in blood pressure (LVSP, from 121.5 ± 6.2 to 140.0 ± 12.4 ; LVEDP, from 7.6 ± 3.0 to 9.3 ± 3.3 ; SBP, from 112.7 ± 10.5 to 113.6 ± 12.8 ; DBP, from 82.7 ± 10.4 to 92.2 ± 11.8 ; MBP, 94.9 ± 10.0 to 103.0 ± 11.4) and maximal rate of pressure development (+dp/dt, from 4078.1 ± 402.0 to 6080.2 ± 891.2). Interestingly, the increase in the heart rate caused by aconitine was attenuated by the addition of 6-gingerol, from 412 ± 57 to 386 ± 24 .

Table 8. Summary of Hemodynamic Data with Combined Use of Aconitine and 6-gingerol

	AC 10ug/kg		AC 10ug/kg+6-gingerol 70ug/kg	
	Before administration	After administration	Before administration	After administration
SBP (mmHg)	96.7±11.4	112.7±10.5**	97.1±9.4	113.6±12.8**
DBP (mmHg)	67.5±10.4	82.7±10.4**	74.3±6.7	92.2±11.8**
MBP (mmHg)	80.1±11.1	94.9±10.0**	85.7±7.2	103.0±11.4**
HR (bpm)	388±47	412±57*	365±35	386±24
LVSP (bpm)	108.6±6.6	121.5±6.2*	123.9±13.4	140.0±12.4*
LVEDP (bpm)	8.9±3.0	7.6±3.0*	6.8±6.2	9.3±3.3
+dp/dt _{max} (mmHg/s)	3473.1±367.4	4078.1±402.0*	5274.4±661.8	6080.2±891.2*

	AC 5ug/kg		AC 5ug/kg+6-gingerol 35ug/kg	
	Before administration	After administration	Before administration	After administration
SBP (mmHg)	101.8±16.2	109.2±18.0	100.4±10.0	115.9±22.7**
DBP (mmHg)	76.5±23.0	84.2±22.1	73.1±9.2	86.9±12.0*
MBP (mmHg)	87.1±20.6	94.9±20.3	86.5±9.6	100.9±15.8*
HR (bpm)	395±43	405±16	358±46	368±30
LVSP (bpm)	115.3±9.6	121.6±8.9	119.1±16.3	135.7±18.0
LVEDP (bpm)	7.5±1.1	7.4±1.0	3.8±6.2	7.3±4.2
+dp/dt _{max} (mmHg/s)	3879.7±515.0	4156.7±301.5	4948.3±592.6	5529.2±535.0**

SBP, systolic blood pressure; DBP, diastolic blood pressure; medium blood pressure; HR, heart rate; LVEDP, left ventricular end-diastolic pressure; LVSP, left ventricular systolic pressure; +dp/dt_{max}, the maximum rate of change of ventricular systolic Values; AC, aconitine.

Data shows as mean ± SD, n=3, * p<0.05, ** p<0.01

3.4.4 The Validation of Predicted Targets with Constituents in SND

3.4.4.1 The Validation of Aconitine to Beta-1 Adrenergic Receptor

By administrating simultaneously with propranolol, we can validate whether the propranolol, a long-known beta-1 adrenergic antagonist, can block the cardiac inotropic effect caused by administration of aconitine. As shown in **Figure 26**, the increase in HR and $\pm dp/dt_{\max}$ due to the administration of aconitine was blocked by propranolol, indicating the possibility that aconitine may have its inotropic cardiac effect via acting on beta-1 adrenergic receptor. Moreover, the change rates in HR and $\pm dp/dt_{\max}$ after administration were almost the same for the two groups: propranolol and aconitine, propranolol and saline, but the change rates for another group with treatment of aconitine alone is significantly larger than the two groups. This result indicated that propranolol could block most of aconitine's effect on heart function, indicating the possibility that aconitine may act on beta-1 adrenergic receptor to have its therapeutic function.

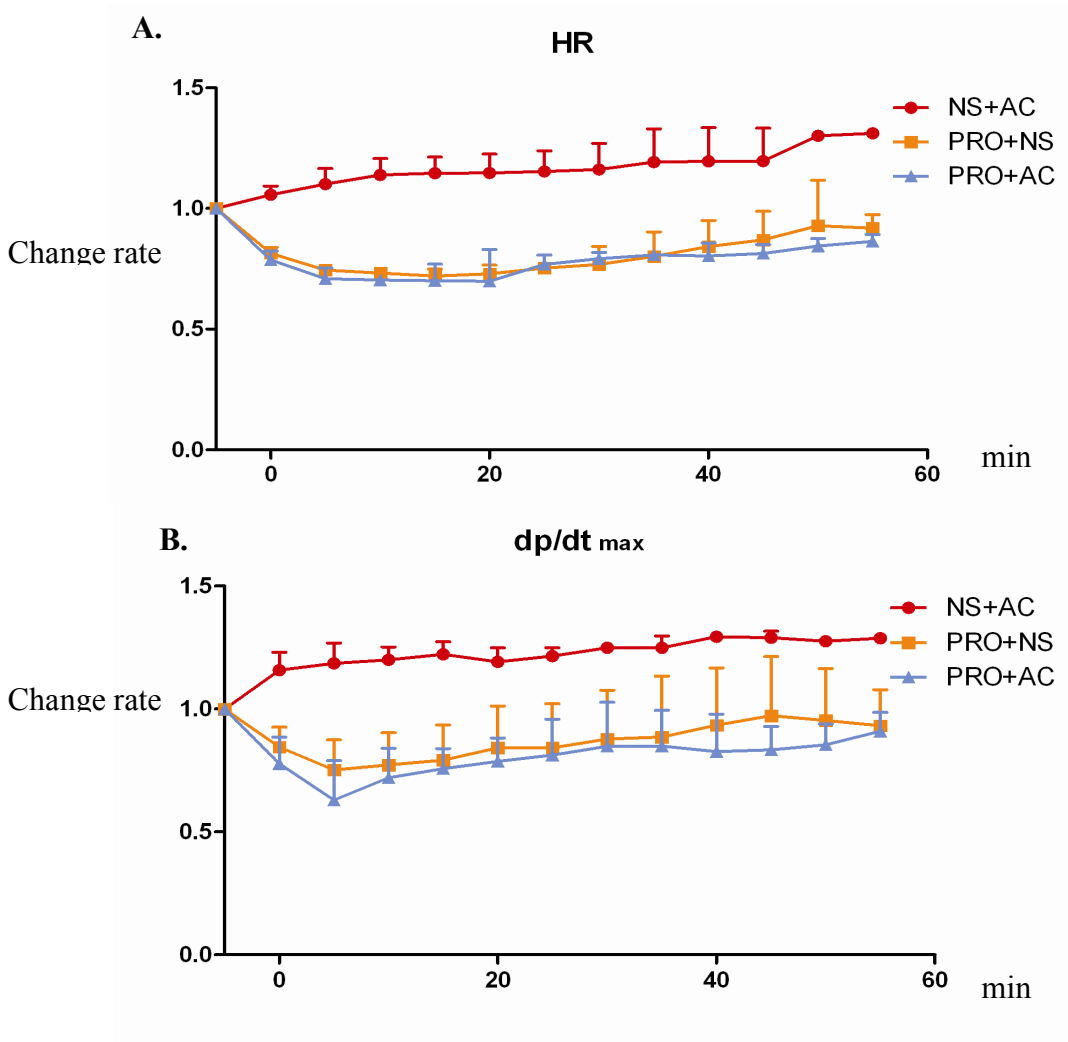


Figure 26. The Change Rate of HR and dp/dt after treatment of Propranolol and Aconitine
The change rate of heart rate (A) and the maximum rate of change of ventricular systolic values dp/dt_{max} (B) after administration of aconitine (AC) and propranolol (PRO), aconitine and normal saline (NS), and propranolol and NS.

4.0 DISCUSSION

4.1 SYNERGISTIC EFFECT OF THREE INGREDIENTS IN SND

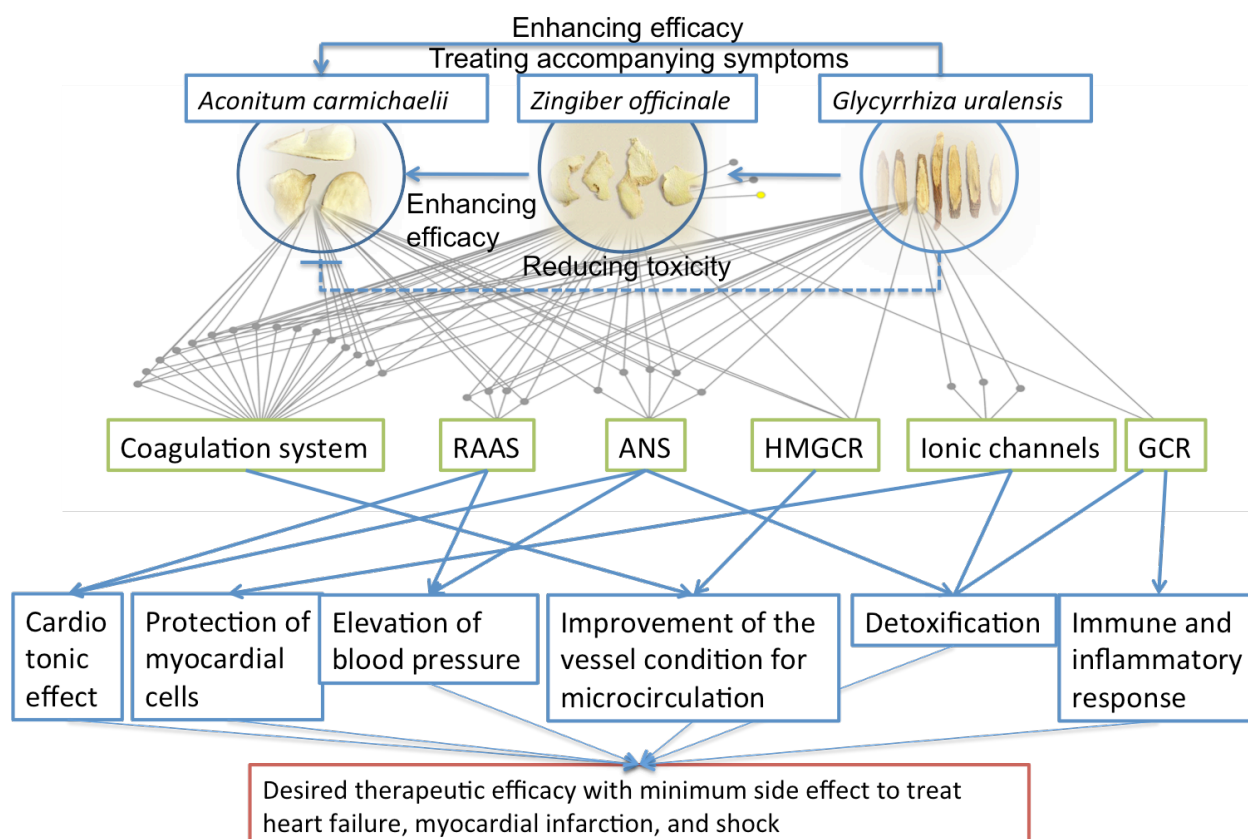


Figure 27. The predictions of synergistic effect mechanism for SND

Multiple constituents in Sini Decoction (SND) act on multiple targets in the context of several physiological systems to achieve synergistic effects. The large circles with figures inside show the three herbs in SND. The gray nodes represent our predicted therapeutic targets. These targets are linked with the herbs and related pathways by gray lines. Green rectangles represent the

pathways that the predicted therapeutic targets are involved in. Blue rectangles represent the therapeutic effects according to different targets, pathways, and herbs. Red rectangles show the synergistic effects of the combined use of three herbs in SND. The therapeutic effects are linked with their corresponding targets and synergistic effects by lines.

SND, originally recorded in *Treaties of Febrile diseases*, has a long history of use as a treatment for cardiovascular diseases (CVDs). People applied SND as a life-saving drug to treat patients with heart failure, myocardial infarction, shock, and other serious diseases [58]. According to the previous literature, SND can ameliorate lipid profiles, improve microcirculation [59], and increase blood pressure to help blood reflux to the heart and to help improve circulation. This process keeps people warm and can help to treat Yang deficiency. SND can also restore the function of heart, thus pulling the blood to the system circulation more powerfully with a higher frequency [60, 61]. Thus SND is useful to treat patients with diseases caused by weak circulation, such as rheumatism, general debility, cardiac weakness, weak circulation, and decreased kidney function [62].

In the SND formula, aconite (emperor) plays a dominating role in treating the primary causes of disease [63, 64]. Herbalists believed that aconite could resurrect the dead. Previous studies indicated that the hydrophilic parts of AC showed a strong cardio tonic effect in the heart of frogs, toads, and warm-blooded animals, either in their normal or diseased condition [65]. Some research claimed that aconite and its extract could protect the myocardial cells of animal models and patients with heart failure, myocardial infarction, cardiac hypertrophy, and other CVDs [66]. However, aconite is well known as a poisonous herb whose improper use can cause human respiratory paralysis, cardiac arrest, and even death [67, 68].

Ginger (minister) might enhance the effect of aconite and treat accompanying symptoms of CVDs [69]. Ginger extract can ease pain [70], prevent inflammation [71, 72], temporarily elevate blood pressure [73], fight against hypercholesterolemia [74], and prolong thrombus formation time in rats [60, 75].

Licorice as “zuoshi” (adjuvant-courier) in SND formulation is used to reduce the toxicity of aconite in fighting arrhythmia and inducing glucuronide-like detoxification [76]. Licorice also has other functions that can help to alleviate CVD symptoms, such as antibacterial [77], antiviral, anti-inflammatory [77], and hypertensive effects [78]. Licorice is used as a unique “guide drug” in many herbal formulations in TCM. It works through altering the enzyme activity of P450 and modulating of the drug transporter protein such as P-glycoprotein [79].

By using the systems polypharmacology approach to further investigate the target proteins connected with multiple compounds, we found most of these shared targets belong to a few physiological systems: the renin-angiotensin-aldosterone system (yellow square), the coagulation pathway (purple square), lipid metabolism (blue square), and the auto nervous system (rubber red square). These shared targets contribute to the synergistic effect of SND, revealing the underlying mechanism of SND formulation.

4.1.1 Major Constituents from Three Herbs Acting Synergistically on RAAS

Multiple constituents in SND are predicted to act on four targets in RAAS (renin-angiotensin-aldosterone system): ACE, AGTR, AGT, and renin. As shown in **Figure 28A**, renin is an enzyme that breaks down angiotensinogen (AGT) into angiotensin I. Angiotensin I is further cleaved in the lung by ACE into angiotensin II. Angiotensin II, the most potent compound in this system, can act on AGTR to attain two functions: (1) causing vasoconstriction, which increases

the peripheral vascular resistance that the heart needs to overcome, thus enhancing cardiac output and blood pressure; and (2) inducing the release of aldosterone, which stimulates the epithelial cells in kidneys distal tubule and collecting ducts to increase re-absorption of sodium and water, and increase excretion of potassium, leading to an increased blood volume and pressure [80, 81]. Moreover, the inhibitors for RAAS are widely used to treat cardiovascular diseases, like hypertension and heart failure [82, 83]. As shown in **Figure 28A**, GU, ZO, and AC exert synergistic efficacy by increasing the plasma concentration of angiotensin II via three targets (ACE, AGT, and renin) or by achieving the angiotensin II effect by directly interacting with AGTR, thus boosting blood pressure, increasing cardiac output, and improving circulation. GU [84-86] and ZO [87-90] have already been demonstrated to act on RAAS, whereas the influence of AC on RAAS requires further investigation.

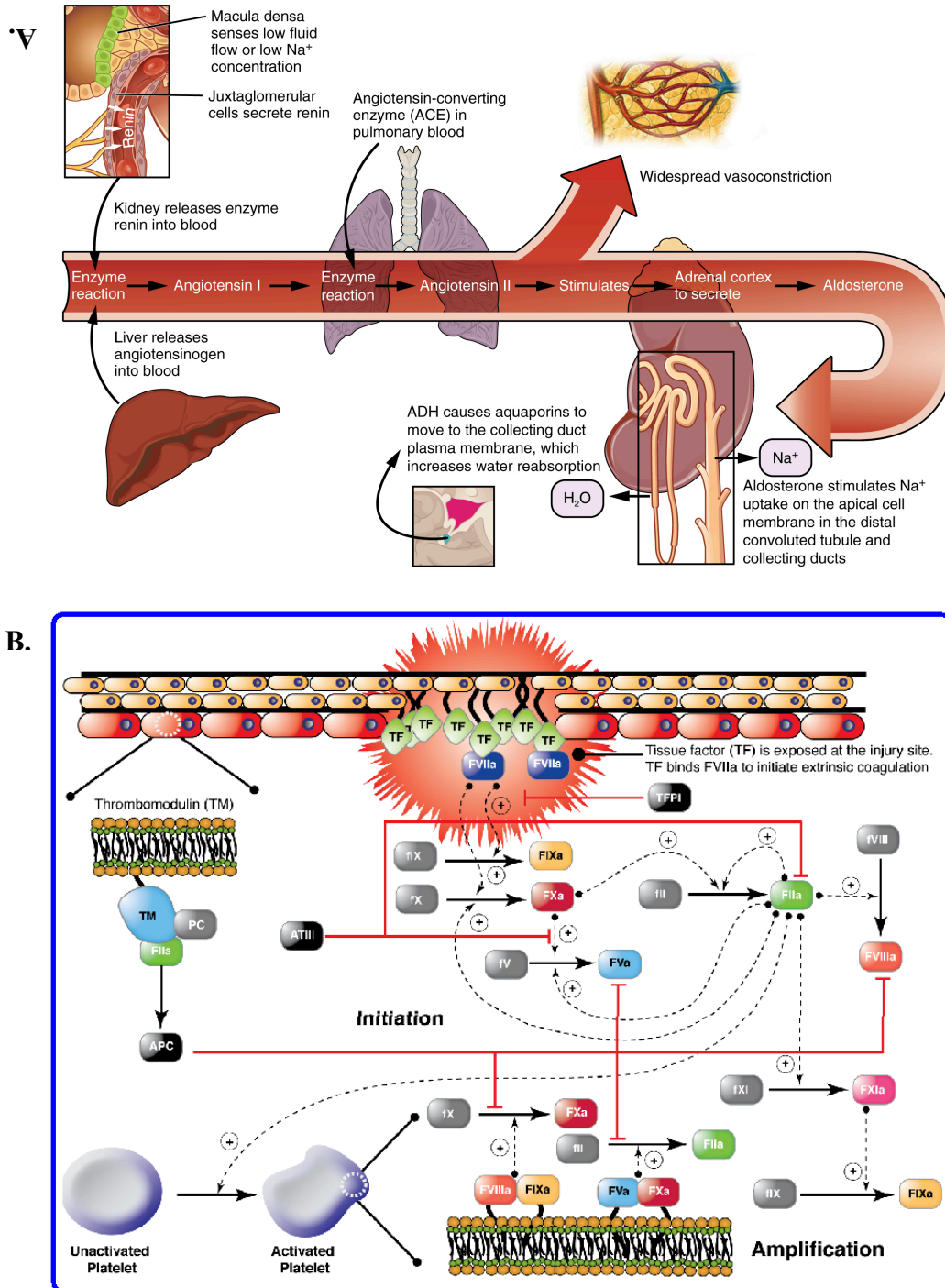


Figure 28. Multiple Targets from the RAS System and Coagulation Pathway

(A) The role of the four targets (ACE, AGT, AGTR, and REN) in the RAS physiological system (the figure was adapted from the website: <http://bookcoverimgs.com/renin-angiotensin-system/>).

(B) The roles of multiple potential targets in the coagulation pathway (the figure was adapted from [91]).

4.1.2 Multiple Components Interact with Multiple Targets in the Coagulation System

Multiple constituents in SND are predicted to interact with five targets in the coagulation system: FII, FX (coagulation factor X), FVII (coagulation factor FVII), PAF (platelet activation factor), and antithrombin III (ATIII). As shown in **Figure 28B**, the coagulation system includes three parts: fibrinolysis, platelet aggregation, and coagulation cascade; most of our potential targets are involved in the coagulation cascade. The intrinsic pathway and the extrinsic pathway, both found in the blood coagulation cascade, lead to the activation of FX, which converts prothrombin (FII) to thrombin, resulting in fibrin formation [92]. The pathways are a series of reactions, in which inactive pro-enzymes and their cofactors are turned into active forms that can catalyze the next reaction in the cascade, amplifying the process and culminating in the formation of thrombin [93]. Most coagulation factors are serine proteases that can be converted to their active forms to act on a downstream reaction; but FVIII and FV are glycoproteins cofactors. The intrinsic pathway is initiated by the activation of FXII, followed by the sequential activation of FXI and FIX, leading to the activation of FX [94]. The extrinsic pathway is initiated by the formation of the complex TF-FVII; TF-FVIIa activates FX; FXa convert FII (prothrombin) to thrombin, which not only converts fibrinogen to fibrin, but also activates platelet, FVIII, FV, and FXIII, which forms covalent bonds that crosslink the fibrin polymers, stabilizing fibrin clotting [92].

Herbs in SND interrelate with FII, FX, and FVII. Each factor plays a role in the coagulation cascade, thus allowing SND to inhibit the process of blood coagulation and reduce thrombus and blood clots through blocking these coagulation factors. In addition, some target proteins, hit by compounds of SND, are involved in the anticoagulation processes (ATIII) and platelet aggregation (PAF). Antithrombin III (also termed as ATIII) is a serine protease inhibitor

that is constantly active to degrade the serine proteases: thrombin, FIXa, FXa, FXIa, and FXIIa. Fibrinolysis is the process in which the tissue plasminogen activator (t-PA) and urokinase (uPA) trigger the transformation from plasminogen (PLG) to active plasmin, which breaks down fibrin, in order to maintain the size of clots and prevent thrombosis [93]. SND might have the potential of addressing multiple targets to keep hemostatic balance for smooth blood circulation, therefore conquering and preventing many complex cardiovascular diseases.

4.1.3 Herbs in SND Acting Synergistically to Improve the Lipid Profile

Multiple compounds from three herbs in SND target HMGCR, the rate-limiting enzyme in the process of synthesis of cholesterol. There are mainly four sources of cholesterol in human bodies: dietary uptake, retake from recycling bile acid, biosynthesis in the liver, and uptake from circulation by low-density lipoprotein (LDL) receptors on the liver [95]. When HMGCR is inhibited, less cholesterol will be synthesized. The liver can take in more LDL, leaving less LDL in the plasma, thus resulting in lower LDL and cholesterol plasma concentration in the body.

Multiple constituents in SND can also interact with peroxisome proliferator-activated receptor gamma (PPARG), to regulate fatty acid storage and glucose metabolism. PPARG is a regulator of adipocyte differentiation, and it stimulates lipid uptake and adipogenesis [96]. PPARG knockout mice cannot generate adipose tissue even when fed with a high-fat diet [97]. PPARG has been emphasized in the etiology of numerous diseases including obesity, diabetes, atherosclerosis, and cancer. PPARG decreases the inflammatory response of many cardiovascular cells [98], and increases synthesis and release of paraoxonase 1 from the liver by gene regulation, thus reducing atherosclerosis [99]. In addition, known agonists of PPARG have been used in the treatment of hyperglycemia [100] and hyperlipidaemia [101]. Many insulin-

sensitizing drugs used in the treatment of diabetes, such as the thiazolidinediones, target PPAR γ as their molecular mechanisms to lower serum glucose without enhancing secretion of pancreatic insulin [102, 103]. According to our predictions, PPAR γ might interact with glycyrrhetic acid, one of the major constituents in liquorice, thus reducing the inflammatory response of many cardiovascular cells, regulating fatty acid storage to improve plasma lipid profile, and controlling glucose metabolism to reduce the blood glucose level. This prediction is consistent with the experimental data, which reported that glycyrrhetic acid did shown activity binding with PPAR γ [104].

The constituents in SND can act on both PPAR γ and HMGCR to improve serum lipid profile. An improved serum lipid profile will enhance circulation and provide a more efficient vessel condition to prevent CVDs, such as atherosclerosis, shock, and stroke [105]. Recent research have also shown that aconite extract increased the hepatic LDL receptor, decreased HMGCR expression, and lowered cholesterol levels in rats [106]. Rats treated with ginger extract displayed a significant dose-dependent reduction in the serum cholesterol level, LDL-C, and serum triglyceride (TC) level, demonstrating a more efficient anti-hypercholesterolemic effect of ginger at a higher dose than Atorvastatin [107]. Glycyrrhizin (27) is also able to fight against hyperglycemia and hyperlipidemia [108]. Clinical studies demonstrated that licorice has desirable effects on preventing inflammatory processes in blood vessels, decreasing LDL, reducing plasma lipid levels, and lowering systolic blood pressure [109]. The results of these studies all match our predictions that SND can improve lipid profile.

4.1.4 Liquorice can Alleviate Arrhythmia Caused by Aconitum

Aconites from *Radix Aconiti* were proven to have cardiac toxicity, like causing arrhythmia [110]. According to the prescription database analysis platform of *Radix Aconiti*, 29.52% of 3188 prescriptions that contains aconite, are combined with liquorice to reduce the toxicity of aconite [111]. GU contains isoliquiritigenin (31), liquiritin (28), licoricidin (34), glycyamarin (30), isoliquiritin (37), and glycyrol (33), which are predicted to interact with potassium channels, sodium ion channels and beta-1 adrenergic receptor respectively. These targets are coincident to be some of the drug targets for the treatment of arrhythmia. The following drugs are all in the market or clinical trials for the treatment of arrhythmia: Procainamide, Lidocaine, Pyrazole amine, Phenytoin sodium, and Propafenone acting as sodium channel blockers; Amiodarone, Bromine, Sotalol, Benzyl ammonium, and Ibutilide blocking potassium current of myocardial cells and extending action potential duration; and, Metoprolol, Esmolol, and Bisoprolol inhibiting ADRB1 [112]. Liquorice was reported to fight against arrhythmia via inhibitory effects on the potassium current [113] and sodium channel [114]. Some compounds in liquorice can have an antitoxin effect similar to glucocorticoid (GC), to help reduce the toxicity of aconitum [115]. The anti-inflammatory and anti-shock effect of Glucocorticoid receptor (GCR) from liquorice and ginger also help to heal accompanying illness and contribute to the synergistic effect of SND.

One of the major components in liquorice, glycyrrhetic acid, is predicted to interact with the 11 β -hydroxysteroid dehydrogenases (11 β -HSDs) to mimic the effect of glucocorticoid, which is consistent with the literature reports [116]. As shown in **Figure 29**, the 11 β -hydroxysteroid dehydrogenase isozymes 1 (11 β -HSD1) and 2 (11 β -HSD2) are the catalysts for

the inter-conversion between cortisone and cortisol [116]. 11 β -HSD1 converts cortisone to the active glucocorticoid cortisol while the 11 β -HSD2 catalyzes the transformation from active cortisol to inactive cortisone. Inhibition of 11 β -HSD2 could be used to potentiate the anti-inflammatory effects of glucocorticoids due to a reduction in the amount of glucocorticoid. Aldosterone and glucocorticoids exerted a similar, concentration-dependent chronotropic action on cardiomyocytes, which was mediated by both the mineralocorticoid and glucocorticoid receptors [115]. Components in liquorice and ginger that interact with targets in RAAS influencing the function of aldosterone (mineralocorticoid), which might also aid to fight against cardio toxicity of aconite [117].

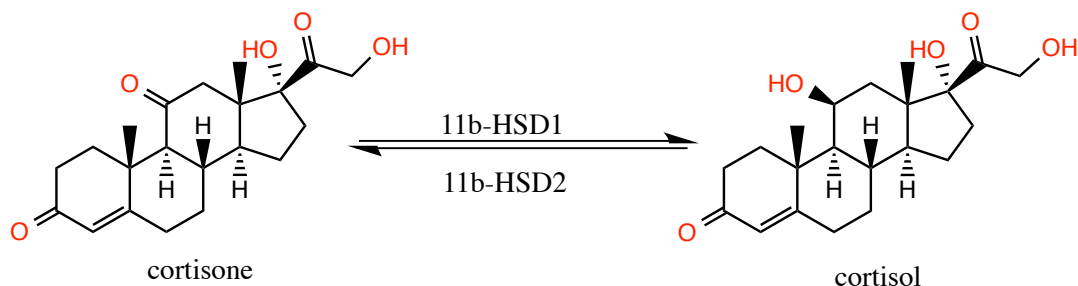


Figure 29. Interconversion of Cortisone and Cortisol Catalyzed by 11 β -HSD 1 and 11 β -HSD 2

Liquorice is frequently used in TCM for detoxification, and previous studies reported that paired use of GU and AC will reduce the toxicity of aconite and are declared to be safe, which matches our prediction [76, 111, 118, 119].

Among all constituents in liquorice, liquiritin seems to be more representative as it is predicted to act the sodium, the voltage-gated potassium channels, and the beta-1 adrenergic

receptor, according to our results. Then we tested the selected active components pair of liquiritin and aconitine (selected active compound in aconitum) by recording the electrocardiograms of normal ECG, premature beats, ventricular tachycardia and cardiac arrest. We observed that the administration of liquiritin could alleviate the cardio toxicity of arrhythmia caused by aconitine in mice, shown by significantly delayed time of premature beats, ventricular tachycardia, and cardiac arrest, induced by aconitine. This result validated our prediction that the liquiritin was the active component responsible for the antiarrhythmic effect of liquorice (**Figure 23, Figure 24, Figure 25, Table 7, and Table 8**).

4.1.5 The Synergistic Effect of Ginger and Aconitum Pair

We also tested the synergistic effect for the combination of our selected compounds 6-gingerol and aconitine to evaluate whether 6-gingerol is the active component in ginger, which can improve the therapeutic effect of aconitum. As shown in previous reports, Ganjiang (ginger) –Fuzi (aconitum) pair has been used for more than 2000 years in a ratio of one to one for ginger and aconitum in weight. This herbal pair has dispelled internal cold and recuperates depleted yang activities to treat patients with Yang deficiency, which can be reflected as deadly cold limbs and a sunken and feeble pulse [7, 120, 121]. After being combined with ginger, the cardiac effect of aconitum was enhanced, reflected by the increased force of cardiac muscle systole, improved cardiac energy metabolism, reduced left ventricular end-diastolic pressure (LVEDP), improved heart compliance and altered hormone regulation [122-124]. Thus, aconitum are reported to have improved therapeutic effect in curing heart failure when combined use with ginger. In order to evaluate whether the 6-gingerol in ginger or the aconitine in aconitum is responsible for their therapeutic and synergistic effects in treating heart failure, we measured the

effect of aconitine combined with 6-gingerol, compared with aconitine alone by recording the hemodynamic parameters, such as left ventricular systolic (LVSP) and end-diastolic pressures (LVEDP) and heart rate (HR), Systolic blood pressure (SBP), diastolic blood pressure (DBP), maximal rate of pressure development (+dp/dt). We observed increase of all the hemodynamic measurements on mice induced by the administration of aconitine, indicating that aconitine is at least one of the major components possess therapeutic activity. These increases were further improved by the combination with 6-gingerol, indicating the 6-gingerol is responsible for the synergistic effect in ginger. These results validate our prediction about active components in ginger and aconitum that participate in the synergistic effect of SND (**Table 9**).

4.1.6 Compounds act on targets in autonomic nerves system (ANS)

Beta-1 adrenergic receptor, a G-protein coupled receptor, predominantly expresses in cardiac tissues. ADRB1 can raise heart rate in sino atrial node (SA node), enhance contractility and automaticity of ventricular cardiac muscle, and elevate conduction of atrioventricular node (AV node), thus increasing cardiac output [125]. ADRB1 is the potential target linked to the largest number of components in our prediction. Higenamine, a constituent in AC, was reported to have a cardio tonic effect on cardiac chronotropic and inotropic actions mediated by ADRB1, which matches our prediction [126]. Low dose of mesaconitine was shown to stimulate beta-adrenoceptors in hippocampus, evoking long lasting excitatory effects, to exert accompany function like hypertensive effect and analgesia effect [127]. Our experiments results shown the inotropic actions and following pressure changes induced by aconitine was compromised/counteracted by the pre-administration of propranolol, a well-known beta adrenergic antagonist, indicating the possibility that the aconitine may act on beta adrenergic

receptor, especially beta-1 adrenoceptor, to achieve its effect on increasing heart rate and blood pressure [128] (**Figure 26**).

The M2 muscarinic receptors (M2AChR) are cholinergic receptors that act on myocardium to slow down the heart rate and lessen the cardiac output by delaying the speed of depolarization, reducing conduction of AV node, and decreasing contractile forces of the atrial cardiac muscle [129]. Multiple compounds from SND target M2AChR to regulate the heart rate and heart output, and to achieve cardio tonic effect against disease conditions. M3AChR mediates vessel constriction by regulating intracellular calcium in smooth muscles, which is also correlated closely to blood pressure. Liquorice and ginger [130] may act on M3AChR to exert precondition-mediated cardio protective efficacy against aconite-induced arrhythmia [131]. Acetyl cholinesterase (AChE) inhibits the metabolism of acetylcholine (ACh), resulting in the accumulation of ACh in the synaptic cleft, which will stimulate sympathetic nervous system for a long time [132]. Liquorice is demonstrated to interact with AChE, which matches our prediction [133]. According to previous studies, 6-gingerol [134] and glycyrrhetic acid [135] have shown binding affinity with AChE, for K_i of 10.6nM and 31.2nM respectively, which is in consistent with our prediction. We predicted that Liquiritin can interact with ADBR2, this prediction has already been demonstrated by qHTS screening for beta2-adrenergic receptor with an IC_{50} of 6 μ M [128].

As shown in Table 10, some of our predicted targets for the constituents have already been validated by other literature reports, indicating the reliability of our prediction

Table 9. The Validated Interaction between SND Components and Predicted Targets

Compound Name	Abbreviation	Target Name	Assay	Value	Reference
6-gingerol	AChE	Acetylcholinesterase	Ki	0.0106	[134]
6-gingerol	TRPV1	Transient receptor potential cation channel subfamily A member 1	Efficacy	0.114	[136]
6-gingerol	LTAH4	Leukotriene A4 hydrolase	Efficacy	0.114	[137]
aconitine	CHRNA7	Neuronal acetylcholine receptor protein alpha-7 subunit	Ki	2.12nM	[138, 139]
glycyrrhetic acid	PPARG	Peroxisome proliferator-activated receptor gamma	Activity	Active	[104]
glycyrrhetic acid	HSD-11 β	11-beta-hydroxysteroid dehydrogenase 2	IC50	1nM	[120]
glycyrrhetic acid	AChE	Acetylcholinesterase	INH	0.0312	[135]
liquiritin	ADRB2	Beta-2 adrenergic receptor	IC50	6.5131uM	
glycyrrhetic acid	AKR1B10	Aldo-keto reductase family 1 member B10	IC50	=4.9uM	[140]
glycyrrhetic acid	POLL	DNA polymerase kappa	Active	Active	[141]
Aconitine		Tetrodotoxin-sensitive, voltage-dependent sodium channels	Active	Active	[128]
Glycyrrin	GCR	Glucocorticoids receptor	IC50	2.6uM	[142]
Higenamine	ADRB1	Beta-1 adrenergic receptor	Active	Active	[126]

5.0 CONCLUSION

To summarize, we initially constructed a comprehensive database for CVDs research. We then applied this database to predict the active constituents linked to potential targets for SND through the construction of the biological target-compound network at the molecular level. The results showed that 31 constituents interacting with 33 targets, which have a significant relationship with pathological processes of cardiovascular diseases (CVDs), such as the thrombosis process, lipid profile (HMGCR, PPARG), and blood pressure regulation (RAAS, AGTR, ADBR, and M2AChR). Also, multiple compounds in this formula could interact with the same targets simultaneously, which offers a good explanation for the synergistic mechanisms of TCM. Based on the network analysis, we further explored the underlying mechanism of the SND formula with the “Jun-Chen-Zuo-Shi” principle.

The results revealed that aconite (empire) plays an important role in RAAS, HMGCR, ANS, and the coagulation system to cure symptoms of CVDs. Multiple constituents in aconitum might interact with multiple targets, such as renin, ADRB1, ACE, HMGCR, ADRB1, and FII, to treat the primary cause of the disease. On the other hand, ginger and liquorice reacted with multiple targets, some of which were also targeted by aconite. Some other targets may not share by different herbs, but still in the same pharmacological process and will produce similar actions to improve the efficacy of aconite. Interestingly, ginger (Chen) was predicted to not only interact with many target proteins (PPARG, HMGCR) in the same physiological system as the other two

herbs to strengthen the effect of aconitum, and but also act on other targets (TRPV1, LTAH4, and COX2) relevant to the immune and inflammatory processes to remedy concomitant complications with CVDs. Liquorice (Zuo) can alleviate arrhythmia caused by aconite via reaction with potassium ion channels, sodium ion channels, ADBR1 and HSD-11 β , thus reducing toxicity of aconite.

These predicted results are in agreement with the rationality of the formula, involving the mutual reinforcement of therapeutic efficacy and reduction of adverse effects. In addition, some of our predicted interactions (like AChE-6-gingerol, glycyrrhetic acid-PPARG) are also in accordance with the previous literature (as shown in Figure 10). We did further experimental validation on normal rats and HF and MI rat models to validate the function of the constituents (liquiritin, 6-gingerol, and aconitine), which we selected for each herb from SND and predicted would have therapeutic and synergistic effects,. We found that aconitine is effective and powerful in improving heart function on HF, MI and normal rats; liquiritin can reduce the arrhythmia induced by aconitine; and 6-gingerol can improve the effect of aconitine on heart function. Finally, we selected ADBR1 as an example and partially validated our prediction that aconitine act on ADBR1.

6.0 FUTURE PROSPECTIVE

To further evaluate the molecular mechanism of the synergistic effects in SND and to make sure our predictions were correct, we will need more specific experimental validation. We plan to perform some protein binding assays between our selected representative compounds (liquiritin, aconitine, and 6-gingerol) and our predicted target proteins (PPARG, HMGCR, and ACE). We selected the protein-binding assay of these target proteins based on the following reasons: first, these target proteins are well-known therapeutic targets for the treatment of CVDs in the clinic. Moreover, the effects induced by the activations or inhibitions of these targets are identical with the therapeutic effects of SND and effects of individual herbs in SND. Furthermore, the purified proteins for these targets used in the binding assays are commercially available, and the experimental protocols are easily found with the well-established binding assays for these proteins. Lastly, the protein-binding assay is simple and specific to validate our prediction about target-drug interaction. If the constituents were demonstrated to interact with the proteins, we could do more cell-based assays or *in vivo* animal studies.

APPENDIX. ABBREVIATION

5HT	Serotonergic synapse
$+dp/dt_{\max}$	The maximum rate of change of ventricular systolic Values
AC	Aconitine
ACE	Angiotensin Converting Enzyme
AChE	Acetyl cholinesterase
AD	Alzheimer's disease
ADR	Adrenergic signaling in cardiomyocytes
ADRA1	Alpha-1 adrenergic receptor
ADRA2	Alpha-2 adrenergic receptor
ADRB1	Beta-1 adrenergic receptor
ADRB2	Beta-2 adrenergic receptor
ADRB3	Beta-3 adrenergic receptor
AGT	Angiotensinogen
AGTR	Angiotensin II receptor
AKR1B10	Aldo-keto reductase family 1 member B10
AMPK	AMP-activated protein kinase signaling pathway
ANPR	Atrial natriuretic peptide receptor A
ANS	Autonomic nervous system
APN	Aminopeptidase N
ARVC	Arrhythmogenic right ventricular cardiomyopathy (ARVC)
ATIII	Antithrombin-III
CACN	Voltage-dependent L-type calcium channel

CAMP	cAMP signaling pathway
CHD	Coronary heart disease
CHO	Cholinergic synapse
CHRNA7	Neuronal acetylcholine receptor protein alpha-7 subunit
COX-2	Prostaglandin G/H synthase 2
CR	Circadian rhythm
CVD	Cardiovascular diseases
DBP	Diastolic blood pressure
DILATED CM	Dilated cardiomyopathy
EDNRA	Endothelin-1 receptor
EF	Ejection fraction
FII	Coagulation Factor II
FIII	Coagulation factor III (tissue factor)
FS	Fractional shortening
FV	Coagulation Factor V
FVII	Coagulation factor VII
FVIIa	Coagulation factor VIIa
FVIII	Coagulation factor VIII
FX	Coagulation factor IX
FXa	Coagulation factor Xa
FXI	Coagulation factor XI
FXIII	Coagulation factor XIII
GCR	Glucocorticoid receptor
GU	Glycyrrhiza Uralensis
HCM	Hypertrophic cardiomyopathy (HCM)
HF	Heart failure
HMGCR	3-hydroxy-3-methylglutaryl-coenzyme A reductase
HR	Heart rate
HRH1	Histamine H1 receptor
HSD-11 β	11-beta-hydroxysteroid dehydrogenase 2
HTR	Serotonin receptor

INSULIN	Insulin signaling pathway
KCN	Potassium channel
KvCN	Potassium voltage-gated channel subfamily D member 3
LDL	Low density lipid protein
LTAH4	Leukotriene A4 hydrolase
LV	Left ventricle
LVEDP	Left ventricular end-diastolic pressure
LVEDV	Left ventricular end-diastolic volume
LVESV	Left ventricular end-systolic volume
LVIDd	Left ventricular internal diameter in diastole
LVIDs	Left ventricular internal diameter in systole
LVSP	Left ventricular systolic pressure
M2AChR	M2 muscarinic acetylcholine receptor
M3AChR	M3 muscarinic acetylcholine receptor
MBP	Medium blood pressure
MCR	Mineralocorticoid receptor
MI	Myocardial infarction
MM	Multiple myeloma
NS	Normal saline
PAF	Platelet activating factor
PDE3	cGMP-inhibited 3',5'-cyclic phosphodiesterase
PI3K-AKT	PI3K-Akt signaling pathway
PLATELET	Platelet activation
PLG	Plasminogen
PN3	Sodium channel protein type 10 subunit alpha
POLL	DNA polymerase kappa
PPAR	Peroxisome proliferator-activated receptor signaling pathway
PPARG	Peroxisome proliferator-activated receptor gamma
PRO	Protein digestion and absorption
RAAS/RAS	Renin-angiotensin-aldosterone system
REN	Renin

SBP	Systolic blood pressure
SCN	Sodium
SND	Sini Decoction
SV	Stroke volume
TC	Serum triglyceride
TCM	Traditional Chinese medicine
THR	Thyroid hormone signaling pathway
TNF-alpha	Tumor necrosis factor alpha
TRP	Inflammatory mediator regulation of TRP channels
	Transient receptor potential cation channel subfamily A
TRPV1	member 1
TTSCN	tetrodotoxin-sensitive, voltage-dependent sodium channels
uPA	Urokinase-type plasminogen activator
VEGFR	Vascular endothelial growth factor receptor
vWF	Von Willebrand factor
ZO	Zingiber Officinale

BIBLIOGRAPHY

1. Yang, H., *Experimental research on effects of anti-heart failure of sini decoction in terms of oxidative stress-apoptosis*. 2000, Dissertation.
2. Tan, G., et al., *Metabonomic profiles delineate the effect of traditional Chinese medicine sini decoction on myocardial infarction in rats*. PloS one, 2012. **7**(4): p. e34157.
3. Luo, J., et al., *The effects of modified sini decoction on liver injury and regeneration in acute liver failure induced by d-galactosamine in rats*. Journal of ethnopharmacology, 2015. **161**: p. 53-59.
4. Wu, S., et al., *Lipidomic profiling reveals significant alterations in lipid biochemistry in hypothyroid rat cerebellum and the therapeutic effects of Sini decoction*. Journal of ethnopharmacology, 2015. **159**: p. 262-273.
5. Zheng, J.-P., *Experience in clinical application of Danggui Sini Decoction*. Zhong xi yi jie he xue bao = Journal of Chinese integrative medicine, 2005. **3**(4): p. 289-293.
6. Cai, Y., et al., *Myocardial lipidomics profiling delineate the toxicity of traditional Chinese medicine Aconiti Lateralis radix praeparata*. Journal of Ethnopharmacology, 2013. **147**(2): p. 349-356.
7. Chen, S., et al., *Investigation of the therapeutic effectiveness of active components in Sini decoction by a comprehensive GC/LC-MS based metabolomics and network pharmacology approaches*. Molecular bioSystems, 2014. **10**(12): p. 3310-3321.
8. Zhang, H., et al., *Absorption and metabolism of three monoester-diterpenoid alkaloids in Aconitum carmichaeli after oral administration to rats by HPLC-MS*. Journal of ethnopharmacology, 2014. **154**(3): p. 645-652.
9. Wu, S., et al., *Serum metabonomics coupled with Ingenuity Pathway Analysis characterizes metabolic perturbations in response to hypothyroidism induced by propylthiouracil in rats*. Journal of pharmaceutical and biomedical analysis, 2013. **72**: p. 109.

10. Tan, G., et al., *Characterization of constituents in Sini decoction and rat plasma by high-performance liquid chromatography with diode array detection coupled to time-of-flight mass spectrometry*. Biomedical Chromatography, 2011. **25**(8): p. 913-924.
11. Plake, C. and M. Schroeder, *Computational Polypharmacology with Text Mining and Ontologies*. Current Pharmaceutical Biotechnology, 2011. **12**(3): p. 449-457.
12. Peters, J.-U., *Polypharmacology - foe or friend?* Journal of medicinal chemistry, 2013. **56**(22): p. 8955-8971.
13. Tan, G., et al., *Analysis of phenolic and triterpenoid compounds in licorice and rat plasma by high-performance liquid chromatography diode-array detection, time-of-flight mass spectrometry and quadrupole ion trap mass spectrometry*. Rapid communications in mass spectrometry : RCM 2010. **24**(2): p. 209-218.
14. Tan, G., et al., *Detection and identification of diterpenoid alkaloids, isoflavonoids and saponins in Qifu decoction and rat plasma by liquid chromatography–time-of-flight mass spectrometry*. Biomedical Chromatography, 2012. **26**(2): p. 178-191.
15. Tan, G., et al., *Screening and analysis of aconitum alkaloids and their metabolites in rat urine after oral administration of aconite roots extract using LC-TOFMS-based metabolomics*. Biomedical chromatography : BMC, 2011. **25**(12): p. 1343.
16. Zhang, H., et al., *Comparative pharmacokinetics of three monoester-diterpenoid alkaloids after oral administration of Acontium carmichaeli extract and its compatibility with other herbal medicines in Sini Decoction to rats*. Biomedical Chromatography, 2014: p. n/a-n/a.
17. Luo, G., et al., *Introduction of Systems Biology in Traditional Chinese Medicine (TCM)*. John Wiley & Sons, Inc: Hoboken, NJ, USA. p. 1-37.
18. Wu, L., et al., *Identifying roles of Jun-Chen-Zuo-Shi" component herbs of QiShenYiQi formula in treating acute myocardial ischemia by network pharmacology*. Chinese medicine, 2014. **9**: p. 24-24.
19. Tao, W., et al., *Network pharmacology-based prediction of the active ingredients and potential targets of Chinese herbal Radix Curcumae formula for application to cardiovascular disease*. Journal of ethnopharmacology, 2013. **145**(1): p. 1-10.
20. Li, S., B. Zhang, and N. Zhang, *Network target for screening synergistic drug combinations with application to traditional Chinese medicine*. BMC Systems Biology, 2011. **5**(1): p. S10-S10.
21. Wang, L., et al., *A network study of chinese medicine xuesaitong injection to elucidate a complex mode of action with multicomponent, multitarget, and multipathway*. Evidence-based complementary and alternative medicine : eCAM, 2013. **2013**: p. 652373.
22. Reddy, A.S. and S. Zhang, *Polypharmacology: drug discovery for the future*. Expert Review of Clinical Pharmacology, 2013. **6**(1): p. 41-47.

23. Peters, J.-U., *Polypharmacology in Drug Discovery*. 2012, US: John Wiley & Sons Inc.
24. Anighoro, A., J. Bajorath, and G. Rastelli, *Polypharmacology: challenges and opportunities in drug discovery*. Journal of medicinal chemistry, 2014. **57**(19): p. 7874.
25. Simon, Z., et al., *Drug effect prediction by polypharmacology-based interaction profiling*. Journal of Chemical Information and Modeling, 2012. **52**(1): p. 134-145.
26. Wertheimer, A.I., *The Economics of Polypharmacology: Fixed Dose Combinations and Drug Cocktails*. Current medicinal chemistry, 2013. **20**(13): p. 1635-1638.
27. Bottegoni, G., et al., *The role of fragment-based and computational methods in polypharmacology*. Drug Discovery Today, 2012. **17**(1-2): p. 23-34.
28. Pérez-Nueno, V.I., et al., *GES Polypharmacology Fingerprints: A Novel Approach for Drug Repositioning*. Journal of Chemical Information and Modeling, 2014. **54**(3): p. 720-734.
29. Proschak, E., *In silico polypharmacology: retrospective recognition vs. rational design*. Journal of Cheminformatics, 2014. **6**(S1): p. 1-1.
30. World Health Organization, W.H.F., World Stroke Organization, *Global atlas on cardiovascular disease prevention and control----Policies, strategies and interventions*. 2011.
31. World Health Organization, *Guidelines for primary health care in low-resource settings Cancer, diabetes, heart disease and stroke, chronic respiratory disease*. 2012.
32. World Health Organization,, *Fact sheets on cardiovascular diseases*. 2015.
33. World Health Organization,, *Global Health Observatory (GHO) data-----Deaths from cardiovascular diseases and diabetes*. 2012.
34. World Health Organization,, *A global brief on hypertension-----Silent killer, global public health crisis*. 2013.
35. Wang, Y., et al., *Pathophysiology and Therapeutics of Cardiovascular Disease in Metabolic Syndrome*. Current pharmaceutical design, 2013. **19**(27): p. 4799-4805.
36. Wang, L., et al., *TargetHunter: an in silico target identification tool for predicting therapeutic potential of small organic molecules based on chemogenomic database*. The AAPS journal, 2013. **15**(2): p. 395-406.
37. DuBois, P., *MySQL: the definitive guide to using, programming, and administering MySQL 4.1 and 5.0*. 2005, Indianapolis, Ind: Sams Pub.
38. Anonymous, *Axitinib*. Formulary, 2012. **47**(1): p. 3.
39. Knox, C., et al., *DrugBank 3.0: a comprehensive resource for 'omics' research on drugs*. Nucleic acids research, 2011. **39**: p. D1035-D1041.

40. MetaCore GeneGo, *Proteostasis Therapeutics licensing agreement*. R & D Focus Drug News, 2009.
41. Gaulton, A., et al., *ChEMBL: a large-scale bioactivity database for drug discovery*. Nucleic acids research, 2012. **40**(D1): p. D1100-D1107.
42. Sandeep, G., et al., *AUDocker LE: A GUI for virtual screening with AUTODOCK Vina*. BMC research notes, 2011. **4**(1): p. 445-445.
43. Liu, H., et al., *AlzPlatform: an Alzheimer's disease domain-specific chemogenomics knowledgebase for polypharmacology and target identification research*. J Chem Inf Model, 2014. **54**(4): p. 1050-60.
44. Wang, M., et al., *Alkaloid profiling of the Chinese herbal medicine Fuzi by combination of matrix-assisted laser desorption ionization mass spectrometry with liquid chromatography–mass spectrometry*. Journal of Chromatography A, 2009. **1216**(11): p. 2169-2178.
45. Glans, J.H., *SciFinder.(Website overview)*. 2014, American Library Association CHOICE: Middletown. p. 1248.
46. Chen, J., et al., *A new model of congestive heart failure in rats*. American Journal of Physiology - Heart and Circulatory Physiology, 2011. **301**(3): p. H994-H1003.
47. Lindqvist, P., A. Calcuttea, and M. Henein, *Echocardiography in the assessment of right heart function*. European Heart Journal - Cardiovascular Imaging, 2008. **9**(2): p. 225-234.
48. Tan, G., et al., *Hydrophilic interaction and reversed-phase ultraperformance liquid chromatography TOF-MS for serum metabonomic analysis of myocardial infarction in rats and its applications*. Molecular bioSystems, 2012. **8**(2): p. 548-556.
49. Anversa, P., et al., *Left ventricular failure induced by myocardial infarction. II. Tissue morphometry*. American Journal of Physiology - Heart and Circulatory Physiology, 1985. **248**(6): p. H883-H889.
50. Pacher, P., et al., *Measurement of cardiac function using pressure–volume conductance catheter technique in mice and rats*. Nature protocols, 2008. **3**(9): p. 1422-1434.
51. Liu, H., et al., *AlzPlatform: an Alzheimer's disease domain-specific chemogenomics knowledgebase for polypharmacology and target identification research*. Journal of chemical information and modeling, 2014. **54**(4): p. 1050-1060.
52. *Huang di nei jing'tong shi*. 1st Edition ed. ISBN 7509128854, ed. H. Zhang, Ma, Lieguang, Tong, Xuanwen. 2009, Beijing, China: People's Military Medical Press.
53. Xie, X.-Q., et al., *Chemogenomics knowledgebased polypharmacology analyses of drug abuse related G-protein coupled receptors and their ligands*. Frontiers in pharmacology, 2014. **5**: p. 3.

54. Cheung, J., et al., *Structures of human acetylcholinesterase bound to dihydrotanshinone I and territrein B show peripheral site flexibility*. ACS medicinal chemistry letters, 2013. **4**(11): p. 1091-1096.
55. Binda, C., et al., *Structures of human monoamine oxidase B complexes with selective noncovalent inhibitors: Safinamide and coumarin analogs*. Journal of medicinal chemistry, 2007. **50**(23): p. 5848-5852.
56. Istvan, E.S. and J. Deisenhofer, *Structural Mechanism for Statin Inhibition of HMG-CoA Reductase*. Science, 2001. **292**(5519): p. 1160-1164.
57. Gampe, J.R.T., et al., *Asymmetry in the PPARgamma/RXRalpha crystal structure reveals the molecular basis of heterodimerization among nuclear receptors*. Molecular cell, 2000. **5**(3): p. 545.
58. Su, J., et al., *Study on influence of Sini Decoction on quality of life of patients after percutaneous transluminal coronary angioplasty*. Chinese Journal of Integrated Medicine, 2000. **6**(2): p. 108-111.
59. Zhang, H., et al., *Sinitang (Shigyaku-to), a traditional Chinese medicine improves microcirculatory disturbances induced by endotoxin in rats*. Journal of ethnopharmacology, 1999. **68**(1-3): p. 243-249.
60. Cui, H.Z., et al., *Ginseng-Aconite Decoction elicits a positive inotropic effect via the reverse mode Na.sup.+ /Ca.sup.2+ exchanger in beating rabbit atria*. Journal of Ethnopharmacology, 2013. **148**(2): p. 624.
61. Tan, G., et al., *Metabonomic profiles delineate the effect of traditional Chinese medicine sini decoction on myocardial infarction in rats*. PloS one, 2012. **7**(4): p. e34157.
62. Yong, L., et al., *Effects of Sini decoction on vascular stenosis of iliac artery in rabbits after injured by balloon and levels of serum cholesterol*. Heart, 2011. **97**(Suppl 3): p. A18-A19.
63. Zhang, H., Y. Sugiura, and Y. Goto, *Aconiti tuber (Bushu) improves microcirculatory disturbances induced by endotoxin in rats*. Phytotherapy Research, 2000. **14**(7): p. 505-509.
64. Chohachi, K., S. Masayoshi, and H. Hiroshi, *Cardioactive Principle of Aconitum carmichaeli Roots I*. Planta Medica, 2009. **35**(2): p. 150-155.
65. Chen, L., et al., *Effects of diammonium glycyrrhizinate on the pharmacokinetics of aconitine in rats and the potential mechanism*. Xenobiotica, 2009. **39**(12): p. 955-955.
66. Meng HL, C.T., *Study on the influence of aconite on aorta vascular extracellular matrix of cardiac hypertrophy rat model induced by thyroxine*. Asia Pacific Traditional Medicine, 2009. **5**(2): p. 32-34.
67. Chan, T.Y.K., *Aconite poisoning presenting as hypotension and bradycardia*. 2009, SAGE

PUBLICATIONS, INC: Sage UK: London, England. p. 795-797.

68. Singhuber, J., et al., *Aconitum in Traditional Chinese Medicine—A valuable drug or an unpredictable risk?* Journal of Ethnopharmacology, 2009. **126**(1): p. 18-30.
69. Marx, W.M., et al., *Ginger*. Nutrition Reviews, 2013. **71**(4): p. 245-254.
70. Black, C.D., et al., *Ginger (Zingiber officinale) reduces muscle pain caused by eccentric exercise*. The journal of pain : official journal of the American Pain Society, 2010. **11**(9): p. 894-903.
71. Mashhadi, N.S., et al., *Anti-oxidative and anti-inflammatory effects of ginger in health and physical activity: review of current evidence*. International journal of preventive medicine, 2013. **4**(Suppl 1): p. S36.
72. Mahluji, S., et al., *Anti-inflammatory effects of zingiber officinale in type 2 diabetic patients*. Advanced pharmaceutical bulletin, 2013. **3**(2): p. 273-276.
73. *Ginger attenuates acetylcholine-induced contraction and Ca²⁺ signalling in murine airway smooth muscle cells*. Canadian Journal of Physiology and Pharmacology, 2008. **86**(5): p. 264-271.
74. Al-Amin, Z.M., et al., *Anti-diabetic and hypolipidaemic properties of ginger (Zingiber officinale) in streptozotocin-induced diabetic rats*. British Journal of Nutrition, 2006. **96**(4): p. 660-666.
75. Shih, H.-C., et al., *Synthesis of Analogues of Gingerol and Shogaol, the Active Pungent Principles from the Rhizomes of Zingiber officinale and Evaluation of Their Anti-Platelet Aggregation Effects*. International journal of molecular sciences, 2014. **15**(3): p. 3926.
76. Peter, K., et al., *A novel concept for detoxification: Complexation between aconitine and liquiritin in a Chinese herbal formula ('Sini Tang')*. Journal of Ethnopharmacology, 2013. **149**(2): p. 562-569.
77. Söderling, E., et al., *The effect of liquorice extract-containing starch gel on the amount and microbial composition of plaque*. Clinical oral investigations, 2006. **10**(2): p. 108-113.
78. Tolstikova, T.G., et al., *Glycidipine, a Promising Hypotensive and Cardioprotective Agent*. Bulletin of Experimental Biology and Medicine, 2011. **151**(5): p. 597-600.
79. Cai, J., et al., *Design and synthesis of novel 4-benzothiazole amino quinazolines Dasatinib derivatives as potential anti-tumor agents*. European journal of medicinal chemistry, 2013. **63**: p. 702-712.
80. Bader, M., *Renin–Angiotensin–Aldosterone System*. 2008. p. 1066-1069.
81. De Mello, W.C., *Beyond the circulating Renin-Angiotensin aldosterone system*. Frontiers in endocrinology, 2014. **5**: p. 104.

82. Shearer, F., C.C. Lang, and A.D. Struthers, *Renin–Angiotensin–Aldosterone System Inhibitors in Heart Failure*. Clinical Pharmacology & Therapeutics, 2013. **94**(4): p. 459-467.
83. Calhoun, D.A., M.A. Zaman, and S. Oparil, *Drugs targeting the renin-angiotensin-aldosterone system*. Nature Reviews Drug Discovery, 2002. **1**(8): p. 621-636.
84. Celik, M.M., et al., *Licorice induced hypokalemia, edema, and thrombocytopenia*. Human & experimental toxicology, 2012. **31**(12): p. 1295-1298.
85. Farese, R.V., et al., *Licorice-Induced Hypermineralocorticoidism*. The New England journal of medicine, 1991. **325**(17): p. 1223-1227.
86. Mumoli, N. and M. Cei, *Licorice-induced hypokalemia*. International journal of cardiology, 2008. **124**(3): p. e42-e44.
87. Akinyemi, A.J., A.O. Ademiluyi, and G. Oboh, *Aqueous Extracts of Two Varieties of Ginger (Zingiber officinale) Inhibit Angiotensin I–Converting Enzyme, Iron(II), and Sodium Nitroprusside-Induced Lipid Peroxidation in the Rat Heart In Vitro*. Journal of Medicinal Food, 2013. **16**(7): p. 641-646.
88. Akinyemi, A.J., A.O. Ademiluyi, and G. Oboh, *Inhibition of Angiotensin-I-Converting Enzyme Activity by Two Varieties of Ginger (Zingiber officinale) in Rats Fed a High Cholesterol Diet*. Journal of medicinal food, 2014. **17**(3): p. 317-323.
89. Granzow, M., et al., *Die Rolle des Renin-Angiotensin-Systems in der Fibrose und Zirrhose in Renin-überexprimierenden Ratten*. Zeitschrift für Gastroenterologie, 2011. **49**(8): p. P447.
90. Yodjun, M., A. Karnchanatat, and P. Sangvanich, *Angiotensin I-Converting Enzyme Inhibitory Proteins and Peptides from the Rhizomes of Zingiberaceae Plants*. Applied Biochemistry and Biotechnology, 2012. **166**(8): p. 2037-2050.
91. Kazemi, B., *Using Factor VII in Hemophilia Gene Therapy*. 2011.
92. Anonymous, *common pathway of coagulation*. 2012, Elsevier Health Sciences.
93. Anonymous, *Coagulation Pathway*. 2008, Springer: Berlin, Germany. p. 715.
94. Anonymous, *intrinsic pathway of coagulation*. 2011, Elsevier Health Sciences.
95. Katzung, B.G., *Basic & clinical pharmacology*. 2002, The McGraw-Hill Companies: New York
96. Aprile, M., et al., *PPARG in Human Adipogenesis: Differential Contribution of Canonical Transcripts and Dominant Negative Isoforms*. PPAR research, 2014. **2014**: p. 537865.
97. Jones, J.R., et al., *Deletion of PPAR γ in adipose tissues of mice protects against high fat diet-induced obesity and insulin resistance*. Proceedings of the National Academy of Sciences of the United States of America, 2005. **102**(17): p. 6207-6212.

98. Hamblin, M., et al., *PPARs and the Cardiovascular System*. Antioxidants & Redox Signaling, 2009. **11**(6): p. 1415-1452.
99. Khateeb, J., et al., *Paraoxonase 1 (PON1) expression in hepatocytes is upregulated by pomegranate polyphenols: A role for PPAR- γ pathway*. Atherosclerosis. **208**(1): p. 119-125.
100. Li, Y., et al., *Pomegranate flower: a unique traditional antidiabetic medicine with dual PPAR- α / γ activator properties*. Diabetes, Obesity and Metabolism, 2008. **10**(1): p. 10-17.
101. Kakiuchi-Kiyota, S., et al., *Effects of the PPAR γ agonist troglitazone on endothelial cells in vivo and in vitro: Differences between human and mouse*. Toxicology and applied pharmacology, 2009. **237**(1): p. 83-90.
102. Takano, H., et al., *Pleiotropic Actions of PPAR γ Activators Thiazolidinediones in Cardiovascular Diseases*. Current pharmaceutical design, 2004. **10**(22): p. 2779-2786.
103. Le, J., et al., *Muscle-specific Pparg deletion causes insulin resistance*. Nature medicine, 2003. **9**(12): p. 1491-1497.
104. Chintharlapalli, S., et al., *Structure-dependent activity of glycyrrhetic acid derivatives as peroxisome proliferator-activated receptor γ agonists in colon cancer cells*. Molecular cancer therapeutics, 2007. **6**(5): p. 1588-1598.
105. Canner, D., *Proteopedia entry: HMG-CoA reductase*. Biochemistry and Molecular Biology Education, 2011. **39**(1): p. 64-64.
106. Huang, X., et al., *Polysaccharide from fuzi (FPS) prevents hypercholesterolemia in rats*. Lipids in health and disease, 2010. **9**(1): p. 9-9.
107. ElRokh, E.-S.M., et al., *Antihypercholesterolaemic effect of ginger rhizome (Zingiber officinale) in rats*. Inflammopharmacology, 2010. **18**(6): p. 309-315.
108. Sen, S., M. Roy, and A.S. Chakraborti, *Ameliorative effects of glycyrrhizin on streptozotocin-induced diabetes in rats*. Journal of Pharmacy and Pharmacology, 2011. **63**(2): p. 287-296.
109. Fuhrman, B., et al., *Antiatherosclerotic effects of licorice extract supplementation on hypercholesterolemic patients: increased resistance of LDL to atherogenic modifications, reduced plasma lipid levels, and decreased systolic blood pressure*. Nutrition (Burbank, Los Angeles County, Calif.), 2002. **18**(3): p. 268-273.
110. Wang, T. and T.H. Xu, *Advances in studies on compatibility of Radix Aconiti Laterlis and Radix Glycyrrhizae*. Chinese Traditional and Herbal Drugs, 2009. **40**(8): p. 1332-1334.
111. Wang, X., et al., *Liquorice, a unique guide drug of traditional Chinese medicine: a review of its role in drug interactions*. Journal of ethnopharmacology, 2013. **150**(3): p. 781-790.
112. Hondeghem, L.M. and B.G. Katzung, *Antiarrhythmic Agents: The Modulated Receptor*

Mechanism of Action of Sodium and Calcium Channel-Blocking Drugs. Annual Review of Pharmacology and Toxicology, 1984. **24**(1): p. 387-423.

113. Wu, D., et al., *Inhibitory effects of glycyrrhetic Acid on the delayed rectifier potassium current in Guinea pig ventricular myocytes and HERG channel*. Evidence-based complementary and alternative medicine : eCAM, 2013. **2013**: p. 481830-11.
114. Yi-mei, D., et al., *18[beta]-Glycyrrhetic acid preferentially blocks late Na current generated by [Delta]KPQ Nav1.5 channels*. Acta Pharmacologica Sinica, 2012. **33**(6): p. 752.
115. Anonymous, *Arrhythmia; Investigators at University Hospital target arrhythmia*, in *Cardiovascular Week*. 2008, NewsRx: Atlanta. p. 35.
116. Vicker, N., et al., *A novel 18 beta-glycyrrhetic acid analogue as a potent and selective inhibitor of 11 beta-hydroxysteroid dehydrogenase 2*. Bioorganic & medicinal chemistry letters, 2004. **14**(12): p. 3263-3267.
117. Gravez, B., A. Tarjus, and F. Jaisser, *Mineralocorticoid receptor and cardiac arrhythmia*. Clinical and Experimental Pharmacology and Physiology, 2013. **40**(12): p. 910-915.
118. Pei, M., Duan,X.,Pei,X, *Compatibility chemistry of acid-alkaline pair medicine of Fuzi and Gancao in Sini decoction*. J of Chinese Traditional Medicine 2009. **34**: p. 2047–2050.
119. Huangcai Yun, X.S., Yang Jingxian, etc., *The role of licorice water extract on experimental arrhythmias*. [J] Dalian Medical University, 2003. **25**(1): p. 13-15.
120. Peng, W.-W., et al., *The effects of Rhizoma Zingiberis on pharmacokinetics of six Aconitum alkaloids in herb couple of Radix Aconiti Lateralis-Rhizoma Zingiberis*. Journal of ethnopharmacology, 2013. **148**(2): p. 579-586.
121. Zhang, W., et al., *Comparative Pharmacokinetics of Hypaconitine after Oral Administration of Pure Hypaconitine, Aconitum carmichaelii Extract and Sini Decoction to Rats*. Molecules, 2015. **20**(1): p. 1560.
122. J.P. Chen, H.M.T., W.K. Wu, H.C. Luo, T.W. Liang, H.Q. Huang, X.R. Zhao, *Effect of Si-Ni-Tang on ischemic myocardium*. Academic Journal of First Military Medical University, 19 (1999), pp. 120–121, 1999(1999): p. 120-121.
123. Lv, Y., *Research on Pharmacodynamics and Toxicity of Aconite Dry Ginger of Compatibility*. Changchun University of Traditional Chinese Medicine, Changchun 2012.
124. H.X. Zhan, C.P., *Effect of the compatibility with Radix Aconiti Lateralis Preparata and Rhizoma Zingiberis on adrephrin, angiotensin II, aldosterone, ANP and NT of blood plasma in Xinyang declination rats*. Pharmacology and Clinics of Chinese Materia Medica, 2006(22): p. 12-14.
125. Wallukat, G., *The beta-adrenergic receptors*. Herz, 2002. **27**(7): p. 683.

126. Kimura, I., M.A. Islam, and M. Kimura, *Cholera toxin accentuates the antagonism by acetylcholine of higenamine-induced positive chronotropy in isolated right atria of mice*. Biological & pharmaceutical bulletin, 1995. **18**(11): p. 1509.
127. Ameri, A., *Effects of the Aconitum alkaloid mesaconitine in rat hippocampal slices and the involvement of alpha- and beta-adrenoceptors*. British journal of pharmacology, 1998. **123**(2): p. 243.
128. Bryan Roth and Bob Lefkowitz, N.M.L.P.P.N., NIH Chemical Genomics Center, *qHTS assay of beta-arrestin-biased ligands of beta2-adrenergic receptor*. NCGC Assay, 2010.
129. Masaru, I. and K. Yoshihisa, *Muscarinic Acetylcholine Receptors*. Current Pharmaceutical Design, 2006. **12**(28): p. 3573-3581.
130. Heinz, H.P., et al., *Effects of Ginger Constituents on the Gastrointestinal Tract: Role of Cholinergic M3 and Serotonergic 5-HT3 and 5-HT4 Receptors*. Planta Medica, 2011. **77**(10): p. 973-978.
131. Liu, Y., et al., *Role of M3 receptor in aconitine/barium-chloride-induced preconditioning against arrhythmias in rats*. Naunyn-Schmiedeberg's archives of pharmacology, 2009. **379**(5): p. 511-515.
132. Anonymous, *acetylcholinesterase*. 2011, Elsevier Health Sciences.
133. Sandhya, K.D., H.P. Chandan, and S.M. Smruti, *MEMORY STRENGTHENING ACTIVITY OF AQUEOUS LIQUORICE EXTRACT AND GLABRIDIN RICH EXTRACT IN BEHAVIOURAL MODELS*. International Journal of Pharmaceutical Sciences Review and Research, 2012. **16**(1): p. 120.
134. Brunhofer, G., et al., *Exploration of natural compounds as sources of new bifunctional scaffolds targeting cholinesterases and beta amyloid aggregation: the case of chelerythrine*. Bioorganic & medicinal chemistry, 2012. **20**(22): p. 6669.
135. Schwarz, S., et al., *Amino derivatives of glycyrrhetic acid as potential inhibitors of cholinesterases*. Bioorganic & medicinal chemistry, 2014. **22**(13): p. 3370.
136. Morera, L., et al., *Synthesis and biological evaluation of [6]-gingerol analogues as transient receptor potential channel TRPV1 and TRPA1 modulators*. Bioorganic & medicinal chemistry letters, 2012. **22**(4): p. 1674-1677.
137. Jeong, C.-H., et al., *[6]-Gingerol suppresses colon cancer growth by targeting leukotriene A4 hydrolase*. Cancer research, 2009. **69**(13): p. 5584.
138. Frazier, C.J., et al., *Synaptic Potentials Mediated via alpha -Bungarotoxin-Sensitive Nicotinic Acetylcholine Receptors in Rat Hippocampal Interneurons*. Journal of Neuroscience, 1998. **18**(20): p. 8228.
139. Ivy Carroll, F., et al., *Synthesis, nicotinic acetylcholine receptor binding, antinociceptive and*

seizure properties of methyllycaconitine analogs. Bioorganic & medicinal chemistry, 2007. **15**(2): p. 678-685.

140. Endo, S., et al., *Selective inhibition of the tumor marker AKR1B10 by antiinflammatory N-phenylanthranilic acids and glycyrrhetic acid*. Biological and Pharmaceutical Bulletin, 2010. **33**(5): p. 886-890.
141. Mizushina, Y., et al., *Inhibitory effects of glycyrrhetinic acid on DNA polymerase and inflammatory activities*. Evidence-based Complementary and Alternative Medicine, 2012. **2012**: p. 650514.
142. Mae, T., et al., *A Licorice Ethanolic Extract with Peroxisome Proliferator-Activated Receptor- γ Ligand-Binding Activity Affects Diabetes in KK-Ay Mice, Abdominal Obesity in Diet-Induced Obese C57BL Mice and Hypertension in Spontaneously Hypertensive Rats*. The Journal of Nutrition, 2003. **133**(11): p. 3369-3377.